Evaluation of the pinocytic uptake and cellular processing of antibody-N-(2-hydroxypropyl)methacrylamide copolymer conjugates and estimation of their potential use in "targeted" drug delivery.

by

Pauline Ann Flanagan B.A. (Hons)

A thesis submitted to the University of Keele in partial fulfilment of the requirement for Degree of Doctor of Philosophy.

Biochemistry Research Laboratory,
Department of Biological Sciences,
University of Keele

November 1987

For Mum

with love

Acknowledgements

I wish to thank Dr. Ruth Duncan for her consistent help and support throughout this study, and for her faith in me when I felt uncertain. Also, I wish to thank Professor Lloyd for the help and advice he readily gave whenever asked.

I wish to thank Dr. Ian Troubridge for his kind gift of monoclonal antibody B3/25, without which I could not have completed these series of experiments. Also thank you to Dr. Kopecek and co-workers for preparing all the HPMA copolymer conjugates used in this study.

Special thanks to my husband Patrick, without whose continued support I could not have undertaken this study. At this point I should also thank my children, Miles and Nicola, for putting up with me during the last few years!

Thank you to all the research staff, in both the Biochemistry Research Unit and Department of Biological Sciences for their help, in particular Kathryn O'Hare for help and advice, and both Aylsa Hume and Lynne Scarlett for their technical assistance.

A special thank you to Dr. Blanka Rihova for allowing me to visit her laboratory in Prague, and for her great hospitality and kindness.

A very big thank you to Margaret Cowen for typing this thesis, again to my husband Patrick for drawing all the diagrams, and to both Kathryn O'Hare and Len Seymour for proof-reading. I am certain that it seemed a never-ending task!

Last, but certainly not least, thank you to the Medical Research Council who funded this work.

Abstract

^{125}I-labelled protein (antibody or transferrin)–N-(2-hydroxypropyl)methacrylamide (HPMA) copolymer conjugates were characterised using gel permeation chromatography and their average molecular weight ($\bar{M}w$) determined (Chapter 3). It was estimated that within a protein-HPMA copolymer conjugate each protein residue was probably bound to 10-20 molecules of HPMA copolymer.

The human transferrin receptor was used as a model target antigen/receptor. Pinocytic uptake of HPMA copolymer conjugated to monoclonal antibody B3/25 (specific for the transferrin receptor) or transferrin (as potential targeting residues) was up to 9-fold higher than the uptake of parent copolymer (Chapter 4). The ability of these conjugates to bind specifically was confirmed by Scatchard analysis of their cell-surface binding (Chapter 6). Also, using a Percoll density gradient (Chapter 5), it was shown that internalisation of protein-HPMA copolymer conjugates is dependent upon their $\bar{M}w$ and that internalised conjugates reach the lysosomal compartment.

The transferrin receptor was found to have limited potential as an *in vivo* model antigen/receptor. HPMA copolymer conjugates containing either monoclonal antibody B3/25 or transferrin were detected in all rapidly dividing organs/tissues studied (Chapter 7). Conjugates containing anti-Thy-1.2 polyclonal antibody (as a targeting residue) were shown to localise preferentially in the thymus, spleen, liver, skin and bone marrow. The ability of only <1% (administered dose) of conjugate to reach a major target organ, the thymus, was consistent with published values (Chapter 8).

Conjugation of HPMA to antibody (IgG) was shown to produce a 250-fold reduction in immunogenicity of the antibody (Chapter 9,

preliminary results).

Although the stoichiometry and stereochemistry of the conjugates used in this study were not ideal (Chapters 3, 10) use of similar conjugates in targeted drug-delivery has potential.

Abbreviations

CFA	Complete Freund's adjuvant
CURL	Compartment involved in the uncoupling of receptor and ligand
ELISA	Enzyme-linked immunosorbent assay
Fab	Monovalent antibody antigen binding fragment (released by papain cleavage)
$F(ab')_2$	Divalent antibody antigen binding fragment (released by pepsin cleavage)
Fc	Antibody complement binding fragment (released by papain cleavage)
ffp	Fluid-phase pinocytosis
HPMA	N-(2-hydroxypropyl)methacrylamide
HBSS	Hank's balanced salt solution
IgG	Immunoglobulin, class G
i.p.	Intraperitoneal
i.v.	Intravenous
McAb	Monoclonal antibody
$\bar{M}_w$	Molecular weight average
PBS	Phosphate buffered saline
r_{av}	Average radius
SOL	In solution
Tf(apo)	Apotransferrin
$Tf(Fe)_2$	Diferric transferrin

Correction: All references in this thesis have been written with a comma before et al. This is incorrect.

CONTENTS

CHAPTER 1

General Introduction

1.1 INTRODUCTION

Conventional chemotherapy is still associated with the complication of undesirable side-effects, arising from a lack of specificity of drug action. Other major problems include early loss of a great deal of administered drug via the kidney, together with first pass metabolism by the liver. This often necessitates frequent administration of drug, in relatively high dose, in order to maintain optimal blood level and optimal pharmacokinetic behaviour. The small size of conventional drugs together with their chemical properties have the added disadvantages of facilitating entry into all cells by the process of simple diffusion and/or active transport across membranes, resulting in ubiquitous rather than specific distribution of drug in the body. This is exemplified in cancer therapy, where treatment is based on the selective destruction of rapidly dividing cells. The targets of such therapy are the cancerous cells, but rapidly dividing cells such as those found in the lining of the intestine, hair follicles and in bone marrow are equally accessible to, and affected by, drug. Conventional chemotherapy can be wasteful, inefficient, and unselective.

Conventional chemotherapy is, however, on the verge of a radical and exciting change. The advent of this new era of drug delivery has been made possible by the many exciting advances in our fundamental knowledge of cell and molecular biology, such as the first description of monoclonal antibodies by Milstein (reviewed Milstein, 1980). Ehrlich, the father of chemotherapy, once stated "corpora non agunt nisi fixata" (agents cannot act unless they are bound); it is the ambition of scientists working in the area of drug delivery not simply to have drugs which bind, but bind specifically to a pre-determined cell type such as cancer cells. The increasing number of cell-surface antigens being catalogued, and the raising of

antibodies specific for these antigens (Baldwin & Byers, 1985) may offer a possibility of cell-specific targeting of drug as once dreamt of by Ehrlich when he talked of "magic bullets". In the following study the transferrin receptor will be explored as a model cell-surface antigen, to which the soluble, synthetic, polymeric drug-carrier poly-N-[2-hydroxypropyl]methacrylamide (HPMA), will be targeted by conjugation with either transferrin, or monoclonal antibody B3/25 (specific for the transferrin receptor).

To achieve selective cell death it is necessary to deliver drug specifically and at an optimal concentration to the target cell. If antibodies per se are loaded with drug there is the possibility that denaturation of the antibody may result leading to a loss of antigen recognition and binding. Baldwin & Byers (1986) report that substitution ratios of three drug residues per antibody molecule may result in a loss of antibody specificity. The use of a drug-carrier, which can be optimally loaded with drug and then subsequently bound to antibody in a ratio approaching one to one, offers the potential of reducing the limitation of drug-loading when using antibody directed conjugates and would therefore allow site-specific delivery of effective concentrations of drug.

1.2 DRUG CARRIERS

Potential drug-carriers may be divided into two major groups, natural and synthetic macromolecules (see Table 1.1).

Natural macromolecules (Duncan & Kopecek, 1984) have the advantage that they may be of discrete size, be non-toxic, and may contain the necessary targeting residues within their structure. Their disadvantages include the fact that they tend to be immunogenic (either in native form or when chemically modified to bind drug), and that they are sensitive to denaturation during binding of drug and also when handled experimentally. An example of such instability was

Table 1.1

A selection of Potential Drug Carriers

Type of Carrier	Reference
Natural macromolecules	
Proteins	Trouet, et al. (1982)
DNA	Hulhoven & Harvengt (1982)
Antibodies	Worrell, et al. (1986)
Hormones	Poznanzky, et al. (1984)
Erythrocyte Ghosts	Ihler, et al. (1973)
Serum Albumin	Garnett, et al. (1983)
Lipoproteins	Vitols, et al. (1985)
Synthetic macromolecules	
Colloidal carriers:-	
emulsions	Davis (1984)
liposomes	Poste, et al. (1984)
microspheres	Davis, et al. (1984)
nanoparticles	Davis, et al. (1986)
Poly(amino acids)	Ryser & Shen (1978)
Poly(phosphazenes)	Grolleman (1982)
Polyvinyl analogues of nucleic acid	Pitha, et al. (1981)
Copolymer of PVP	Pato, et al. (1983)
Dextran	Konieczny, et al. (1982)
N-(2-hydroxypropyl)-methacrylamide copolymer	Kopecek, et al. (1985)

observed by Trouet, et al. (1980) when using DNA as a carrier non-covalently bound to drug.

Synthetic carriers (Duncan & Kopecek, 1984; Kopecek, 1984; Lloyd, et al., 1984) have the great advantage that they can be tailor-made to suit the requirements of any particular drug-delivery system. Within the overall structure of such a carrier it is possible to provide limited degradation together with an optimal number of functional groups for the subsequent binding of both drug and targeting residues (Duncan & Lloyd, 1980; Duncan, et al., 1983; Kopecek, 1984). Synthetic carriers including HPMA are of lower immunogenicity than natural molecules (see Chapter 8; Rihova,et al., 1985), but do become slightly more immunogenic with the incorporation of amino-acid side chains (Rihova, et al., 1984; Rihova,et al., 1985). A disadvantage of synthetic carriers may be their polydispersity (Kopecek, 1984).

Synthetic carriers fall broadly into two main groups, colloidal particles and polymers (see Table 1.1). Colloidal particles (Davis & Illum, 1986) include liposomes, microspheres, nanoparticles and emulsions. A major problem of this type of synthetic carrier has been its preferential uptake by the reticulo-endothelial (R.E.) system, in particular capture by Kupffer cells of the liver following intravenous administration (Duncan & Kopecek, 1984). This uptake by the R.E. system has been attributed to the size, shape, charge, surface polarity and rigidity of the carriers (Poste & Kirsch, 1983; Posnansky & Juliano,1984; Poste, 1985). Using combinations of polyoxamine and polyoxamer coated microspheres, Davis & Illum (1986) have reported that the capture of microspheres by the R.E. system can be reduced by 55% with a redistribution of particles to the bone marrow, or retention within the vascular system. Targeting, however, to specific cell types remains a major problem with these carriers

(Davis & Illum, 1986).

The carrier used in this study is a soluble, synthetic polymer whose structure has a backbone of N-(2-hydroxypropyl)methacrylamide (HPMA) (see Fig. 1.1). This relatively inert structure was originally developed as a plasma expander (Kopecek,et al., 1973). Reactive groups have been incorporated into this structure by copolymerisation of HPMA with N-methacryloylated oligopeptides terminating in p-nitrophenyl esters (Kopecek, 1984; Fig. 1.2). The presence of reactive p-nitrophenyl (ONp) ester linkages allows subsequent binding of drugs and targeting residues which contain an aliphatic amino group, by aminolysis of the ONp ester linkage (Kopecek, 1984; Fig. 1.3). The combination of amino-acids within the oligopeptide side-chain can be designed to give controlled release of terminal group X (where X may be drug, or targeting-residue) within the lysosomal compartment of the cell (Duncan & Lloyd,1980; Duncan, et al., 1983; Rejmanova,et al., 1985). The rate of release of drug from such oligopeptide side-chains is influenced by the chemical nature of the drug itself (Kopecek, 1984). Incubation of HPMA copolymers containing daunomycin or puromycin with lysosomal enzymes (Duncan,et al., 1987) has shown that more than 20% of daunomycin and more than 80% of puromycin can be released from HPMA conjugates containing a gly-phe-leu-gly oligopeptide side-chain.

HPMA copolymers are taken into cells by fluid-phase pinocytosis (see Chapter 4). An understanding of the pinocytic pathway reveals that there are a number of ways to increase both the specificity and rate of uptake, of the HPMA carrier (see Section 1.4.2). Using the rat visceral yolk sac system, Duncan,et al., (1984) have demonstrated an enhanced rate of uptake of HPMA resulting from non-specific adsorption after incorporation of tyrosinamide (10-20%) into the structure of the copolymer. Incorporation of a gly-gly spacer

between [^{125}I]-tyrosinamide and the HPMA copolymer backbone resulted in subsequent release of [^{125}I]-tyrosine within the lysosome.

Polycations also bind strongly to membranes. Shen & Ryser (1978; 1979; 1981) showed that covalent attachment of poly-(L-lys) to serum albumin, horseradish peroxidase, or methotrexate resulted in a large increase in their rate of pinocytosis. In particular the transport of methotrexate into cells normally drug-resistant was achieved (Shen & Ryser,1978; 1979; 1981). McCormick,et al. (1986) found that a polycationic derivative of HPMA copolymer bound strongly to cells both in vivo and in vitro. The polymeric cation adsorbed to the cell membrane, or glycocalyx, but did not readily gain access to the cell's interior.

To achieve an increased uptake by specific cell types it is possible to use carbohydrates specific for carbohydrate receptors (see Table 1.2) or antibodies specific for cell surface antigens. Duncan,et al. (1985; 1986) have been able to demonstrate uptake of modified copolymers via galactose (liver) and fucose receptors (L1210 cells). Increased survival of DBA_2 mice bearing L1210 cells, following treatment with HPMA copolymeric drug carriers containing daunomycin and a fucosylamine targeting residue has been shown (Duncan,et al. 1987).

Evaluation of the feasibility of targeting HPMA copolymers by incorporation of antibodies as targeting residues is the primary aim of this study. The field of immunotargeting has expanded rapidly over the last decade, since the advent of monoclonal antibodies (McAb; a pure preparation of one class of antibody with a single defined specificity; Milstein, 1986). A selection of work reported by others in this field is shown in Table 1.3. Immunotargeting of HPMA is still in its infancy. In vitro incubation of HPMA bound to non-specific rat IgG (Duncan, et al., 1985) was shown to enhance both

Figure 1.1

The structure of N-(2-hydroxypropyl)methacrylamide (HPMA)

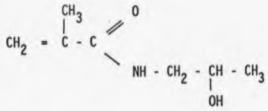

Figure 1.2

Radicle polymerisation of N-(2-hydroxypropyl)methacrylamide with p-nitrophenyl esters of N-methacryloylated oligopeptides

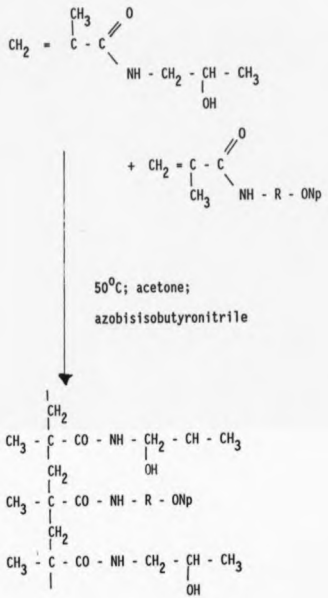

Where R = oligopeptide such as

gly-gly; gly-phe-leu-gly

Figure 1.3

Aminolysis of the p-nitrophenyl ester linkage by an aliphatic amino group on X

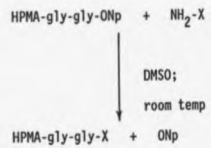

Where X may be drug, for example daunomycin or a targeting residue, for example antibody/transferrin.

Gly-gly may be replaced by an alternative oligopeptide side chain.

Table 1.2

Carbohydrate receptors and their cellular distribution

Carbohydrate receptor	Cells bearing the receptor	Reference
Galactose	hepatocytes	Ashwell & Harford (1982)
	hepatoma	Schwartz, et al. (1982)
Galactose-particle	Kupffer Cells	Teraclaira, et al. (1983)
Mannose-N-acetyl glucosamine	RE cells	Davis & Illum (1986)
Mannose-fucose	monocytes	Stahl (1983)
Mannose-6-phosphate	fibroblasts	Neufeld, et al. (1975)
	liver cells	Ullrich, et al. (1978)
Fucose	hepatocytes	Prieels, et al. (1978)
Mannose	fibroblasts	Tomlinson (1986)
Glucose	Lewis lung carcinoma	Roche, et al. (1983)

Table 1.3

A summary of the various approaches used in immunotargeting

General Reviews: Gregoriadis (1984); Honra & Dass (1984); Baldwin (1985); Feun (1985); Embleton (1986).

Complexity	Reference
Antibody	Scheinberg & Strand (1982)
Antibody-radiolabelled	Hazra & Sharma (1982)
	review: Bradwell et al. (1985)
Antibody-toxin	Worrell, et al. (1986)
	Thorpe, et al. (1984)
Antibody + free drug	Newman & Ford (1977)
antibody-drug conjugate	review: Arnon & Sela (1982)
	Smyth, et al. 1986)
Antibody-bridging reagent-drug	Jung, et al. (1981)
Antibody-carrier-drug	
including as carrier:	
liposomes	Mangat & Patel (1985)
	Senior, et al. (1986)
microspheres	Laasko (1986)
nanoparticle	Illum, et al. (1983)
natural polymers	Garnett, et al. (1985)
soluble synthetic polymers	review: Duncan & Kopecek (1984)

the rate of pinocytic uptake and rate of exocytosis of HPMA by the rat visceral yolk sac system. Rihova & Kopecek (1985) and Rihova et al. (1986) have shown that HPMA conjugated to a cell-surface active drug and anti-Thy-1.2 (monoclonal and polyclonal) antibody was 70-times more cytotoxic against T-lymphocytes than the same conjugates bound to non-specific IgG. Partial inactivation of antibodies occurred during conjugation to HPMA and a slight decrease in the in vitro activity of conjugated, as compared to free drug was reported. This was thought to be due to possible steric hindrance of the drug by the antibody.

In the following study monoclonal antibody (McAb) B3/25, specific for the transferrin receptor will be used as the major model system. The structure of an antibody molecule and the transferrin receptor will now be described.

1.3 THE STRUCTURE OF THE ANTIBODY MOLECULE

To appreciate the potential of antibodies as targeting moieties in drug therapy, it is necessary to have an understanding of the structure of the antibody molecule, and its antigen binding site (Fig. 1.4). Appreciation of the function of the various structural domains is also necessary to enable prediction of the consequences of polymer-antibody conjugation.

Antibodies are secreted by B-lymphocytes and are one of the major proteins found in the blood, being approximately twenty per cent of the total blood protein. A unique feature of these proteins is that their basic structure can produce almost infinite variability, determining the specificity of each particular antibody (reviews by Nisonoff, 1975; Kabat, et al., 1976). Each B-lymphocyte (B-cell) and its clones, is responsible for the secretion of only one of the millions of different antibodies. The differentiation of B-cells into clones of antibody-secreting plasma cells is stimulated by the presence of a foreign substance which is

Fig.1.4 The different classes of immunoglobulin and detailed structure of IgG. (After Alberts, et al., 1983).

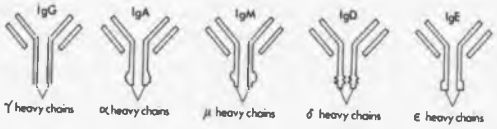

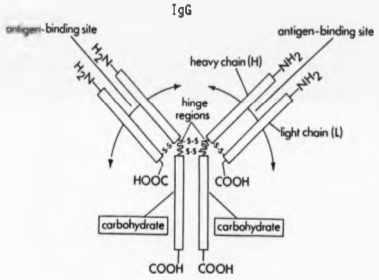

recognised as an antigen of the antibody. If the foreign particle is large then it can contain a number of sites which are capable of eliciting the formation of antibody; each of these sites is known as an antigenic determinant, and is capable of stimulating a different B-cell. At the other extreme there are particles which are too small to elicit a response unless they are attached to a carrier macromolecule. Such small molecules are known as haptens (or haptenic determinants when attached to a carrier). This type of B-cell stimulation is important when the use of an antibody-polymer-drug conjugate is being considered.

Antibodies can be divided into a number of classes depending on the fine structure of the molecule (see Fig. 1.4). The simplest structure is found in the IgG class, which form the predominant type of antibody found in the blood of higher vertebrates, and as such have been the most extensively studied. A molecular weight of 160K led Porter (1973) to propose that the molecule is composed of approximately 2.3×10^4 atoms. The overall shape of the molecule is that of a Y, with a two-fold axis of symmetry passing through the tail of the Y (comprehensively reviewed by Amazel & Poljak, 1979; Davies & Metzer, 1983; Gorevic, et al., 1985). Chemical manipulation of the molecule, using mercaptoethanol, to reduce disulphide bonds, and 6M urea to disrupt non-covalent bonding, resulted in the production of two identical 50K Dalton chains, and two identical 25KD Dalton chains, which were designated the heavy chain and the light chains respectively. This gave an IgG subunit structure of H_2L_2. Each half of the molecule is composed of one H and one L chain, and the whole is held together by covalent and non-covalent bonding to form a highly ordered molecule. The heavy chain has been shown to contain one or more carbohydrate side-chains, the function of which are still not absolutely clear.

The function of the antibody molecule was related to this structure by the use of specific enzyme cleavage using papain and pepsin (see Fig. 1.5). Porter (1973) showed that papain cleaves the heavy chain on the amino-terminal side of the disulphide bond which links the heavy and light chains, to produce three fragments of approximately equal size. Two of these fragments are identical being derived from the arms of the Y, the remaining fragment is formed from the tail of the Y. The two identical fragments are able to bind antigen and are therefore given the name antigen-binding fragments, (F_{Ab}). The second fragment-type from various IgGs was found to crystallise readily, that is, these fragments formed a homogeneous population. They were given the name constant, or crystalline, fragments (Fc). The Fab fragments are composed of the entire L chain plus the amino-half of the H chain, whereas the Fc fragments are composed of the carboxyl-terminal ends of two H chains. The binding of antigen was therefore confined to the arms of the Y. The tail of the Y has a complementary role in directing various physiological events, such as the fixation of complement, and the uptake of an opsonised particle by macrophages.

Pepsin cleavage is specific for the region of the IgG molecule below the disulphide bridge which holds together the H and L chains, to produce an $F(ab')_2$ fragment and a mixture of Fc sub-fragments. The $F(ab')_2$ fragment is bivalent and as such can cross-link antigens to form precipitates. The efficiency of this bivalent linkage is up to 10^4 greater than a univalent linkage, and is further enhanced by the flexibility of the arms of the Y, which have been shown to vary between 113 and 143 degrees (Silverton, et al., 1977). This flexibility optimises the formation of antigen-antibody complexes, since the angle between the arms can be regulated to correct for the distance between specific antigenic determinants.

Fig. 1.5 Enzyme cleavage of IgG using papain and pepsin.
(After Alberts, et al., 1983).

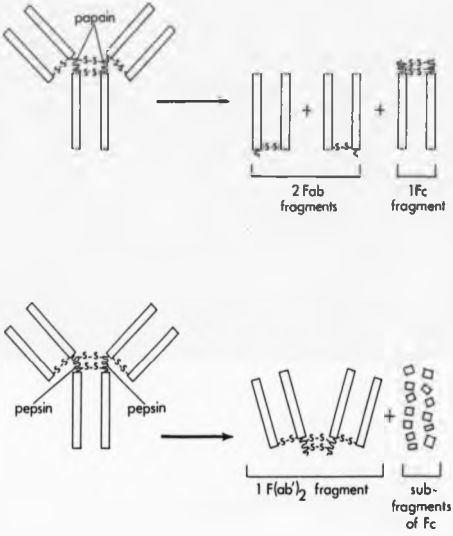

Both the light (L) and heavy chains (H) of the antibody molecule can be sub-divided into distinct regions (Wu & Kabat, 1970). A variable region of 108 amino acids is found at the amino-terminal end of both the heavy and light chains. The remaining amino acids form the constant domains; 106 amino acids in the case of the light chain, 330-440 amino acids in the case of the heavy chain, depending on class of antibody (see Fig. 1.6). Within the constant region of the light chain, at position 191 there is an allotypic site designated Kappa (Leu or Val present) or Llamda (Lys or Arg present).

The structure of the antibody molecule is composed of several distinct domains, each of which is held together by an intra-chain disulphide bridge (Fig. 1.7). The domains are designated V_H V_L (which are homologous), and C_H1 C_H2 C_H3 and C_L (which are homologous). Each domain is thought to contain at least one active site, which in the variable region binds antigen, and in the constant region is important in effector functions (such as binding complement). The structure of each domain is based upon the immunoglobulin fold (Fig. 1.8), that is, two sheets of β-strands, with the hydrophobic side-arms of the constituent amino acids packed very tightly between the sheets to form a hydrophobic cleft.

Each domain has dimensions 4x2.5x2.5nm (Davies, 1977; Davies & Metzger, 1983). Carbohydrate plays a central role in the interaction of the domains, for example, C_H1 and C_H2 are prevented from making close contact by carbohydrate; the C_H2 regions of both chains must interact via carbohydrate.

1.3.1 The characteristics of the antigen-binding site

The variable regions contain hypervariable (H.V.) regions (4 in V_H; 3 in V_L; Capra & Edmundson, 1977). These regions are composed of 25 amino acids in V_L and 30 in V_H, the remaining amino acids being relatively constant (Fig. 1.9). It is within these HV regions that

Fig. 1.6 Constant and variable regions of IgG.

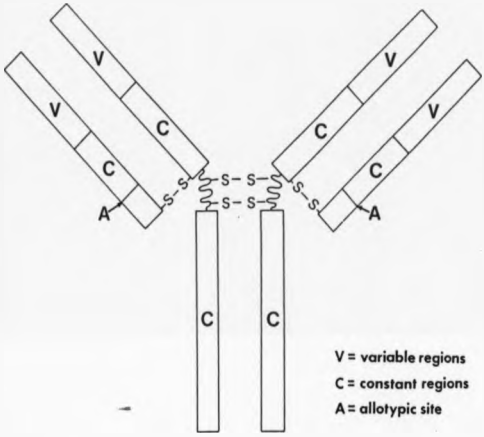

Fig. 1.7 The distinct domains of IgG. (After Edelman, 1973).

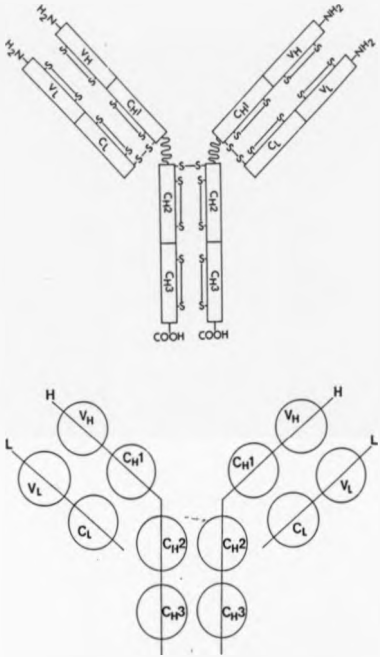

Fig. 1.8 The immunoglobulin fold. (After Capra & Edmundson, 1976).

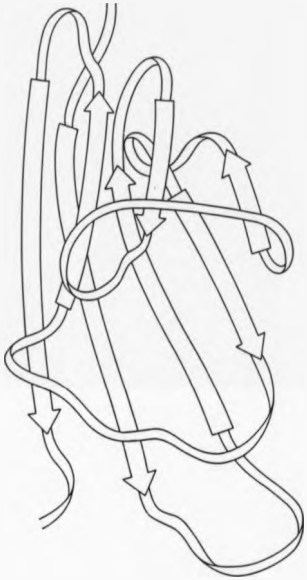

Fig. 1.9 The hypervariable regions of IgG and the antigen-binding site. (After Alberts, et al., 1983).

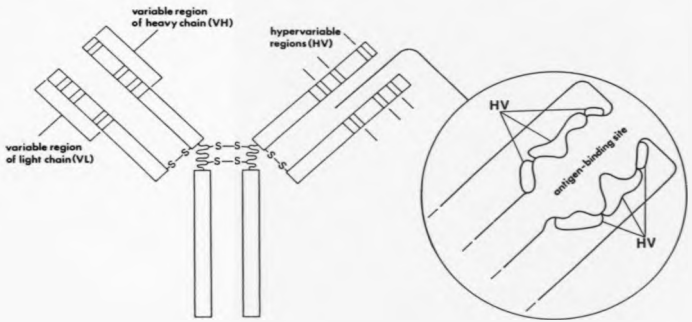

antibody specificity is determined, (Capra & Edmundson, 1977), with the potential of 10^8 different combinations of binding sites (Milstein, 1986).

The strength of antigen binding is determined by the cumulative effect of Van der Waals interactions, H-bonding and electrostatic forces. These weak forces are effective only when antigen is in close enough proximity to the antigen-binding site to allow some of the antigen atoms to fit into complementary recesses on the antibody surface (Amazel, et al., 1974, the binding of vitamin K; Padlan et al. 1976, the binding of phosphorylcholine).

1.3.2 The characteristics of an antigen

An antigen (or antigenic determinant, epitope) may be broadly defined as that region of a molecule which interacts with the binding site of an antibody molecule. Those properties which determine antigenicity, however, are as yet not fully understood. For carbohydrates, the antigen can consist of a sequence of up to five sugars, (Nisonoff, et al., 1975; Williams & Woollett, 1984). Determination of the antigenicity of proteins is more complicated; the antigen is composed of a sequence of 5-8 amino acids (Worobec et al., 1985) which have a continuous, or discontinuous primary sequence. This sequence of amino acids may be flexible or rigid. Investigation of continuous antigens (reviewed Marx, 1984; Tainer et al., 1984; Westhof, et al., 1984) has suggested that flexibility of these regions is an important property of the antigen. However, others have found (Novotny, et al., 1986) (using both continuous and discontinuous epitopes) a greater correlation between accessibility of an antigen to antibody and antigenicity, than between flexibility and antigenicity. Novotny, et al. (1986) support the view that "exceptional surface exposure is the key to antigenicity", flexibility being a consequence of this exposure.

There is also debate as to whether discrete antigenic determinants exist or whether there are a number of mutually overlapping antigens (Benjamin,et al., 1984). It is even possible that the whole surface is potentially antigenic, those regions which elicit a response being the most accessible to antibody (Novotny,et al., 1986). If antibodies are to be used for drug-targeting it may not be necessary to define antigenicity, but rather to use those antibodies which are known to localise efficiently at a target cell.

At the cell surface it is glycoproteins and glycolipids which are accessible to the immune system; often carbohydrate will form a considerable area of possible interaction (Williams,et al., 1985). However, in mammals antigenic determinants are often based on proteins rather than carbohydrates (Williams & Woollett,1984). Antibodies raised against different species also seem to recognize protein rather than carbohydrate. Feizi (1984,1985) has recently found, however, that in some tumour cells antigens are carbohydrate in nature, possibly reflecting novel carbohydrate structures on these cells.

The existence of ideal tumour-specific antigens, as defined in Table 1.4, is at this time thought to be unlikely. Many reports of tumour-specific antigens (Teh,et al., 1985) have been shown to cross-react with antibodies raised against normal tissue. There is growing support for the view of Greaves (1979) that "tumour antigens are normal antigens which have been produced at an inappropriate time, or in an inappropriate tissue". An example of this would be the stabilisation, of a normally transient differentiation antigen, on a tumour cell. Such antigens are not foreign and would not elicit an immune response. If novel antigens are present, however, the tumour has several ways of avoiding destruction (and avoiding binding of an antibody-targeted carrier), these are summarised in Fig. 1.10.

Figure 1.10

Schematic diagram summarising how a tumor avoids destruction

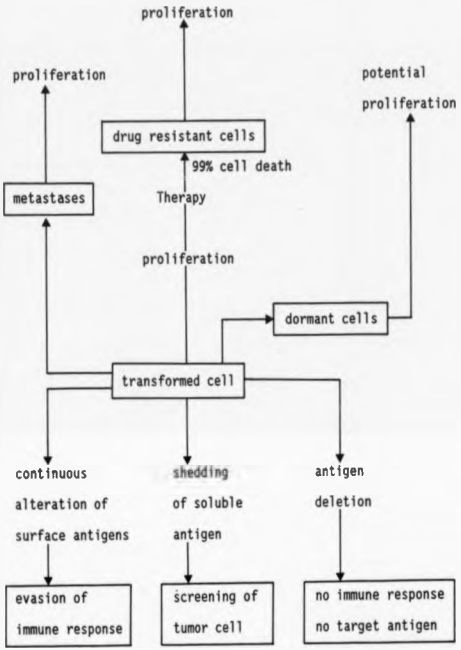

Table 1.4

Characteristics of an ideal tumor antigen

1. It must be present on all cells of the tumour, but not on normal cells
2. The antigen should be characteristic of a particular type of malignancy
3. The primary tumour antigen should be retained in secondary tumours
4. The antigen should readily gain access to the interior of the cell, or at least
5. Not be shed from the cell surface to produce an antigen "screen".

As stated above anti-carbohydrate antibodies have been found to react with novel tumour antigens, and there is increasing awareness of the importance of carbohydrate chains of glycolipids and glycoproteins as oncodevelopmental antigens (Feizi, 1985; Tang et al., 1985). These novel structures may play a role in cell adhesion and hence metastasis of tumour cells.

In the following study the transferrin receptor has been used as a model antigen.

1.4 TRANSFERRIN AND THE TRANSFERRIN RECEPTOR

Use of the transferrin receptor as a model antigen has certain advantages; (a) it has been isolated and well characterised (Schneider, 1983) (b) the density of the receptor is thought to be dependent on cell type and state of growth, being of higher density on rapidly proliferating cells such as cancer cells (Trowbridge, 1985) (c) the receptor-ligand complex is internalised after binding of ligand, be that ligand transferrin or antibody (Schneider & Williams 1985; Testa 1985). Understanding of the physiological receptor-ligand interactions will allow comparison with data reported later using novel antibody or transferrin-containing HPMA copolymer ligands.

1.4.1 Transferrin

Iron is a transition metal essential to all living organisms for biocatalysis and oxygen transport (reviewed Aisen, 1980; Aisen & Listowsky, 1980). The metal can exist in one of two oxidation states, Fe^{II} or Fe^{III}. Under physiological conditions of pH, ionic strength, and pO_2 Fe^{III} is the predominant state. It is essential to any living organism that this cation is sequestered since Fe^{III} is highly hydrolytic and will form insoluble polymers at concentrations

greater than 10^{-17}M at pH7. Normally serum concentration of Fe^{III} is 70µg/dl (10µM) and the solubility problem is overcome by tight chelation of Fe^{III} by the serum protein transferrin, which under physiological conditions is only 20-50% saturated (Aisen, 1980; Aisen & Listowsky, 1980.)

Transferrin is synthesised and secreted by hepatocytes (Finch & Heubers 1982). There are three main types of transferrin, ovotransferrin, serum transferrin, and lactoferrin, the latter being distinctive in amino-acid sequence and immunogenicity (Aisen, 1980; Aisen & Listowsky, 1980). The transferrin described here is that found in the serum; it is acidic and has a molecular weight of approximately 80K Daltons. The protein is composed of a single chain of 676 amino-acids and two carbohydrate side-chains. The carbohydrate is 6% by weight and is composed of two identical, nearly symmetrical heterosaccharide chains. These chains are of the bi-antennary structure common to serum glycoproteins. Both chains are found at the C-terminal region of the protein, joined by β-1 glycosidic linkages to asp residues 415 and 668. Unlike other glycoproteins removal of the terminal sialic acid residue to expose galactose does not increase clearance from the blood (Aisen 1980). The function of the carbohydrate is unknown.

The overall shape of transferrin is that of an ellipsoid, containing two lobes at 30^{o} to each other, which each contain a cleft in the region of the join. The binding equivalent of transferrin for Fe^{III} is 40K, indicating that the carrier is two-sited. None (apotransferrin), one (monoferric), or two (diferric) Fe^{III} molecules may be bound to transferrin. X-ray crystallography has shown that the shape of the carrier changes during Fe^{III} binding, the ellipsoid becoming more spherical and more resistant to denaturation.

Iron has the coordination geometry of an octahedron, as seen in

haemoglobin and transferrin. Transferrin is able to coordinate at only five of the six sites, leaving the absolute requirement of an anion, CO_3^{2-} or HCO_3^- at the sixth coordination site. Schlabach and Bates (1975) have shown, using different anions, that the anion-binding site is a cleft measuring 3x3x6A. The anion is thought to function as a bridging ligand between metal and protein, locking the metal in place by occupying a coordination site that would otherwise be occupied by water, and thus stabilising the metal-protein interaction by preventing hydrolysis of the Fe^{III}. The bond between the anion and protein is relatively labile, having a half-life of 200h at pH7 (Aisen, 1980). It is the nature of this bond which is thought to provide the mechanism for the removal of Fe^{III} from transferrin. If the anion is removed by protonation, or enzymic cleavage, from the sixth coordination site, then the protein will spontaneously fall from the other five sites releasing $Fe(H_2O)_6$. Strong binding of neither anion nor protein is seen in the absence of the other. Without anion binding the transferrin cannot compete with the hydrolytic reactions of Fe^{III}.

When loaded with Fe^{III} transferrin shows a characteristic absorbance in the visible spectrum at 465nm (Aasa,et al., 1963). If the protein is cleaved to produce two one-sited fragments, then it is found that the spectra of each site is different, with the sum of the two spectra being equal to that of the intact spectrum (Aisen, 1980). There has been a large amount of contradictory evidence in the literature pointing to both the equivalence and non-equivalence of these two sites. Today it is generally accepted that there is an acid-labile and an acid-stable site. The two sites have different binding constants, which differ by a factor of 5 at pH7.4 and a factor of 33 at pH6.7. At physiological pH, in the presence of anion, Fe^{III} is essentially locked into either site on the first

encounter. The significance of the differential susceptibility of these sites to acid may be important in the delivery of iron to acidic intracellular compartments (see Section 1.5).

1.4.2 The transferrin receptor

The tranferrin receptor is a protein composed of 760 amino acids (Schneider, et al., 1984) It is a Group II plasma membrane protein (Schneider, et al. 1982; 1984; Serial, et al., 1986), that is, the receptor spans the membrane once and has its N-terminal on the cytoplasmic side of membrane. The C-terminal extracellular domain consists of 671 amino acids, the N-terminal cytoplasmic domain 61, and the intramembrane domain 28 amino acids (Schneider, et al., 1984). The receptor exists as a disulphide-linked dimer of molecular weight 180K Daltons, sub-unit weight 90K Daltons (Schneider, et al., 1982). Trypsin releases a 70K Dalton fragment from the membrane which retains the ability to bind transferrin (Schneider, et al., 1982; Fig. 1.11). Trowbridge & Omary (1981) using the monoclonal antibody B3/25 have shown that the receptor is a cell-surface antigen on a large number of cell types. It is now thought that the receptor may be found on most if not all nucleated cells (Table 1.5) and as such would explain the dependence of cell growth in vitro on the presence of transferrin (Rudland, et al., 1977). The cell-surface density of the receptor has been reported to be dependent upon several factors (Schneider & Williams, 1985; Testa, 1985; Trowbridge, 1985) (a) malignancy; certain malignant cells possess a higher density of transferrin receptor than the corresponding normal cells (b) state of differentiation; the erythroblast has a high density of receptor, the erythrocyte none (c) state of growth; cells which are in their log phase of growth, and cells which are induced to proliferate rapidly in vitro express a higher density of receptor than corresponding cells in a less active phase of growth. The

Fig. 1.11 The transferrin receptor (information taken from May and Cuatrecasas, 1985; Schneider, et al., 1982).

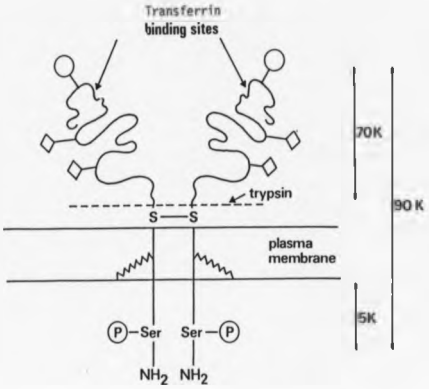

Table 1.5

Cell types which express the transferrin receptor

(references: too numerous for individual citation; please refer to reviews Newman, et al. (1982) Sibille et al. (1982)).

Most human haematopoetic cell lines

- reticulocytes
- human lymphocytes
- choriocarcinoma cell lines
- RPMI 2650 (quasi diploid nasopharyngeal carcinoma)
- WI 38 (embryonic lung fibroblasts)
- HeLa (cervical carcinoma)
- foetal liver
- normoblasts (erythrocyte precursor)
- leukaemia cells
- neuroblastoma
- pancreatic carcinoma
- melanoma
- hepatocytes
- K562 (human erythrocyte leukaemia)
- fibroblasts
- KB cells (human carcinoma)
- CCRF/CEM (pre-T, pre-B cell human lymphoblastic leukaemia)

Now thought to be present on all nucleated cells.

association of receptor density and growth has been demonstrated in fibroblasts, lymphocytic lines, breast tumour cell lines, leukaemic cell lines, and may be a feature of all cell types. There is dispute in the literature as to whether the density of the receptor may play an important role in natural killer (NK) cell recognition (Newman et al., 1982; disputed Bridges & Smith 1985), since normal and malignant cells, which are NK-cell targets, express a high density of the transferrin receptor.

The importance of the interaction between transferrin and its receptor in the control of growth has been implicated in the work of Trowbridge & Lopez (1982) who found that McAb 42/6 and transferrin bind competitively with the ligand binding-site of the transferrin receptor. It has been shown that the growth of cells was inhibited in the presence of McAb 42/6 together with transferrin, the cells remaining in the S-phase of their life cycle. This inhibition could not be overcome by supplying the cells with an alternative source of iron in the form of ferrous sulphate or ferric nitriloacetic acid, which are both potential donors of iron to the cell.

Each monomer of the receptor is capable of binding one molecule of iron-saturated transferrin. It has been shown by trypsin cleavage of the transferrin-binding fragment from the membrane that each site binds independently of the other (Schneider & Williams 1985). There is conflicting evidence in the literature as to whether the receptor-ligand complex becomes clustered in the coated pits following binding of transferrin, or if it is a resident of the pit (Testa, 1985; Dautry-Varsat, 1986; Cheng, 1986).

The complex is internalised by endocytosis (a term which was first used by de Duve, 1963). As the process of endocytosis is central to the following study it will be described in detail with particular reference to transferrin.

1.5 ENDOCYTOSIS

The term endocytosis is very broad, and on the basis of the size of the ingested substrate the process may be sub-divided into the processes of phagocytosis and pinocytosis. Phagocytosis is a substrate-triggered event resulting in the uptake of relatively large particles, such as senescent cells, immune complexes, and bacteria, by specialised scavenger cells, the macrophages. The process of phagocytosis will not be discussed further here.

1.5.1 Pinocytosis

Pinocytosis describes the process of cell drinking, with the consequent uptake of extracellular fluid and the solutes dissolved therein. Pinocytosis, unlike phagocytosis, is a constitutive process, which occurs in most cell types; it may be further sub-divided to distinguish between fluid-phase and adsorptive pinocytosis.

1.5.1.1 Fluid-phase pinocytosis

Fluid-phase pinocytosis (fpp) describes the uptake of extracellular fluid, and solutes in a non-specific manner (Besterman & Low, 1983; Steinman, et al., 1983; Willingham & Pastan, 1984). The rate of uptake of solute is dictated by the rate of invagination and pinching off of the plasma membrane to form pinocytic vesicles, and is not regulated by the availability of substrate. The rate of ffp varies with cell type, for example the macrophage ingests 50% of its volume and 180% of its surface area per hour, as compared with the fibroblast which ingests 5-10% of its volume and 50% of its surface area per hour (Steinman,et al., 1983). It has also been shown (Steinman,et al., 1983) that over a 3h period the surface area of macrophages remained constant suggesting that membrane is constantly recycling to the cell surface after pinocytic internalisation.

The function of fpp is not absolutely clear. Originally it was thought that a major function was plasma membrane lipid and protein recycling. However, the 54-180% of cell surface internalised per hour far exceeds the 2% per hour turnover of plasma membrane protein. It seems more likely that plasma membrane protein turnover is a consequence of the continuous endocytosis-exocytosis shuttle. Bretscher, et al., (1980) explain the relatively low rate of membrane constituent turnover by postulating the involvement of a molecular filter which prevents the majority of proteins being internalised.

1.5.1.2 Adsorptive pinocytosis

Although the rate of pinocytosis is not usually affected by the presence of substrate, substrate selection can occur by means of adsorption to the plasma membrane (Besterman & Low, 1983; Lloyd & Williams,1984). Substrates which have an affinity for the plasma membrane and are selectively concentrated within the cell include cationised ferritin (Besterman & Low, 1983) and denatured bovine serum albumin (BSA) (Lloyd & Williams,1984). The degree of concentration depends upon (a) substrate concentration in the ambient fluid (b) affinity for the plasma membrane and (c) the density of binding sites on the membrane to be internalised. Non-specific binding has been demonstrated using the rat visceral yolk sac cultured *in vitro*. Experiments using BSA, and native bovine insulin (Lloyd & Williams,1984) led to the proposal that the yolk sac membrane contains two types of binding site, one for cationic ligands, and another for hydrophobic ligands, the two sites operating independently. It is conceivable that the natural turnover *in vivo* of non-adsorptive circulating proteins involves such binding sites. Spontaneous denaturation may reveal previously masked hydrophobic, or cationic sites, with the consequent rapid and efficient removal of the protein from circulation.

1.5.1.3 Receptor-mediated pinocytosis

In contrast to simple adsorptive pinocytosis, receptor-mediated pinocytosis is highly specific, a particular receptor being responsible for the uptake of only one particular ligand type. For example, the galactose receptor recognises those glycoproteins with a terminal galactose residue (Wall & Hubbard, 1985), whilst the transferrin receptor recognises transferrin (Schneider, et al., 1982). The former example is less discriminating in that it has specificity for a range of glycoproteins which may only have in common an exposed galactose residue (Wall & Hubbard, 1985) as compared with the latter example, which is specific for only one protein. It is thought that some ligands such as transferrin and $\alpha_2$macroglobulin are also able to bind non-specifically to low affinity membrane binding-sites (Steinman, et al., 1983).

There are a wide variety of receptors found on the surface of animal cells. Characteristically they are intrinsic membrane proteins which are able to move freely in the plane of the lipid bilayer by lateral diffusion, with a diffusion coefficient similar to other membrane proteins (Pastan & Willingham, 1983). Fluorescence labelled ligands have shown that most receptors move randomly and freely in the plane of the membrane (Pastan & Willingham, 1983). At 37^{o}C each receptor encounters one of the 1000, or more, coated pits found on most types of cultured cell, once every 3 seconds.

The distribution of receptors is not always uniform across the whole cell surface, for example the asialoglycoprotein (ASGP) receptor is confined to one side of the hepatocyte by junctional elements (Wall, et al., 1980). Other cell types such as those possessing microvilli, contain a higher density of receptors in certain areas of the cell surface, such as the microvillous area, without the presence of junctional complexes (Weller, 1974) giving

indirect evidence for the existence of domains.

The number of receptors on any one cell specific for a particular ligand is not always constant. There is some evidence of an interchange between cell surface receptors and an intracellular pool, for example the asialoglycoprotein receptor (Steinman, et al., 1983) and the transferrin receptor (Hopkins, 1986) are amongst those which exhibit down regulation.

1.5.2 Intracellular processing

Once ligand is bound to receptor, for example transferrin to the transferrin receptor, there is clustering of the receptors into the coated pits (Pastan & Willingham, 1983). It is possible that receptors such as the transferrin receptor, low density lipoprotein receptor (Willingham & Pastan,1984; Wileman,et al., 1985) may cluster in these pits in the absence of ligand. Internalised ligand enters the early peripheral endosomal compartment, (Wileman,et al., 1985). The endosomal compartment is heterogeneous both in its cellular distribution and morphology (Helenius,et al., 1983; Willingham & Pastan,1983; Wileman,et al., 1985). The vesicles which form the endosome range from 0.3-1μm in diameter and are composed of two or possibly three distinct sub-populations, the early peripheral endosomes, which are usually associated with tubular elements, and a second population which is located near the Golgi-lysosome region of the cell. The latter population are larger, sometimes tubular and possibly identified as CURL (Geuze,et al., 1983).

The heterogeneous nature of endosomes has made separation of these organelles extremely difficult. Indirect studies have shown that the vacuole has an acidic interior (Pastan & Willingham, 1983). Galloway,et al. (1983) have shown acidification of endosomes in vitro, and postulate that an ATPase/H^+ pump (similar to that found in the lysosome) is responsible. The origin of the proton pump

responsible for acidification is thought to be the plasma membrane.

The function of this pre-lysosomal acidic compartment is thought to be that of a "clearing house", sorting out membrane from intravesicular contents, and dissociating receptors from ligands. The prime importance of the endosome is as a site of recycling (Besterman, 1981) of both membrane and receptors (Van Renswoude, et al., 1982). The number of ligands taken up by a cell is very large, for example fibroblasts internalise $2x10^6$ $\alpha_2$macroglobulin molecules per hour despite with the presence of only a few thousand cell-surface receptors (Dickson, 1981). The cell does not have the capacity to resynthesise so many receptors quickly enough to replace those internalised. There must be re-use of receptors resulting from recycling. Evidence that such recycling occurs via a pre-lysosomal compartment is several fold; (a) the relatively long half-life of plasma membrane proteins, and in particular receptors, implies that they are not exposed to lysosomal enzymes (Steinman, et al., 1976) (b) the rapid recycling time (less than five minutes) for receptors such as transferrin is too quick to have involved the lysosome (Van Renswoude, et al., 1982) (c) receptor-mediated uptake of ligands continues at 16-20^{0}C at which temperature there is little movement to the lysosome, if indeed any (Wall & Hubbard, 1985). The role of the endosome in receptor recycling is probably to act as an acid environment in which the ligand-receptor complex dissociates, as seen with the Semliki Forest Virus (SFV) (Marsh, et al., 1983) and transferrin (Van Renswoude, et al., 1982). It is within the acidic environment of the endosome that diferric transferrin is subject to protonation of the anion at the sixth co-ordination site of Fe^{III}. This destabilises the transferrin-metal interaction and releases iron to the cell (Aisen 1980; Octave, et al., 1983; Testa,1985; May & Cuatrecasas, 1985). Iron is transported to ferritin (mechanism

unknown) and the apotransferrin-receptor complex is subsequently recycled back to the plasma membrane. The site of recycling has been variously attributed to the endosome, Golgi, and lysosome (see Table 1.6). This confusion may result from the lack of a common pathway in all cell types. In the field of drug delivery, it is necessary to know the exact intracellular routing of particular drug-conjugates.

The ultimate fate of those receptors which do not recycle (see Table 1.7) is the lysosome (Besterman & Low, 1983; Steinman, et al., 1983). Lysosomes (Barrett, 1969; Thines-Simpoux, 1984; Dean, 1977) are a heterogeneous population of vesicles, whose characteristics are summarised in Table 1.8. There are found to exist two broad populations of lysosomes (i) primary lysosomes, which are newly formed (ii) secondary lysosomes, which result from fusion of a primary lysosome with a second vesicle. The membrane of the primary and secondary lysosome differ, in that the latter contains a high proportion of choline phosphate and sphingomyelin (Thines-Simpoux, 1984), which are normally characteristic of the plasma membrane, thus indicating some interchange between the plasma membrane and the lysosome.

The function of the lysosome is one of degradation. Material which is no longer of use to the cell is degraded to its constituent molecules, which may then be subsequently re-used. The structure of the lysosome is ideally suited to this function of digestive organelle; (i) the vast battery of enzymes, some of which have incomplete substrate specificity (Lloyd & Forster, 1986) are able to degrade all incoming organic material, be that material polypeptide, polysaccharide, polynucleotide, or glycolipid (ii) the acid pH-optima of the enzymes ensures that the maximal effect of these enzymes is within the confines of the lysosome, reducing potential damage by leakage of lysosomal enzymes into the cytosol (pH7.2) (iii) the

Table 1.6.

Putative vacuole involved in recycling of transferrin and its receptor

Cell type	Putative vacuole	Reference
Epidermoid carcinoma	endosome and lysosome	Hopkins (1983)
Human carcinoma A431	lysosome-like compartment	Hopkins & Trowbridge (1983)
K562	non-lysosomal acidic vacuole	van Renswoude, et al. (1982)
Cultured mammalian cells	endosome/lysosome	Octave, et al. (1983)
Rat fibroblasts	lysosome	Octave, et al. (1979)
Embryo fibroblasts	lysosome	Octave, et al. (1981)
K562	golgi	Stein (1984)
K562	golgi	Pastan & Willingham (1983)
HepG2	endosome	Neutra, et al. (1985)
Hepatocytes	golgi	Morgan, et al. (1986)

Table 1.7

Ligands which are ultimately delivered to the lysosome following receptor-mediated endocytosis

Reference: please refer to reviews by Besterman & Low (1983); Steinman, et al. (1983).

Ligand	Cell type
Low density lipoprotein (LDL)	fibroblasts
Transcobalamin II	Many cell types
Transferrin (possibly)	see Table 1.6
Semliki Forest Virus (SFV)	fibroblasts
Cholera Toxin	Many cell types
Insulin	hepatocytes; monocytes; adipocytes
Complement	leucocytes
Epidermal growth factor	fibroblasts
Murine gamma globulin	macrophages; leucocytes
Glycoproteins terminated in	
galactose	hepatocytes
mannose-fucose	macrophages; endothelial cells
mannose-6-phosphate	fibroblasts
Acetylated LDL	macrophages
α_2 Macroglobulin	macrophages

Table 1.8

Characteristics of the lysosome

Membrane	relatively impermeable to
	(i) molecules >220 dalton
	(ii) molecules which are charged
	contains ATPase/H^+ pump
	contains transport proteins
Interior	acid (pH ≃ 5)
	contains >80 enzymes
	(i) incomplete specificity
	(ii) able to degrade all naturally occuring molecules
Function	degradation of unwanted material to its constituent molecules

For more detailed information see

Barrett (1969); Thines-Simpoux (1984);

Dean (1977); Lloyd & Forster (1986)

relatively high impermeability of the lysosomal membrane ensures that only the monomeric units of degraded material are allowed to re-enter the cytosol for subsequent re-use. Material which cannot be degraded is retained within the lysosome, thus restricting contact with the rest of the cell.

The basic design of HPMA drug conjugates is such that free drug is released from the carrier within the lysosomal compartment (Duncan, 1986). It is necessary to determine the intracellular routing of all potential HPMA drug-carrier conjugates after conjugation to the targeting residue, to determine the optimal chemistry of binding drug to the inert HPMA backbone. If, after conjugation to transferrin the HPMA copolymer conjugate does not enter the lysosomal compartment, but rather recycles through the endosomal compartment, then it is possible to incorporate an acid-labile linkage into the overall structure of the carrier to facilitate release of drug within the endosome. If, alternatively, the carrier is not readily endocytosed after conjugation then a surface active drug may be attached to the carrier.

Those properties considered to be desirable in a drug-carrier are summarised in table 1.9 This study has examined the potential of HPMA copolymer-protein conjugates, in particular HPMA-copolymer-antibody conjugates, to fulfil these requirements.

Table 1.9

Characteristics of an ideal drug-carrier

1) possess sites available for the attachment of drug and targeting residues

After conjugation the carrier must be

2) soluble
3) of a defined molecular weight
4) able to bind specifically
5) able to release drug at either the cell surface or intracellularly to facilitate cell death

In vivo the conjugate must be

6) stable in the plasma
7) able to extravasate and reach target tissues
8) eliminated from the body after fulfilling its function
9) biocompatible, non-toxic, and have limited immunogenicity

CHAPTER 2

Materials and Methods

2.1 MATERIALS

2.1.1 Cell Maintenance

Human Skin Fibroblasts: Kindly supplied by Dr. G.T.N. Besley, Dept. Pathology, Royal Hospital for Sick Children, Edinburgh.

$HepG_2$: Kindly supplied by Dr. M. Wilkinson Liver Unit, King's College Hospital, London.

Alexander: Kindly supplied by Dr. H. Thomas, Royal Free Hospital, London.

CCRF/CEM; Clone M_3: Flow Laboratories, Irving, Ayrshire, U.K. CCRF/CEM (Cat. No. 05-520) First isolated by Foley, *et al.* (1965). Clone M_3 (Cat. No. 05-535)

Flow Laboratories, Ayrshire

		catalogue number
Culture flasks	growth area 25cm^2	62-350-07
	75cm^2	62-375-05
	175cm^2	62-380-C3
Tissue culture multi-well plates	96 well	76-063-04
Micro-filters	Flowpore (0.2µm;D26-20)	64-001-04
Medium	Powdered Ham's F10	10-411-22
	Powdered Eagle's minimum essential, with Earle's salts (with glutamine, without sodium bicarbonate)	10-101-20
Serum	Newborn calf	29-121-54
	Foetal bovine	29-102-54
Amino acids	Non-essential	16-810-49
Trypsin	2.5% (w/v)	16-893-49
Phosphate buffered saline:	Dulbecco's formula (modified) without calcium and magnesium	28-103-05

Trysin/versene	(0.4gm/l EDTA)	16-891-49

Gibco (Europe), Uxbridge, Middlesex

Medium	Powdered RMPI 1640	074-1800
Antibiotics	Penicillin-streptomycin (10,000 units ml^{-1})	043-5140 H

LIP (Equipment and services) Ltd, Shipley, Yorkshire

Disposable sterile pipettes	10ml	131 BM
	1ml	D611
Pasteur pipettes	long form, plain	26591
	short form, plain	26534

Equipment

Laminar Flow cabinet	Flow Laboratories	BSB4A Class II, Type A
Pipetus	Flow Laboratories	77-240-00
CO_2 incubator	Heraeus Electronic West Germany	Type B5060 EK/CO_2
Microscope	Zeiss, West Germany	47 1202 9901
Suction pump	Charles Austin Pumps Ltd, Surrey	Capex 2D-C

Freezer -80^{0}C	Denley Instruments Ltd, U.K.	BT 225K 625LV
Coulter Counter	Coulter Electronics Ltd, Harpenden, Herts	Model Ind.St.
Haemocytometer slide	Hawksley, England Depth 0.1mm	B5 748 Improved

2.1.2 Radioiodination

Sodium[^{125}I]iodide	Amersham International plc Aylesbury, Bucks.	
1,3,4,6-tetrachloro-3α, 6α-diphenylglycouril	Sigma, Dorset	T-9018
Visking tubing 8/32"	Scientific Instruments, London	
Hand monitor	Mini-Instruments Essex, England	type 5.40
Gamma Counter	LKB, Croydon, Surrey	Compugamma model 1282
Beta counter		Rackbeta
Spectral		

		Model 1219
Liquicint, scintillation fluid	National diagnostics Bucks	LS 121

2.1.3 Chromatography

Pharmacia, Milton Keynes, Bucks

		catalogue/model number
Sephadex	G-15	17-0020-01
	4B	17-0120-01
	6B	17-0110-01
Sephacryl	S-200	17-0871-01
	S-300	17-0438-01
PD-10	G-25 disposable	17-0851-01
Sepharose Protein-A	Sigma	P3391
Plastic insert tubes	LIP (Equipment and Services) Ltd, Shipley, Yorkshire	28985
Automatic fraction collector	Chemlab, England	270

Peristaltic Perspex pump	LKB	10200
Ultrafiltration unit Immersible cx-10 single use ultrafiltration units	Millipore, Bedford	PT40 11K 25

2.1.4 Proteins and polymer conjugates

	Sigma catalogue/model number
Apotransferrin (human)	14506

Monoclonal antibody B3/25, specific for transferrin receptor	Kind gift from Dr. I. Trowbridge, Salke Institute, California
HPMA copolymer and protein-HPMA copolymer conjugates	Prepared by Kopecek, et al. Institute of Macromolecular Chemistry, Prague.

2.1.5 Subcellular Fractionation

	Pharmacia
Percoll	17-0891-01

Density marker beads		17-0459-01

Beckman, High Wycombe, Bucks

Centrifuge	Preparative Ultra-centrifuge	Model L
Centrifuge head	Fixed angle (23.5) Rav 6.5cm	Type 65
Centrifuge tubes and caps	Thick walled polycarbonate	

Koch-Light, Maidstone, Kent

Fluorescamine	1039-00
4-Methyl-umbelliferyl-2-acetamido-2-deoxy-β-D-glucopyranoside	4080-00

Sigma

Homovanillic acid (4-hydroxy-3-methoxy-pheylacetic acid)	H1252
Peroxidase	P8375
Tryptamine	T2891
Pyruvate	P-2256
$NADH_2$	lot 646-F3

	Perkin-Elmer, Beaconsfield, Bucks	
Fluorimeter	Fluorescence spectrometer	Model 3000
Spectrophotometer	UV/VIS	Model 5505

2.1.6 In vivo

Mice

DBA_2	Bantin and Kingman, The Field Station Grimston, Aldbrough, Hull	male
B10; AJ	Institute Microbiology Prague	male and female
Homogeniser	Camlab	Model K41
Anaesthetic ether	May and Baker, Manchester	

All other chemicals were of analytical grade.

2.2 METHODS

2.2.1 Cell Culture

2.2.1.1 Aseptic technique

All cell culture techniques were carried out in a laminar flow cabinet (Class II). Equipment and materials used were always sterile. Those items not supplied pre-sterilised were sterilised by either (i) autoclaving($120^{o}C$, $15lb/m^2$, 15min); suitable for glassware, certain plastics (ii) micro-filtration ($0.2\mu m$); suitable for solutions (iii) U.V. irradiation (>10min) used where (i) and (ii) not possible. The pipetus, suction pump, all associated tubing and the inside of the cabinet, were wiped down with methylated spirits (70%) before and after use. The inside of the cabinet was irradiated (U.V., 10mins) after each use.

Sterile solutions were dispensed by means of a pipetus attached to a sterile pipette (10ml). Solutions were removed from cell cultures by suction (suction pump) via a sterile Pasteur pipette. Whilst dispensing and removing solutions great care was taken to ensure that neither the pipette, nor solution, touched the neck of any container used.

2.2.1.2 Cell lines

Human skin Fibroblasts (adherent) were routinely grown in complete Ham's F10 medium (that is Ham's F10 medium containing newborn calf serum (20%)) and antibiotics (Penicillin, $10u\ l^{-1}$; Streptomycin, $10\mu g ml^{-1}$) and incubated ($37^{o}C$, CO_2 incubator) in culture flasks (plastic 25, 75, or $175cm^2$ growth area).

CCRF/CEM (human lymphoblastic leukaemia) were routinely grown in RPMI complete medium (that is, RPMI medium containing foetal calf serum, 10% and antibiotics, as above and incubated ($37^{o}C$, CO_2 incubator) in culture tubes (round-bottomed, plastic 10ml).

Clone M_3, Hep G_2 and Alexander cells (used only in Chapter 6)

were maintained by A. Hume and L. Scarlett.

Briefly, Clone M_3 were grown in Ham's F10 medium containing horse serum (15%) and foetal bovine serum (2.5%).

Hep G_2 were grown in Eagle's (modified) minimum essential medium with Earles salts, containing foetal bovine serum (10%).

Alexander cells were grown in Eagle's (modified) minimum essential medium with Earle's salts containing non-essential amino acids (1%) and foetal bovine serum (10%).

2.2.1.3 Subculturing

2.2.1.3.1 Fibroblasts

The following protocol describes the sub-culturing of fibroblasts grown in flasks of 25cm^2 growth area.

At confluence (determined by microscopy) cells were washed (PBS without calcium and magnesium, pH 7.4, 10ml). For initial experiments this was followed by trypsinisation according to the method of Kooistra & Lloyd (1985). Pre-washed cells were incubated in trypsin (0.25% in PBS, pH 7.4, 2.5ml 15min, 37^{0}C) and recovered by centrifugation (1000 rpm, 10min). The resulting pellet was resuspended in Ham's F10 complete medium (4ml), and equally divided into culture flasks (25cm^2) containing complete medium (as above, 5ml). The flasks were gassed (5% CO_2 95% air, 6-12s).

However, this method had a number of disadvantages (i) prolonged contact of fibroblasts with trypsin caused the cells to clump (ii) recovery of cells by centrifugation is potentially damaging (iii) gassing of flasks resulted in a lowering of the pH of the medium to a sub-optimal level. To overcome these difficulties the above method of trypsinisation was modified. The following modification was used in the majority of the experiments.

Trypsin was left in contact with pre-washed cells for one minute. After incubation in residual trypsin (37^{0}C, 15min), and

subsequent resuspension in Ham's F10 complete medium (4ml) the fibroblasts were equally divided into 2 flasks ($25cm^2$) each containing complete medium (5ml).

If flasks of larger growth area were used then the volumes of reagents were scaled up accordingly.

Medium was changed on day 4 after subculturing, and the cells subcultured on day 7.

2.2.1.3.2 CCRF/CEM

CCRF/CEM were grown to an optimal density (determined by cell viability, 2.2.1.5). The cell pellet was resuspended by inversion of the cell culture tube several times, and sub-divided 1:10 into 10 culture tubes each containing RPMI complete medium (9mls).

2.2.1.4 Freezing and thawing of cells

Cells were stored at $-80^{o}C$ (medium term, up to 6 months; $-196^{o}C$ (liquid nitrogen, long term, more than 6 months).

Fibroblasts were washed and trypsinised (2.2.1.3.1). Detached cells were then resuspended in Ham's F10 complete medium containing dimethylsulphoxide (DMSO, 10% , 2ml) and transferred to a screw-topped ampoule. The ampoule was gradually cooled. For medium term storage cells were sequentially cooled at $4^{o}C$ (1h), $-20^{o}C$ (1h) and finally $-80^{o}C$. For long term storage the cells were then further cooled to $-196^{o}C$ (after 24h at $-80^{o}C$).

CCRF/CEM were pelleted (1000rpm, 5min) washed by resuspension in PBS (pH7.4, 10ml) and repelleted (1000rpm, 10min). The pellet was resuspended in RPMI complete medium containing DMSO (10%) and treated as above.

Cells were rapidly thawed by placing the ampoule in a water bath ($37^{o}C$). The cell suspension (in medium containing DMSO) was then

transferred to a centrifuge tube (10ml) and slowly (drop at a time) complete medium (5ml) was added, followed by a further addition of complete medium (5ml). After gentle washing the cells were recovered by centrifugation (1000rpm, 10min). As the cells are very fragile after freezing, they were not subjected to further washing at this time. The cells were resuspended in a large excess of complete medium (20ml) to dilute the effect of any remaining DMSO. Fibroblasts were transferred to a culture flask (75cm^2 growth area). Viable cells were given time to adhere to the flask (24h). Medium and dead cells were removed by suction, and fresh complete medium added (20ml, 75cm^2 flask). In contrast the CCRF/CEM cell suspension was added to culture tubes (2, 10ml) left for 2h and then pelleted (1000 rpm, 10min). The pellet was washed (PBS, pH7.4, 10ml) and resuspended in complete medium (10ml).

2.2.1.5 Cell viability: Trypan blue exclusion test

Pre-washed fibroblasts (PBS pH7.4, 10ml) were trypsinised (2.2.1.3.1), and resuspended in PBS (pH7.4, 2mls). Trypan blue (200µl, 0.4%) was added to a sample of cell suspension (200µl). The cells were allowed to take up the dye (37^{o}C, 10min), then duplicate samples were placed on a haemocytometer slide and the percentage viable cells determined.

CCRF were pelleted (1000rpm, 10min), washed in PBS (pH7.4, 10mls), repelleted (100rpm, 10min) and then resuspended in PBS (2mls). Trypan blue was added and cell viability determined as detailed above. The percentage of viable cells was calculated by the following equation:

Total cell number in xmls of cell suspension = No cells on haemocytometer slide grid (contains $1x10^{-4}$ml) x 10^4 x X

$$\% \text{ viability} = \frac{\text{viable cell number}}{\text{Total cell number}} \times 100$$

All cultures used in this study were > 99% viable.

2.2.1.6 Cell growth

A growth curve was determined for each cell type used. A set of identical flasks (adherent cells) or tubes (non-adherent cells) were set up on day 0. At each time point (t-0, 24h, 48h, over approximately 10 days) cell number and viability were determined as above.

2.2.2 Radioiodination

2.2.2.1 The Iodogen method

The method used was originally described by Fraker & Speck (1978) and later modified by Dean, 1985).

Iodogen (1mg in 25ml dichloromethane) was added (50µl) to the bottom of an Eppendorf tube (500µl). Solvent was allowed to evaporate in a fume cupboard, leaving a coating of the solid-phase Iodogen reagent on the sides of the Eppendorf tube. Catalyst-coated tubes were stored (-20^{0}C, tightly stoppered) until required.

A stock solution of 4.4mg ml^{-1} was prepared for all ligands to be iodinated (the same concentration as McAb B3/25 supplied by Dr. I. Trowbridge). For all protein-HPMA copolymer conjugates the concentration of protein was used as a measure of conjugate concentration. (For example conjugate-associated transferrin 4.8mg ml^{-1}; IgG 6.8mg ml^{-1}; McAb B3/25 2mgml^{-1}). To allow standardisation of the iodination condition used, in terms of a ratio of ^{125}I(µCi) to protein (mg) the volume of protein-HPMA copolymer conjugate used for iodination was determined by the concentration of protein in the preparations as supplied.

In general, (25µl 4.4mgml^{-1}; 110µg) was added carefully to the bottom of the catalyst-coated tube. Sodium [^{125}I]iodide (0.5mCi, 5µl) was added (ensuring thorough mixing with the substrate solution). The lid of the Eppendorf tube was quickly closed and the reaction allowed to proceed at room temperature (≥10min). The reaction was stopped by addition of phosphate buffer (0.05M, pH7.2, 1ml). Diluted sample was eluted through a disposable gel permeation chromatography column (Pharmacia P-10, Sephadex G-25) with phosphate buffer (0.05M, pH7.2). (The column had been pre-washed with BSA, 500µl, 100mgml^{-1}, to prevent non-specific adsorption of protein to the column). Fractions (8-drop) were collected and radioactivity assessed (hand monitor). Those tubes containing the first peak (corresponding to the radiolabelled substrate eluting with the void volume) were pooled and dialysed (8/32" visking tubing) against NaCl (5l, 1%) to remove traces of free [^{125}I]iodide. Radioiodinated preparations were stored at -20^{o}C.

2.2.2.2 Determination of free [^{125}I]iodide using paper electrophoresis

The middle 20cm of a piece of chromatography paper (Whatman-1, 5cmx30cm) was divided into strips (40, 0.5cm wide). Radiolabelled substrate was applied by streaking across the fifth strip, and electrophoresed (30min, 400v) in buffer (barbitone 0.1M, pH8.6). Strips were cut out and assayed for radioactivity (LKB Compugamma, 30s). Under these conditions only free [^{125}I]iodide migrates in the current. Free [^{125}I]iodide was determined as a percentage of the total radioactivity recovered (if >2% the preparation was re-dialysed against NaCl).

Routinely, before all experiments the percentage of free [^{125}I]iodide was determined.

2.2.2.3 Determination of Specific Activity

[^{125}I]iodide has a half-life of 60 days

$$A = A_0 e^{-Kt}$$

Where A = activity on the day of the experiment

A_0 = initial activity

K = the constant for ^{125}I

= 1.155×10^{-2}

t = time (days) from t_0

$$\text{Specific Activity} = \frac{A(\mu Ci)}{\mu g \text{ protein}}$$

A summary of specific activities obtained in this study are given in Chapter 3, Table 3.2.

2.2.3 Chromatography

2.2.3.1 Gel permeation chromatography

2.2.3.1.1 Sephadex G-15 (height 17cm, internal diameter 1.4cm, flow rate 12mlh^{-1}, molecular weight separation of proteins approximately 0-1500k Daltons

Sephadex G-15 columns were used to separate low molecular weight degradation products ([^{125}I]iodide, [^{125}I]iodotyrosine) released during incubation of ^{125}I-labelled HPMA with fibroblasts (Chapter 4).

The column was calibrated with both [^{125}I]iodide and [^{125}I]iodotyrosine. A sample (1×10^4cpm in 1ml) was added to the top of the column and eluted using Tris/HCl buffer (0.2M, pH8, containing NaCl, 0.5M). Fractions (3min) were collected and assayed for radioactivity (LKB, Compugamma, 2min).

For detection of low molecular weight degradation products, duplicate medium samples (1ml) were eluted through the column using

the conditions detailed as above.

2.2.3.1.2 Sephacryl S-200 (height 78cm, internal diameter 1.7cm, flow rate 8mlh^{-1}, molecular weight separation of proteins approximately 5k-250k Daltons).

Sephacryl S-200 columns were used to separate protein-HPMA copolymer conjugates from free unconjugated HPMA copolymer (always found as a contaminant in the preparations supplied). A sample of ^{125}I-labelled conjugate (approximately 500K cpm in 1ml total vol.) was characterised by elution through a S-200 column (0.2M Tris/HCl buffer, pH8, containing 0.5MNaCl). Fractions (6min) were assayed for radioactivity (LKB Compugamma, 2min).

Unlabelled crude reaction mixture (1ml) was then eluted through the column (under the same conditions as above). Those fractions corresponding to protein-HPMA copolymer conjugate (Abs 280nm) were pooled and then concentrated by ultrafiltration (Millipore, CX-10).

2.2.3.1.3 Sephacryl S-300 (height 112cm, internal diameter 1.7cm, flow rate 10mlh^{-1}) and Sepharose 4B/6B (height 65cm, internal diameter 1.7cm, flow rate 13mlh^{-1})

Both Sephacryl S-300 and Sepharose 4B/6B columns were used for the molecular weight determination of the protein-HPMA copolymer conjugates used in this study.

Both columns were calibrated with a range of proteins and HPMA copolymers (of a defined Mw and low polydispersity Table 2.1: see Chapter 3 and Figs. 3.5a,b).

For both calibration and molecular weight determination, a spike of ^{125}I-labelled ligand (approximately 5x10^5cpm in 1ml total vol.) was eluted through the column with buffer (0.2MTris/HCl, pH8, containing 0.5MNaCl). Fractions (6min) were assayed for radioactivity (LKB Compugamma 2min).

Table 2.1

Proteins and HPMA copolymers used to calibrate the S-300 and 4B/6B gel permeation columns.

Protein	Log Molecular Weight
Cytochrome C	4.09
Transferrin (both apo and diferric)	4.90
IgG	5.18
Ferritin	5.67
Thyroglobulin	5.84
HPMA copolymers of differing $\bar{M}_w$ (supplied by Kopecek, et al.)	4.06
	4.32
	4.60
	4.89
	5.17
	5.74

2.2.3.2 Affinity chromatography

Sephadex-protein-A (height 10cm, internal diameter 1.7cm, flow rate $20ml h^{-1}$

Sephadex-Protein-A chromatography was used to separate antibody-HPMA copolymer conjugates on the basis of their ability to interact with Protein-A.

A sample (1ml) of purified antibody-HPMA copolymer conjugate (2.2.3.1.2) was eluted through the column with buffer (0.1M Tris/HCl, pH8). Fractions (3min) were collected and Abs. 280nm determined. Those fractions containing antibody-HPMA copolymer conjugate (Abs. 280nm) were pooled.

Antibody-HPMA copolymer conjugate bound to the column was removed by changing to a new buffer (1M acetic acid, pH3) and reversing the direction of flow through the column. Fractions (3min) were collected and again Abs. 280nm determined. Those fractions containing conjugate were pooled and the pH of the solution brought up to 7.5 (NaOH, 5M).

The two preparations were concentrated by ultrafiltration (Millipore, CX-10), and characterise by gel permeation chromatography (2.2.3.1.3; Chapter 3, Fig 3.2).

All preparations (before and after purification and separation) if not used immediately were stored at -20°C. Freezing and thawing of all preparations was minimised to avoid denaturation.

2.2.4 Preparation of iron-loaded transferrin

The method used was originally described by van Renswoude (1982). Apotransferrin (6mg) was dissolved in buffer (0.1M Tris/HCl, pH8). Sodium nitrilotriacetate (20µl, 100mM, containing ferric chloride 12mM) was added and the reaction mixture incubated (30min, 37°C). The solution was then purified by elution through a column

(Sephadex G-25, height 15cm, internal diameter 1.7cm, flow rate 12mlh^{-1}) with buffer (0.2M Tris/HCl, pH7.4, containing 0.15MNaCl). Fractions (500µl) were collected and those eluting on the void volume pooled.

The criterion used to assess the iron-loading of transferrin was the ratio of Abs. 465nm/Abs.280nm. A ratio of >0.046 was judged to indicate iron saturation of transferrin as first described by Aasa (1963). Samples with a ratio <0.046 were discarded.

2.2.5 Total uptake and internalisation of ^{125}I-labelled ligands by human skin fibroblasts

In all experiments, ligand binding and internalisation were distinguished by trypsinisation (2.2.5.1). Low molecular weight degradation products were quantified by either (i) G-25 chromatography; HPMA copolymer only (2.2.3.1.1), or (ii) an increase in acid soluble radioactivity detected in the incubation medium above that of the corresponding control (2.2.5.2).

2.2.5.1 Determination of the efficiency of trypsinisation to remove cell surface-bound ^{125}I-labelled ligands

These experiments were carried out at 37^{o}C (when there is the potential problem of rapid internalisation of receptor-bound ligand) and at 4^{o}C (when there is the potential problem of slight conformation changes in the receptor within a more rigid plasma membrane).

Cell adherence (determined by microscopy) and cell viability (2.2.1.5) were not reduced by incubation at 4^{o}C.

The experimental protocols at 4^{o}C and 37^{o}C are sufficiently different to require separate description.

2.2.5.1.1 Trypsinisation of surface-bound ligand at 37°C.

Pre-washed (PBS, pH7.4, 10ml) confluent cells (6 flasks, 25cm^2 growth area) were allowed to come into contact with radiolabelled ligand (concentrations as detailed in Table 2.2; total volume 3ml in Hank's balanced salt solution (HBSS), approximately 10s). Duplicate samples of HBSS were assayed for radioactivity (LKB Compugamma, 30s). Cells were rapidly washed (x3, PBS pH 7.4, 10ml) and the flasks divided into two groups of three. In one group of flasks surface-bound ^{125}I-labelled ligand was removed by trypsinisation (0.25M trypsin in PBS pH7.4, 2.5ml, 1min, followed by incubation at 37°C, 15min in residual trypsin). Detached cells were washed (3x, PBS, pH7.4, 10ml) and recoverd by centrifugation (1000rpm, 10min). The cell pellet was digested in NaOH (1M, 1ml, overnight). With the second group of flasks the cells were simply digested in NaOH (1M, 2.5ml, overnight). Cell digests were assayed for both radioactivity (5min) and protein (Lowry).

2.2.5.1.2 Modification required for trypsinisation at 4°C.

(i) Pre-washed confluent cells, stock solutions containing radiolabelled ligand, and all other solutions used were pre-cooled to 4°C.

(ii) It was necessary to increase the time of incubation (4°C) in residual trypsin from 15min (37°C) to 30min.

The percentage of surface-bound ligand removed by trypsinisation was determined as follows

Flasks in group 1 have surface-bound ligand removed by trypsinsation

Flasks in group 2 have not undergone trypsinsation

Percentage trypsin insensitive ligand = $\frac{\text{ligand bound (pm mg}^{-1}\text{cell protein) Group 1}}{\text{ligand bound (pm mg}^{-1}\text{cell protein) Group 2}} \times 100$

= A%

Trypsin sensitive radioactivity expressed as a percentage of total binding

= (100-A)%

The efficiency of trypsinisation at removing the cell surface-bound ligands used in this study is given in Table 2.2.

2.2.5.2.1 Detection of low molecular weight degradation products as an increase in acid-soluble radioactivity.

For HPMA copolymer only refer to 2.2.3.1.1. For protein and protein-HPMA copolymer conjugates duplicate samples (1ml, medium 72h experiments; HBSS, 3h experiments, see Section 2.2.5.3) were taken at each time point. It was necessary at this stage to add protein (100µl serum) to samples contained in HBSS to facilitate precipitation of acid insoluble radioactivity. Trichloracetic acid (TCA, 20%, 500µl) was added to each sample with thorough mixing. Acid insoluble radioactivity and precipitated protein were removed by centrifugation (MSE 4L, $6.5 10^3$ rpm, 30min, 4^0C). The supernatant was assayed for radioactivity (LKB Compugamma, 30s). It was necessary to correct the acid soluble counts (2.2.5.2.2) because of the altered counting geometry of the sample due to (i) an alteration in the counting volume of the supernatant as compared to the original sample and (ii) trapping of acid soluble radioactivity in the protein pellet during centrifugation.

Any increase in acid-soluble radioactivity was related to that seen in a corresponding control.

Table 2.2

Percentage of cell surface-bound ligand sensitive to trypsination.

ligand	concentration (nM)	Trypsin sensitive ligand expressed as a percentage of total cell-associated radioactivity	
		4°C	37°C
Transferrin			
apo	10	72	82.7
diferric	10	99.7	59
Antibody			
IgG	5	ND	93.7
McAb B3/25	5	ND	88.2
Conjugates			
P-gly-gly-IgG	≈5*	ND	99.2
P-gly-gly-Transferrin	≈10*	ND	85.8

P = HPMA copolymer

* See Chapter 3

ND = Not determined

2.2.5.2.2 Determination of the correction factor for acid-soluble radioactivity.

Two sets of 10 tubes were prepared containing either HBSS or Ham's F10 complete medium (1ml). A spike of acid-soluble radioactivity ($1x10^3$cpm; [^{125}I]iodide or 1[^{125}I]Hodotyrosine) was added. Acid soluble radioactivity was then determined as 2.2.5.2.1

$$\text{Correction factor} = \frac{\text{Acid soluble radioactivity cpm in the original sample}}{\text{Acid soluble radioactivity recovered in the supernatant}}$$

A correction factor of 1.3 was used in this study (see Table 2.3).

2.2.5.3 Binding, internalisation and degradation of ^{125}I-labelled ligands by fibroblasts

Controls were identical to experimental flasks in all details but contained no cells. No increase in the degradation of ^{125}I-labelled ligand was found when controls contained medium or HBSS which had previously been in contact with cells. To minimise non-specific adsorption of ligand to the surface of vessels glass containers were used for preparation of stock solutions and for controls.

Pre-washed (PBS, pH7.4, 10mls) confluent cells were incubated (37^0C) in the presence of ^{125}I-labelled ligand (concentrations detailed in Table 2.4) in a total volume of 7ml (Ham's F10 complete medium, 72h experiments) or 3ml (HBSS, 3h experiments). At predetermined time points (for example 0, 30min, 1h, 3h) duplicate sampeles of medium/HBSS were taken from six experimental flasks and two controls. Samples were assayed for both total radioactivity and the presence of low molecular weight degradation products (2.2.5.2.1).

Table 2.3

Calculated correction factor for use in the determination of acid soluble radioactivity.

Substrate	calculated correction factor
[^{125}I] iodide	1.3 ± 0.01
[^{125}I] -iodotyrosine	1.3 ± 0.002

Table 2.4

Concentrations of radiolabelled ligand used for determination of uptake and in subcellular fractionation studies.

Radiolabelled ligand	concentration (M)
PVP	++1nM
HPMA copolymer	50nM
Transferrin	10nM
Antibody	5nM
Protein-HPMA copolymer conjugates	
P-IgG	+126pM
P-Tf	*53nM
P-McAb B3/25	*50nM

*such high concentrations needed to detect any cell-associated radioactivity

+The low molarity of P-IgG is attributable to its very high molecular weight

++Approximate molarity since the average molecular weight is variable between batches (here taken as 30K Daltons).

Fibroblasts were washed (3x, PBS, pH7.4, 10ml, ice-cold) to remove loosely bound ligand and all traces of medium (inactivates trypsin). The flasks were then placed in ice (to minimise internalisation of any surface bound ligand) and divided into two groups for either trypsinisation or direct digestion in NaOH (2.2.5.1.1). Cell digests were assayed for both radioactivity (5min, LKB Compugamma) and total protein (Lowry).

2.2.5.4 Calculations

The uptake of radiolabelled ligand was calculated in terms of µl worth of incubation medium whose contained substrate was endocytosed mg^{-1} cell protein as previously defined by Williams, et al. (1975) and presented in terms of both Total Uptake and Internalisation; and these terms are defined precisely in Chapter 4, Section 4.1.2.

$$\text{Total Uptake (Tu)} \left(\mu l\ mg^{-1}\ \text{cell protein}\right) = \frac{\text{Cell-associated radioactivity (cpm)}}{\text{Medium radioactivity } (cpm\ \mu l^{-1}) \times \text{Total cell protein } (mg)} + \Delta \text{ Degradation products } \left(mg^{-1}\ \text{cell protein}\right)$$

$$\text{Internalisation (In)} \left(\mu l\ mg^{-1}\ \text{cell protein}\right) = \frac{\text{Trypsin insensitive cell-associated radioactivity (cpm)}}{\text{Medium radioactivity } (cpm\ \mu l^{-1}) \times \text{Total cell protein } (mg)} + \Delta \text{ Degradation products } \left(mg^{-1}\ \text{cell protein}\right)$$

In Appendix 5 a detailed example is given together with an explanation of the correction needed to determine TU and In of conjugate 5.

2.2.6 Subcellular fractionation using Percoll density gradient.

2.2.6.1 Standardisation of conditions used.

2.2.6.1.1 Gradient starting density and conditions of centrifugation.

The shape of a density gradient is a product of total force (g) x time, and is affected by rotor geometry, size of tubes, and the density of Percoll used.

First, gradients produced with a Beckman type-65 fixed-angle (23.5^0, r_{av} 5.7cm) head and using thick walled polycarbonate centrifuge tubes with caps, containing 8ml of Percoll gradient were characterised. The following solutions were prepared:-

(i) Standard Iso-osmotic Percoll (SIP) was prepared by mixing stock Percoll (9ml, Pharmacia, $1.128gmml^{-1}$) with sucrose/EDTA (2.5M sucrose, 1mM EDTA, 1ml). Further dilutions of SIP were made using sucrose/EDTA (0.25M sucrose, 1mM EDTA) to produce gradients of the appropriate starting density (expressed in terms of % SIP).

(ii) Density-marker beads (Pharmacia, $1.037-1.138gml^{-1}$) were pre-swollen in water (1ml) and stored (4^0C).

The rotor was pre-cooled (4^0C). A series of gradients (20-90% SIP, total volume 8ml) were loaded with density marker beads (10µl, each density). After capping the tubes tightly the gradients were subjected to various combinations of centrifugation conditions (20K, 29K, 39K rpm, for 15, 30, 40min). A 60% SIP gradient (40min, 20K rpm) was considered to give optimal, even separation of densities associated with all subcellular organelles; the 30% SIP gradient (40min, 20K rpm) optimal separation of densities associated with plasma membrane and lysosomal compartments. For all experiments

described in Chapter 5 a 30% SIP gradient was used.

2.2.6.1.2 Homogenisation of fibroblasts.

Fibroblasts grown to confluence ($75cm^2$ growth area) were washed (PBS, pH7.4, 30ml, x3) and harvested by incubation in PBS/EDTA (1mM EDTA, 37°C, 10min). Detached cells were recovered by centrifugation (1000rpm, 10mins) and resuspended in sucrose/EDTA (0.25M sucrose, 1mM EDTA). The cell suspension was subjected to varying degrees of homogenisation (10-100 strokes of the big head of a Dounce cell-homogeniser) to produce a duplicate series of cell-homogenates. The first series only were spun to remove intact cells. Both sets of homogenates were mixed with SIP Percoll to produce a 30% SIP gradient (5.6ml homogenate, 2.4ml SIP Percoll) and centrifuged (20K rpm, 40min, 4°C). The gradient was sampled from the top (250µl samples) and the suitability of homogenisation conditions assessed by determination of the lysosomal enzyme hexosaminidase (see below 2.2.1.6). The lysosomes are of prime importance in this study, too many burst lysosomes would make results difficult to interpret. A compromise between cell breakage, to release organelles, and maintenance of lysosomal integrity was necessary. Optimal conditions were found to require 20 strokes of the Dounce homogeniser, followed by a short spin to remove whole cells (1000rpm 10mins).

2.2.6.1.3 Enzyme assays used to determine the buoyant densities of subcellular organelles.

2.2.6.1.3.1 Plasma membrane marker: 5'-nucleotidase:.

The method of Avruch & Wallach (1971) was used.

A substrate solution containing [^{3}H]-5'-AMP ($25ng\ ml^{-1}$) 5'-AMP(0.15M), para-nitrophenol (6mM) in buffer (Tris/HCl, pH 9, 54mM, containing $MgCl_2$, 13mM) was prepared immediately before use.

Substrate solution (500µl) was mixed thoroughly with sub-cellular fraction (100µl) and incubated (37°C, 30min). The

reaction was stopped by placing the tubes on ice and adding $ZnSO_4$ (0.25M, 200µl). The tubes were vortexed and $Ba(OH)_2$ added (0.25M, 200µl). After thorough vortexing the precipitate was removed by centrifugation (MSE, 4L, 6500rpm, 20min). Supernatant (500µl) was added to scintillation fluid (Liquicint, 4.2ml) and assayed for radioactivity (LKB Rack β-counter, 10min). The counting standard (representing 100% hydrolysis) was composed of 1:1 substrate:H_2O. Quenching was checked by addition of a spike [^3H] (1000cpm) to each and recounting.

2.2.6.1.3.2 Nuclear Marker: DNA

The method of Erwin, et al. (1981) was used.

Subcellular fraction (10µl) was precipitated by incubation (4°C, >4h) with TCA (10%, 15µl). The solution was centrifuged (MSE 4L, 6.5K rpm, 20min, 4°C) and the precipitate resuspended in TCA (5%, 500µl) and hydrolysed by incubation at 90°C (30min). The resulting solution was cooled (4°C) and centrifuged (to remove solubilised aldehydes resulting from DNA hydrolysis; 6.5k rpm, 20min, 4°C). The supernatant was decanted and DABA (100µl, 200mgml^{-1} aqueous solution, decolorised by addition of activated charcoal). The solution was incubated (1h, 60°C) and the reaction stopped by addition of HCl (2ml, 1N). Fluorescence was read (Extinction (Ex) 420nm, Emission (Em) 520nm).

To ensure that Percoll was not a fluorophore at the wavelength used in this assay a control gradient (identical to the one used for separation of organelles, but containing no homogenate) was fractionated and the fluorescence of fractions determined (Ex 420nm, Em 520nm). Percoll was found not to act as a fluorophore under these conditions. Similar control studies were performed for each of the following fluorescence based assays:-

2.2.6.1.3.3 Protein Assay: Fluorescamine

The method of Weigele, et al. (1972) was used.

Subcellular fraction (25µl) was mixed with buffer (borate, 0.2M, pH9.25, 2m). Fluorescamine (450µl, 30mg/100ml acetone) was added and the solution mixed. The fluorescence was read after more than 1min (Ex 390nm, Em 475nm)

2.2.6.1.3.4 Lysosomal Marker: hexosaminidase

The method of Griffiths, et al. (1978) was used.

A substrate solution containing 4-methyl-umbelliferyl-2-acetamido-2-deoxy-β-D-glucopyranoside (2.5mM) in citrate buffer (0.2M, pH4.3) containing Triton X100 (0.1%) was prepared immediately before use.

Substrate solution (50µl) was added to subcellular fraction (25µl), and the resulting solution incubated ($37^{o}C$, 10min). The reaction was stopped by the addition of Na_2CO_3 (1mM, 1.95ml, pH10). Fluorescence was read (Ex 365nm, Em 450nm).

2.2.6.1.3.5 Mitochondrial Marker: monoamine oxidase

The method of Sherwin (1980) was used.

A substrate solution containing homovanillic acid ($2.5mgml^{-1}$, 50µl), peroxidase ($0.75mgml^{-1}$, 50µl) tryptamine (1.3mM, 300µl), phosphate buffer (0.26M, pH7.4, 1ml containing Triton x100, 0.1%) was prepared immediately before use.

Subcellular fraction (100µl) and substrate (1.4ml) were incubated ($37^{o}C$, 30min) fluorescence was read (Ex 339nm, Em 425nm).

2.2.6.1.3.6 Cytosolic Marker: LDH

The method of Lowry, et al. (1957) was used.

A substrate solution containing pyruvate ($1.1mgml^{-1}$) $NADH_2$ ($7.1mgml^{-1}$) in phosphate buffer (0.1M, pH7.5) was prepared immediately before use.

Substrate solution (20µl) was added to subcellular fraction

(10µl) and incubated (37°C, 30min). HCl (0.5M, 20µl) was added to the reaction mixture and left >30s. Na(OH) (7.5M, 200µl) was added and the solution incubated (37°C, 30min). The reaction was stopped by addition of water (2ml) and fluorescence read (Ex 364nm Em 465nm).

2.2.6.2 Subcellular distribution of [^{125}I]-labelled ligands.

Pre-washed confluent fibroblasts (75cm^2 growth area) were incubated (37°C) in the presence of [^{125}I]-labelled ligand (for concentrations see Table 2.4) in HBSS (10ml) for predetermined times (2h, 5h, sometimes 24h). At each time point cells were washed (3xPBS pH7.4, 30mls) to remove any loosely bound ligand. The fibroblasts were then harvested and fractionated as detailed above (2.2.6.1.2). Each and every fraction was assayed for both hexosaminidase (25µl) and radioactivity (225µl).

The shape of the gradient was determined for every homogenisation by inclusion of a control density gradient, calibrated with density marker beads, in the position directly opposite a density gradient containing homogenate in the rotor head.

2.2.6.3 Calculations

For all subcellular fractionation experiments the radioactivity recovered in each fraction was expressed as a percentage of the total radioactivity recovered from the gradient.

Total radioactivity (cpm) on the gradient was determined by addition of the radioactivity (cpm) in each fraction as follows:-

$$\text{Total radioactivity (cpm)} = \sum_{1}^{32} \text{cpm}$$

The percentage radioactivity (cpm) in each fraction was then expressed as a percentage of the total radioactivity:

$$\text{Percent radioactivity in fraction (n)} = \frac{\text{cpm in tube n}}{\sum_{1}^{32}\text{cpm}} \times 100$$

2.2.7 Determination of the cell surface density of and the affinity of ^{125}I-labelled ligand for the transferrin receptor.

These experiments were carried out at 4^{o}C and required that all materials (cells, solutions) were pre-cooled.

Cells (see Table 6.4) were grown to confluence or an equivalent density. After washing (PBS, pH 7.4, 10ml x 3, ice-cold) cells were placed on ice. A series of flasks/tubes were prepared containing a spike of [^{125}I]-labelled ligand (for concentrations see Table 2.5) and increasing concentrations of unlabelled ligand (approximately 0-400pm) in a total volume of 3ml (HBSS). Cells were incubated (4^{o}C) for 45min in the presence of ligand (after which time binding was shown to have plateaued). Duplicate samples of HBSS were taken and assayed for radioactivity (30s, LKB Compugamma). Cells were washed (PBS, pH7.4, 10ml, ice-cold x3) to remove loosely bound ligand and then digested by incubation (37^{o}C, overnight) in NaOH (0.5M, 2.5mls). The cell digest was assayed for both radioactivity (5min) and protein (Lowry).

2.2.7.1 Calculations

The data were processed in several ways:-

1. To show a plateau of specific binding.

Total binding (pm mg^{-1}cell protein) was plotted against total concentration of ligand present (nm ml^{-1}).

2. To show the percentage of non-specific binding.

The binding of [^{125}I]-labelled ligand was plotted against increasing concentrations of unlabelled ligand.

Table 2.5

Typical concentrations of radiolabelled ligand used for determination of the density of, and affinity of ligand for, the transferrin receptor.

Ligand	concentration (M)	
	radiolabelled ligand	unlabelled ligand
Transferrin (aps and diferric)	10nM	0-400nM
McAb B3/25	5nM	0-200nM

3. Scatchard analysis to allow determination of the density of the transferrin receptor, and the affinity of ligand for the receptor. Data was plotted according to the linear expression of the Scatchard equation (Scatchard, 1948):

$$\frac{B}{F} = \frac{B}{K_D} + \frac{Bmax}{K_D}$$

Where

B = concentration of ligand bound to a cell surface receptor/antigen

F = concentration of free ligand present in the incubation medium

K_D = dissociation constant of binding

B_{max} = intercept on x axis and in these data includes high and low affinity binding.

Experimentally determined values were plotted individually (since there were two variables, bound and free). Triplicate results were denoted by joining individual points with a tie-line.

2.2.8 Determination of the body distribution of ^{125}I-labelled ligands after administration (either intraperitoneal or intravenous) to DBA_2 male mice.

Mice (DBA_2, male, up to 20-weeks of age; Chapters 7 and 8) were always injected under mild conditions of anaesthetic (judged by the ability of the mouse to move freely immediately after injection). Radiolabelled ligand (usually 1-2x10^6cpm in 0.1ml total volume, approximately 10µg protein) was administered via either the peritoneal cavity (ip) or the tail vein (iv). After injection mice were kept in metabolic cages to facilitate collection of urine and

faeces. At predetermined times (2h, 5h, sometimes 24h) the mice were weighed and anaesthetised (from this point it was ensured that mice were always under anaesthetic). Following ip injection of radiolabelled ligand the peritoneal cavity was washed (to recover any residual radioactivity) by injection of saline (1%, 37°C, 3ml). The abdomen was massaged gently, and the washings removed via a small incision. Following all routes of administration the bladder and its contents were removed from the animal before death (to minimise loss of urine-associated radioactivity). Animals were then killed by opening the thoracic cavity and puncturing the heart. A sample of blood (50µl) was taken from the ventricle of the heart and immediately added to NaOH (1M, 1ml; prevents coagulation of blood and consequent loss of blood-associated radioactivity within the micropipette). Organs/tissue (Table 2.6) were removed and weighed. A sample of skin (known weight, uncontaminated with blood), stomach and intestine were digested in NaOH (1M, 37°C, overnight) and the femur in HCl (6M, 37°C, overnight). All other organs, plus urine and faeces, were frozen overnight (easier to homogenise organs after freezing) and subsequently homogenised in as little water as possible (usually 3ml); the faeces were blended. The total volume of each homogenate, the faeces total urine (and peritoneal wash when taken) were measured and duplicate samples (1ml) assayed for radioactivity (LKB Compugamma, 5min). Blood counts were corrected to give total blood radioactivity using the relationship that a mouse contains 5.77mls of blood per 100g body weight (Dreyer and Ray, 1911). Femur counts were corrected to give total bone marrow radioactivity using the a correction factor of 15.87 (Benner, et al., 1981).

Table 2.6

Organs/tissues and body fluids routinely sampled.

Heart

Liver

Lung

Kidney

Spleen

Thymus

Submaxillary gland plus surface lymph nodes

Skin

Bone marrow

Stomach

Intestine

Urine

Faeces

Peritoneal wash

Blood

2.2.8.1 Calculations

Results were expressed in terms of a percentage of the administered dose, and sometimes as a percentage of administered does recovered per gram of organ.

$$\% \text{ (Administered Dose)} = \frac{\text{Radioactivity (cpm) present in the organ}}{\text{Radioactivity (cpm) administered}} \times 100$$

In Appendix 6 a detailed example is given together with an explanation of the correction needed to determine the body distribution of conjugate 5.

2.2.9 Determination of the immunogenicity of protein-HPMA copolymer conjugates

This work was carried out in the laboratory of Dr. B. Rihova, Institute of Microbiology, Prague (March 7-28th 1987).

2.2.9.1 Protocol of immunisation

Ligand was administered using either a combination of complete Freund's adjuvant (CFA) for the first injection, followed by two further injections using alum precipitate or by three injections in solution(SOL). Mice (AJ and B10) were injected with ligand (100µg protein per immunisation per mouse) (Table 2.7) according to the protocol shown in Fig. 2.1. On the seventh day after the final injection mice were exsanguinated. Blood of six mice, which had been immunised identically, was pooled and allowed to stand overnight ($4^{o}C$). Serum was separated from the resulting blood clot and spun (2000rpm, 10min) to remove any contaminating erythrocytes and stored at $-20^{o}C$.

Control sera (used to determine if there were any naturally occurring antibodies to the ligands used in this study) was prepared from unimmunised mice of the same strain.

2.2.9.2 Serial dilution of sera.

Serial dilution of sera was carried out immediately before use.

Sera were serially diluted using PBS containing albumin or gelatin, (1%). One volume of serum was mixed thoroughly with one volume of PBS/albumin (usually 150[1+150µl). Of this 1:1 dilution one volume was taken and mixed thoroughly with one volume of PBS/albumin in the next well, and so on. The resulting dilutions of sera are given in Chapter 9 (Table 9.2).

2.2.9.3 Estimation of antibody titre; ELISA assay.

Ligand (50µl, 500mgml^{-1} or 2mgml^{-1}) was bound to microtitre plate wells (96 well ELISA plate) overnight (4^{o}C). Unbound ligand was removed by suction and the plates thoroughly washed with PBS (200µl pH7.2 x 3). PBS (50µl containing albumin (1%) and gelatin (0.02%) or gelatin (1%; when the ligand itself contains albumin) was added to each well and the plates left to stand at room temperature (ensures that the plates are evenly coated with some form of protein). This solution was removed after 1h and again the plates were thoroughly washed with (i) PBS (200µl) (ii) PBS containing Tween-20 (0.2%; 200µl) (iii) PBS (200µl). Serially diluted serum (2.2.9.2; 50µl) was added to wells coated with corresponding ligand, starting with the highest dilution (lowest concentration), to produce a series of wells containing the same antigen (ligand) but different concentrations of antibody. The plates were now incubated (37^{o}C, 90min) to allow antibody to interact with antigen. Sera was then removed and the plates thoroughly washed as above (PBS, PBS containing 0.2% Tween-20 x 3, PBS). Anti-(murine)IgG conjugated to horseradish peroxidase (50µl, diluted 1:500 in PBS/albumin) was now added to each well and the plates incubated again (37^{o}C, 1h). Unreacted anti-(murine)IgG-horseradish peroxidase conjugate was removed from the plates, which were again thoroughly washed (PBS,

Fig. 2.1 Immunisation Protocol

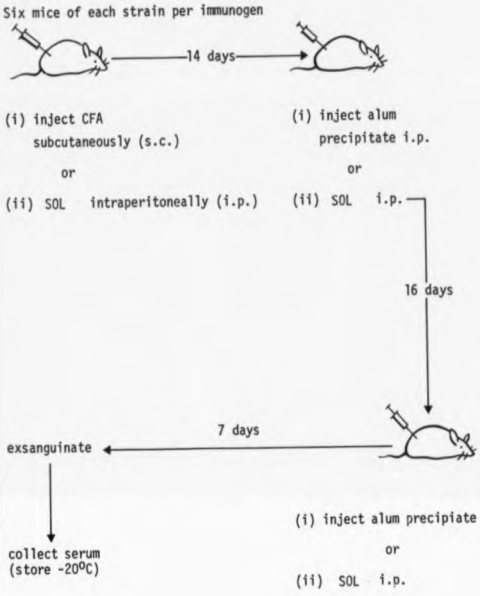

Table 2.7

Summary of immunisation protocol

Ligand antigen	Dose per immunisation	Immunisation	Strain of Mouse
Human Serum Albumin	100μg 100μg	CFA SOL	AJ;B10
Human Gamma Globulin (IgG)	100μg 100μg	CFA SOL	AJ; B10
Human Transferrin (Tf)	100μg 100μg	SOL SOL	AJ; B10
P-gly-gly-Tf	100μg 100μg	CFA SOL	AJ; B10
P-gly-gly-IgG	100μg 100μg	CFA SOL	AJ; B10

P HPMA copolymer

CFA complete Freund's adjuvant

SOL solution

PBS/Tween x 3, PBS). Orthophenlenediamine (substrate for horseradish peroxidase; 50µl 0.5mg ml^{-1} in phosphate buffer 0.1M, pH6 containing H_2O_2, 30%) was added to each well. The reaction was stopped after 1-5min (depending on the intensity of colour) by addition of H_2SO_4 (50µl, 2M). The absorbance 492nm was read (ELISA Titertek Multiscan). The highest antibody dilution (HAD) at which a positive antibody-antigen reaction could be detected waas noted.

2.2.9.4 Calculations

Each graph was drawn to show the well number of the HAD at which a positive antibody-antigen reaction could be detected on the ordinate, against strain of mouse, antigen concentration used to coat the ELISA place well and form of immunisation (CFA or SOL) on the abscissa.

CHAPTER 3

Characterisation of ^{125}I-labelled HPMA copolymer conjugates using several chromatographic methods

3.1 INTRODUCTION

Both HPMA copolymer and HPMA copolymer conjugates used in this study were synthesized by Kopecek, et al. (reviewed Kopecek, 1984) at the Institute of Macromolecular Chemistry, Prague. Optimal conditions for the synthesis of HPMA copolymer-protein, in particular HPMA copolymer-antibody, conjugates are not yet fully understood. Using an aminolysis reaction to attach protein to HPMA copolymers (see Chapter 1, 1.2) there is an inherent problem of copolymer characterisation. Reaction involves conjugation of two multifunctional compounds, with potential for multiple substitutions (resulting in the formation of high molecular weight complexes), and also there is no control over the orientation of the protein within the conjugate. The criteria used for binding protein to HPMA copolymer have been defined by Kopecek (1984); (i) the conjugate should contain a bond between the protein and HPMA copolymer which is stable in vivo and in vitro (ii) the protein should retain its cell-specific binding affinity (iii) high molecular weight complexes should be minimised. Using these criteria HPMA copolymer conjugates were supplied (detailed in Table 3.1, and Appendices 1 and 2) as crude reaction mixtures, which contained both free polymer and conjugate, but no detectable free protein (typical elution profile provided Fig. 3.1). No evaluation of molecular weight, stoichiometry, or orientation of protein had been made.

In order to make any meaningful biological assessments of these conjugates it was necessary that as detailed a characterisation as possible should be attempted. It was not possible to obtain characterisation with the accuracy required, but without some form of characterisation the biological evaluation of such conjugates would be totally worthless. With this qualification in mind, an attempt was made to determine purity, molecular weight average ($\bar{M}w$), and

Table 3.1

Coding of the HPMA copolymer and the protein-HPMA copolymer conjugates used in this study*.

Code number	Structure
1	P†-gly-gly-aminopropanol-$TyrNH_2$
2	P-gly-gly-transferrin
3	P-gly-gly-IgG
4	P-gly-gly-anti-Thy-1.2
5	P-gly-gly-B3/25 McAb

*Also refer to Appendix 1

†P; HPMA copolymer backbone

Fig. 3.1 Typical elution profiles of HPMA copolymer precursor, unconjugated antibody, and HPMA copolymer-antibody conjugate, using Sephadex 4B/6B.

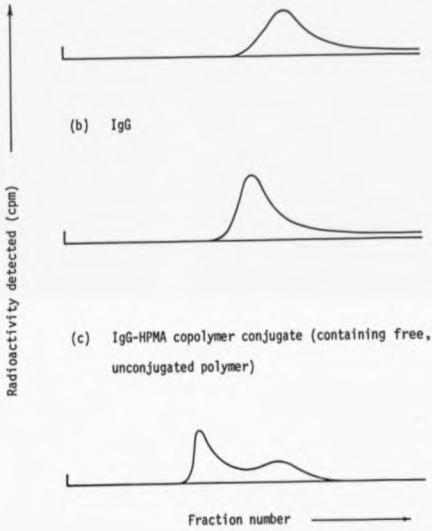

stoichiometry of the HPMA copolymer-protein conjugates. A number of gel permeation chromatography techniques were employed and their interrelationships are shown in Fig. 3.2. The orientation of antibody in immunoconjugate 4 was investigated using protein-A affinity chromatography (Fig. 3.3). To facilitate efficient detection of these substrates they were usually radiolabelled ([^{125}I]iodide, Iodogen method of radiolabelling, Fig. 3.4).

A range of analytical columns were used (Fig. 3.2). Sephacryl S-200 superfine (Mol. wt. range suitable for protein separation 5K-250K Daltons) was used to separate polymer-protein conjugates from free unconjugated HPMA copolymer precursor ($\bar{M}w$ approximately 7K Daltons). Sephacryl S-300 superfine (Mol. wt. range suitable for protein separation 10K-1.5M Daltons and sepharose 4B/6B (Mol. wt. range suitable for protein separation 20K-10M Daltons) were used to determine the $\bar{M}w$ of purified conjugates. These conjugates were composed of both protein and soluble synthetic polymer, which makes molecular weight evaluation very difficult. Gel permeation columns can be calibrated using either polymers or proteins (Fig. 3.5a,b). However the calibration relationship between molecular weight and elution volume obtained for proteins and polymers is not usually superimposable. The elution profile derived from a protein-polymer conjugate could therefore theoretically correspond to either the polymer-based, or protein-based, calibration curves, or in fact neither of these, but at some position dependent upon an indefinable relationship between the protein and polymer. For experimental purposes columns were calibrated with a range of HPMA copolymers of defined $\bar{M}w$ and low polydispersity ($\bar{M}w/\bar{M}n$=1.2) and a number of protein molecules (Fig. 3.5a,b).

Fig. 3.2

Flow chart to show how protein-HPMA copolymer conjugates were purified by gel permeation chromatography and their molecular weights subsequently determined.

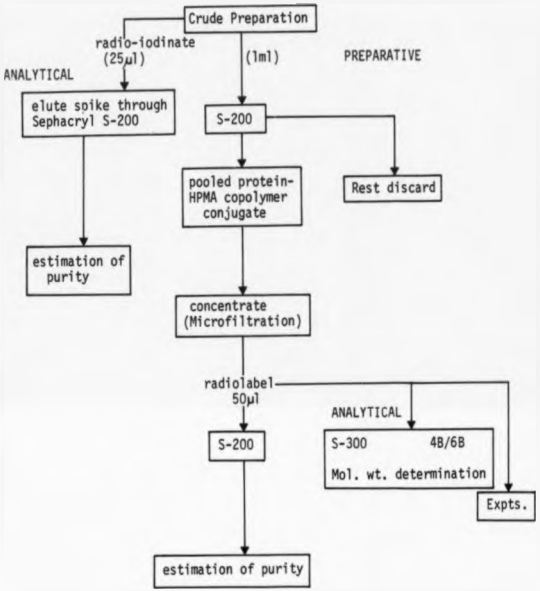

Fig. 3.3

Flow chart to show the sub-division of anti-Thy-1.2-HPMA copolymer using Protein-A affinity chromatography.

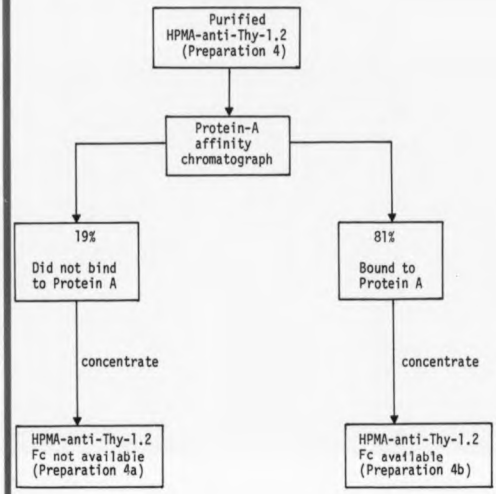

Fig. 3.4

Structure of the solid-phase catalyst Iodogen

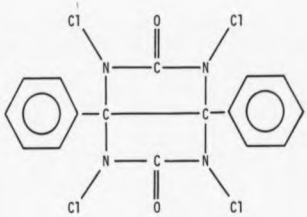

M.W. 432.09

1,3,4,6-Tetrachloro-3α,6α-diphenylglycouril

Fig. 3.5a Calibration of a S-300 superfine gel permeation column, using both protein and HPMA copolymers of defined $\bar{M}w$ and low polydispersity ($\bar{M}w/\bar{M}n$ = 1.2).

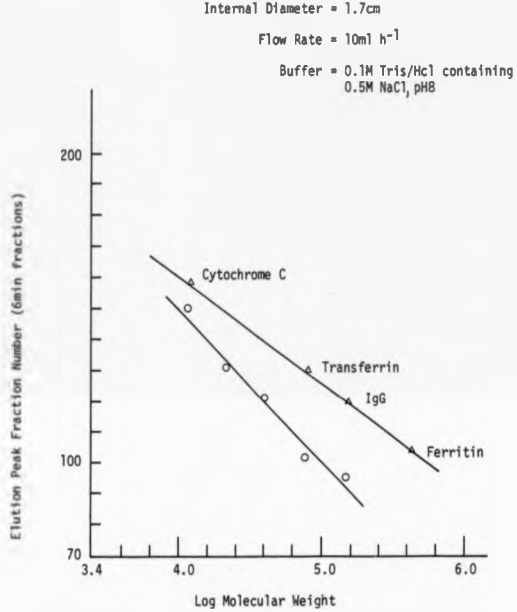

○ HPMA of defined $\bar{M}w$; $\bar{M}w/\bar{M}n$ = 1.2

△ Protein

Fig. 3.5b Calibration of a 4B/6B Sepharose gel permeation column, using both protein and HPMA copolymers of defined $\bar{M}w$ and low polydispersity ($\bar{M}w/\bar{M}n$ = 1.2)

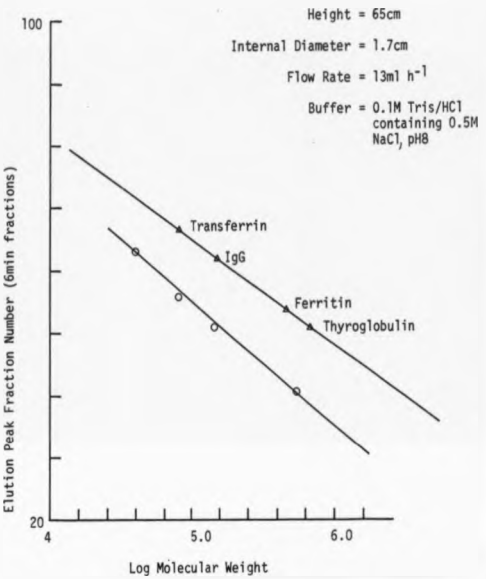

○ HPMA of defined $\bar{M}w$; $\bar{M}w/\bar{M}n$ = 1.2

▲ Protein

3.2 RESULTS AND DISCUSSION

3.2.1 Radioiodination

Of the wide range of oxidizing agents available for radioiodination of proteins (Salacinski, et al., 1981; reviewed by Mather, 1986) the Iodogen method, first described by Fraker & Speck (1978) was chosen to radiolabel the macromolecules investigated in this study for a number of reasons:-

(i) the solid-phase catalyst was considered to subject substrates, in particular monoclonal antibodies, to the mildest denaturing conditions. Gel permeation chromatography of radioiodinated HPMA copolymer conjugates, HPMA and protein revealed no formation of breakdown products, and subsequent binding experiments showed little, if any, loss of affinity (see Chapters 4,5,6). These data, suggesting minimal or no degradation by Iodogen are in agreement with the findings of Fraker & Speck (1978), Salacinski, et al. (1981) and Mather (1986).

(ii) High radiolabelling efficiencies have been reported in the literature using Iodogen (Mather, 1986), and labelling efficiencies of 60-80% were routinely achieved in this study (Table 3.2).

(iii) The solid-phase catalyst is easily separated from the reaction mixture, and therefore ensures that the radioiodinated preparations are catalyst free, and do not contain unwanted chemicals (such as sodium metabisulphite used in the Chloramine-T method of radio-iodination).

Although Salacinski, et al. (1981) had reported that proteins radiolabelled by Iodogen are stable for up to three months when stored at either $4^{o}C$ or $-20^{o}C$, in this study it was shown that [^{125}I]iodide was released from both proteins and HPMA copolymer-protein conjugates (stored at $-20^{o}C$) relatively rapidly (7% over 4 weeks) necessitating the re-dialysis of all preparations

Table 3.2

A summary of typical iodination data.

Molecule	Mol. wt.	binding efficiency of [125I]iodide %	Specific Activity μCi/μg	Approx. number of [125I]iodide molecules per molecule of substrate
Diferric transferrin	80K	80	3.1	1:9
Antibodies				
B3/25	150K	80	3.6	1:4
anti-Thy-1.2	150K	5	0.04	1:360
HPMA copolymers				
6 protein-HPMA copolymer conjugates				
1	15K	60	32	1:3
2	~219K	75	2.97	1:3
3	>2M	70	0.05	1:64
4	~331K	80	13.2	2:1
5	~457K	72	0.24	1:24

* Low specific activity of ^{125}I-labelled anti-Thy-1.2 was consistently obtained.

immediately prior to their use in experiments.

In agreement with Mather (1986) it was found that the antibodies used in this study labelled with different efficiencies. A summary of typical iodination data is given in Table 3.2. It can be seen that substitution ratios of [^{125}I]iodide varied between 1:360 and 2:1 (^{125}I:HPMA copolymer conjugate). To minimise damage to radioiodinated substrate substitution ratios were kept as low as possible. Conjugate 4 (which was to be used only for *in vivo* experiments; Chapter 8) was radiolabelled more heavily (2:1 [^{125}I]iodide:HPMA copolymer conjugate) to allow subsequent detection of radioactivity in the organs of sacrificed mice. It was considered desirable to administer conjugate 4 to mice at a protein equivalent dose in the range 100ng-10μg as discussed previously by Rihova & Kopecek (1985) (also see Chapter 9). Consequently for all radiolabelled ligands to be used *in vivo* the degree of [^{125}I]iodide substitution was increased.

Unconjugated polymer radioiodinated in a stable manner (Fig. 3.6) necessitating its removal from all preparations supplied.

3.2.2 Purification

S-200 gel permeation chromatography was used as a final preparative step to remove the excess unconjugated polymer from the reaction mixtures as provided. A S-200 column was chosen because its separation range meant that polymer-conjugate passed quickly through the column, eluting on, or close to, the void volume (Vo), therefore ensuring minimal dilution of the purified copolymer-conjugate. The lower molecular weight, unconjugated copolymers eluted later. Fig. 3.7a,b shows a typical elution profile from S-200. Fractions corresponding to copolymer-protein conjugates (fractions 50 to 65) were selected according to their absorbance at 280nm and their molecular weights calculated (see methods; Fig. 3.2).

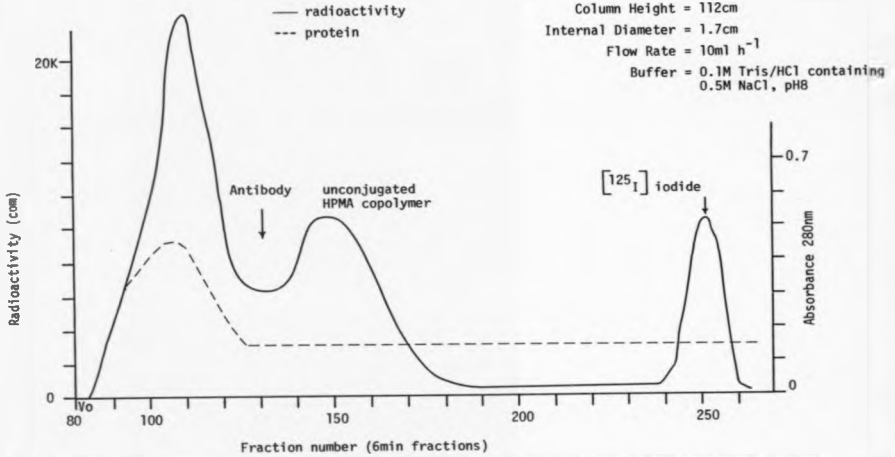

Fig. 3.6 S-300 profile of a preparation of HPMA copolymer-anti-Thy-1.2 conjugate (as supplied by Kopecek et al.).

Fig. 3.7 Typical S-200 profile of HPMA copolymer-protein conjugates
(a) containing free, unconjugated HPMA copolymer
(b) containing only conjugate.

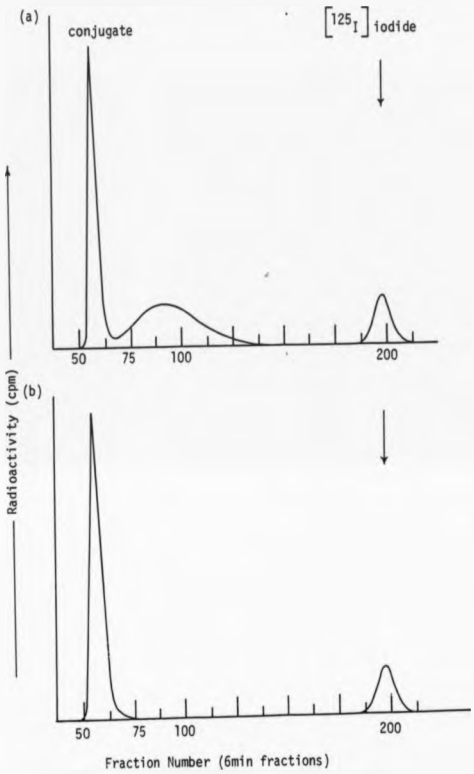

Purification of conjugate 5 was particularly difficult due to the low starting concentration of monoclonal antibody in the reaction mixture with HPMA copolymer precursor (4.4mg ml^{-1} as compared with 25mg of transferrin or IgG). After conjugation the concentration of monoclonal antibody was further reduced to 2.7mg ml^{-1}. S-200 chromatography (Fig. 3.8a) showed the presence of a high percentage of radiolabelled unconjugated polymer (60%). An attempt at purification, using S-200 as above, resulted in degradation of the conjugate, as can be seen by comparing the 4B/6B elution profiles of conjugate 5 before and after purification (Fig. 3.8b,c). In Fig. 3.8b the peaks corresponding to conjugate 5, free unconjugated polymer and the [^{125}I]iodide internal marker are clearly visible. After purification the peak corresponding to conjugate has disappeared and protein is detectable in that region of the elution profile corresponding to low molecular weight proteins. There was also some evidence of aggregation of conjugate to produce excessively high molecular weight protein-HPMA copolymer conjugate eluting on the Vo. For these reasons it was only possible to use the crude reaction mixture of ^{125}I-labelled copolymer 5 in biological experiments, subsequently correcting for the presence of unconjugated copolymer. The uptake (Chapter 4), subcellular localisation (Chapter 5), and body distribution (Chapter 7) of unconjugated copolymer were always determined in control experiments, and therefore in each type of experiment the component attributable to radiolabelled, unconjugated polymer could be accounted for and subtracted (for calculations see the relevant chapters).

3.2.3 Molecular Weight Determination

Sephacryl S-300 and Sepharose 4B/6B were chosen to determine the molecular weights of the protein-copolymer conjugates because of their range of separation of proteins (S-300, 10K -1.5M Daltons;

Fig. 3.8 Gel permeation profiles of the preparation of HPMA copolymer-McAb B3/25 conjugate (a) S-200 before purification (b) S-300 before purification (c) S-300 after purification (buffer used and column characteristics detailed earlier).

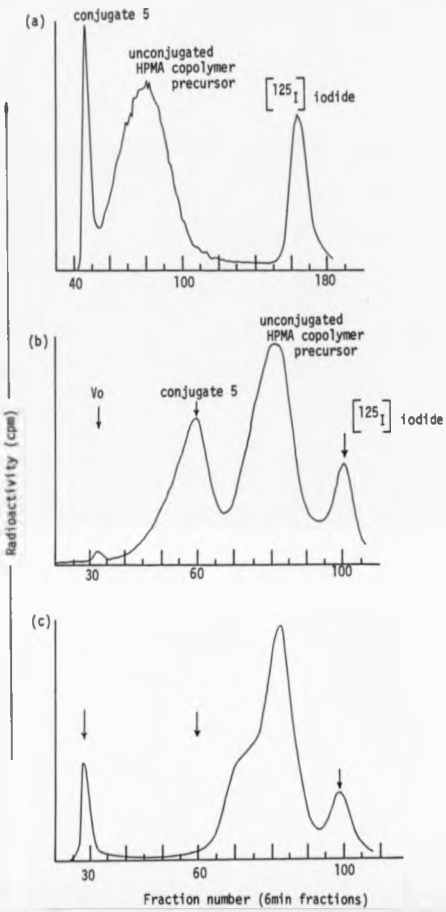

4B/6B, 20K-10M Daltons). Any conjugate eluting on the Vo of the 4B/6B column would probably have such a high molecular weight that use as a potential drug-carrier would be limited. Duncan, et al. (1981), using PVP, and Cartlidge, et al. (1986) using HPMA copolymers of increasing molecular weight have shown, in rat visceral yolk sacs cultured in vitro, there is a decrease in the rate of the pinocytic uptake of PVP and HPMA copolymers with increasing size (>110K Daltons).

Preparation of HPMA copolymeric precursors is by radical precipitation polymerisation (Kopecek, 1984). The products of such a reaction contain molecules of many different chain lengths and upon elution through a gel permeation column they tend to give asymetrical profiles (Fig. 3.9). Determination of $\bar{M}w$ using a calibration graph is not possible, but instead a statistical approach must be used. Such an approach can be represented graphically by a plot of the weight fraction w(M) of HPMA copolymer having a given molecular weight M against the molecular weight (Fig. 3.9). For molecular weight determinations carried out in this Chapter it was assumed that within any one preparation all the molecules were radioiodinated to the same degree of substitution of [^{125} I]iodide. It was therefore possible to plot the radioactivity (cpm) detected in each fraction against fraction number. Using the appropriate calibration graphs it was then possible to obtain a value for $\bar{M}w$ based on the following calculations:-

Let W_i = the weight of that portion of the conjugate having molecular weight M_i

and n_i = the number of moles of conjugate with molecular weight Mi

Fig. 3.9 Typical elution profiles obtained for polymers eluting through a gel permeation column.

(a) Asymmetrical elution profile

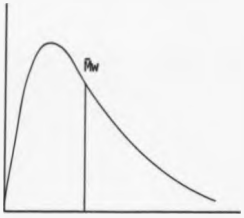

$\bar{M}_w \neq$ elution peak volume

need to use a statistical determination of $\bar{M}_w$

(b) Symmetrical elution profile

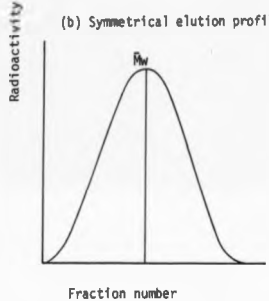

$\bar{M}_w \equiv$ elution peak volume

can determine $\bar{M}_w$ by reference to a calibration graph.

Definition of average molecular weight, $\bar{M}_w$ (Batzer and Lohse, 1979).

Summation over the participating individual molecular weights of a polymer substrate with respect to the weight to give $\bar{M}_w$ of the participating macromolecules under consideration.

Then $w_i = n_i M_i$

$\bar{M}_n$ = the number average molecular weight

$$= \frac{\sum w_i}{\sum n_i} = \frac{\sum n_i M_i}{\sum n_i}$$

$\bar{M}w$ = the weight average molecular weight

$$= \frac{\sum n_i M_i^2}{\sum n_i M_i}$$

For all such calculations performed in this chapter the computer programme found in Appendix 4 was used.

Upon conjugation of the relatively low molecular weight copolymeric precursor (17K Daltons; Table 3.1) to relatively high molecular weight protein (transferrin, 80K Daltons; antibody 150K Daltons) the asymmetry of the elution profiles tended to disappear giving a symetrical profile from both S-300 and 4B/6B (Fig. 3.10a-g). Symmetrical profiles were obtained for conjugates 2, 4, 4a and 4b, and allowed direct determination of their $\bar{M}w$ from calibration curves (protein and HPMA: Table 3.3). The validity of this approach is seen by the fact that $\bar{M}w$ of conjugate 2 shows little difference when calculated by either this method, or statistically (see Appendices 3 and 4; Table 3.4). A summary of $\bar{M}w$ estimated for all HPMA copolymers and conjugates used is given in Table 3.4. The $\bar{M}w$ determined by reference to the HPMA copolymer calibration line indicated that the protein-HPMA copolymer conjugates were not eluting from the gel permeation columns in a manner characteristic of polymer since the

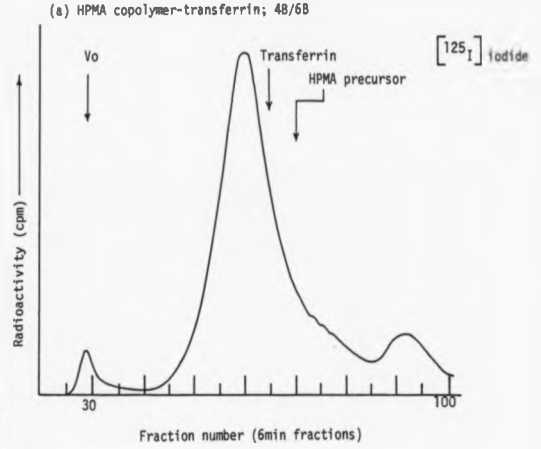

Fig. 3.10(a-g) Gel permeation profiles (48/6B; S-300) of HPMA copolymer-protein conjugates used in this study. (For profiles referring to polymer-McAb B3/25 refer to Fig. 3.3a,b,c).

(b) HPMA copolymer-IgG; S-300

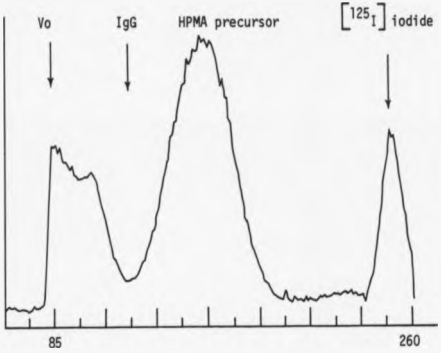

(c) HPMA copolymer-IgG 4B/6B

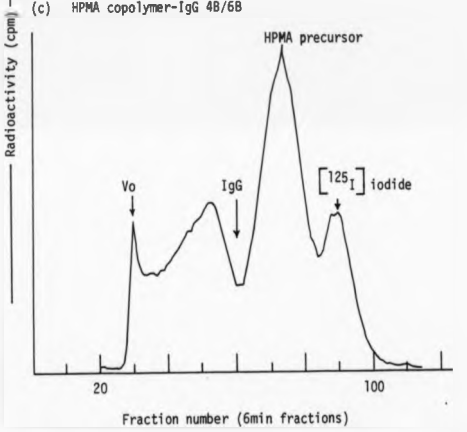

(d) HPMA copolymer-anti-Thy-1.2; S-300

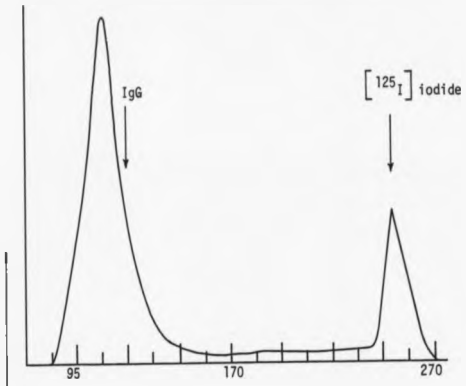

(e) HPMA copolymer-anti-Thy-1.2; 4B/68

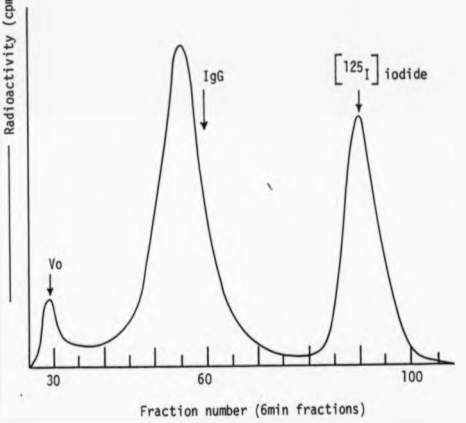

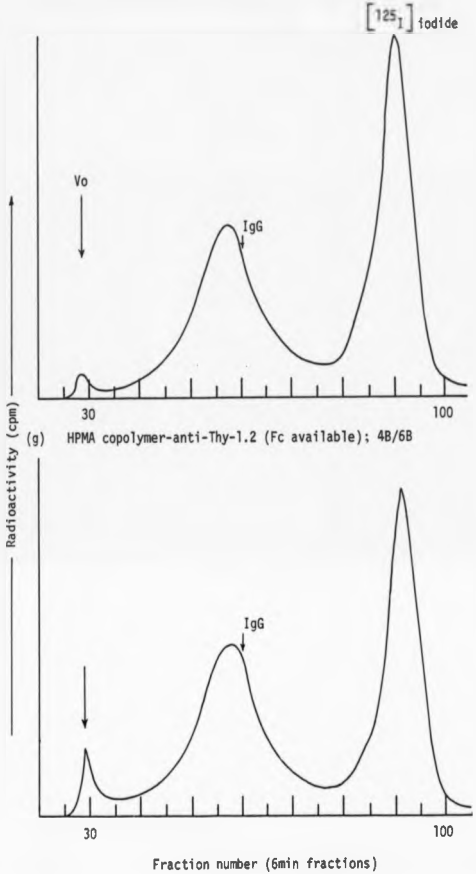
(f) HPMA copolymer-anti-Thy-1.2 (Fc not available); 4B/6B
[125I] iodide
Vo
IgG
30
100
(g) HPMA copolymer-anti-Thy-1.2 (Fc available); 4B/6B
IgG
30
100
Radioactivity (cpm)
Fraction number (6min fractions)

Table 3.3

Proteins and HPMA copolymers used to calibrate the S-300 and 4B/6B gel permeation columns.

Protein	Log Molecular Weight
Cytochrome C	4.09
Transferrin (both apo and diferric)	4.90
IgG	5.18
Ferritin	5.67
Thyroglobulin	5.84
HPMA copolymers of differing $\bar{M}_w$ (supplied by Kopecek *et al.*)	4.06
	4.32
	4.60
	4.89
	5.17
	5.74

resulting values of $\overline{M}w$ were less than those of the known molecular weight of the protein component (Table 3.4). Alternatively, $\overline{M}w$ determined by reference to the protein calibration line may be equally invalid since polymer bound to the surface of protein may alter the passage of protein through the gel permeation column. For experimental purposes $\overline{M}w$ of the protein-HPMA copolymer conjugates was determined by reference to the protein calibration curve. Data in Chapters 4 and 5 seems to support this method of $\overline{M}w$ determination.

The similarity in $\overline{M}w$ of preparations 4a and 4b, and the fact that this $\overline{M}w$ was slightly lower than that of the parent conjugate 4, is difficult to explain. It is possible that the more random orientation of antibody in the parent conjugate has some indefinable effect on the passage of the conjugate through the gel permeation column. Or, the presence of a relatively low percentage of aggregated conjugate eluting on Vo (Fig. 3.10f,g) may have resulted from interaction of conjugates of high molecular weight, which have consequently been removed from the preparation and therefore resulted in reducing the $\overline{M}w$ of the preparation as a whole. Or more simply, this difference may be the result of a slight difference in flow rate during elution through the column, since the difference in $\overline{M}w$ is the result of only a 1-2 tube difference in the elution peak fraction.

The elution profile of conjugate 3 was asymmetrical, indicating the presence of a diverse population of conjugated polymer, which was of high molecular weight(eluting on and close to the Vo). During the course of this study two preparations of conjugate 3 were supplied and both conjugates had this very high $\overline{M}w$. The limited biological application of such large high molecular weight conjugates is discussed in Chapters 4 and 5. As stated earlier, it was desirable that conjugates should elute within the range of a 4B/6B column. However, further purification of HPMA-copolymer conjugate 3, to

Fig. 3.11 Correction of the S-300 gel permeation profile of HPMA copolymer-IgG, to facilitate a statistical determination of an approximate $\bar{M}w$ (also see Appendix 3).

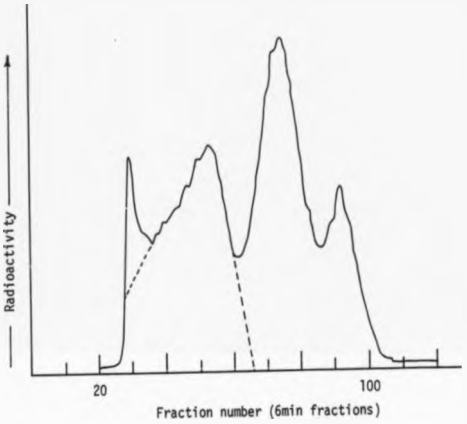

—— actual gel permeation profile

--- extrapolation (full data is stored in Appendix 3)

Table 3.4

A summary of the molecular weight averages ($\bar{M}w$) of conjugates used in this study.

Conjugate	††column and molecular weight markers used: S-300		4B/6B		**Statistical approach: Calculation
	*polymer	protein	polymer	protein	using 4B/6B profile
2	52.5K	219K	52K	229K	240K†
4	70.8K	331K	70K	302-331K	ND
4a	ND	ND	66K	251K	ND
4b	ND	ND	66K	251K	ND
5	ND	ND	151K	457K	ND
3(i)	Asymmetrical				>>2M
(ii)	Asymmetrical				>2M

* see Appendix 3 and 4

† Using 4B/6B protein calibration line.

ND Not determined

†† Based on a symmetrical elution profile (Fig. 3.9)

** Based on a non-symmetrical elution profile (Fig. 3.9).

produce fractions of a more discrete $\bar{M}w$ was not considered advisable, in the light of the observed denaturation of copolymer 5 (formation of aggregates and degradation products) during any further attempt at purification. Conjugate 3 was not therefore purified further, and the crude reaction mixture was used for $\bar{M}w$ determination to minimise the possibility of denaturation. From Fig. 3.11 it can be seen that some material elutes at the V_0 and that the polymer profile overlaps that of the conjugate. Therefore, to obtain a rough estimate of molecular weight, the conjugate profile was corrected (Fig. 3.11) by extrapolation of the IgG-HPMA copolymer peak to the x axis. The values used to extrapolate the conjugate peak were calculated as follows (full data is stored in Appendix 3):-

(1) The slopes of the extrapolated lines were determined.

$$\text{Slope} = \frac{\Delta y}{\Delta x}$$

where y = the radioactivity (cpm) detected in each tube
x = the tube number

(2) To determine the radioactivity (cpm) in each tube due to the presence of conjugate 3, where profiles of conjugate and free polymer, or conjugate and aggregates, overlapped the following relationship was used:-

y = slope x tube number (see Appendix 3.2)

When elution data is processed in this way the calculated $\bar{M}w$ for conjugate would be less than the actual $\bar{M}w$, because the high

molecular weight fractions at the V_o have been ignored. With this limitation in mind, the $\bar{M}w$ of conjugate 3 (preparation 2) was found to be >2M Daltons. As can be appreciated such a molecular weight is too great, the conjugate probably containing at least 10 antibody molecules. The chemistry of binding of protein to HPMA copolymer precursor must be optimised to produce a stoichiometry approximating 1HPMA:1 protein molecule, that is <200K Daltons. The molecular weights of protein-HPMA copolymer conjugates given in Table 3.4 (using the calibration line based on protein standards) indicate that stoichiometries of >1:1 are present for all protein-HPMA copolymer conjugates, with possibly 10 HPMA copolymer molecules:1 transferrin (conjugate 2), 10 HPMA copolymer molecules:1 anti-Thy-1.2 (conjugate 4) and 20 HPMA copolymer molecules: 1 McAb 83/25 (conjugate 5) (Table 3.4). The higher substitution ratio found in conjugate 5 is readily explained by the relatively low proportion of McAb:HPMA copolymer used in the reaction mixture (see earlier). These substitution ratios are in agreement with Rejmanova (1987).

In the future it will also be important to modify binding to control the orientation of the protein, particularly antibody within a protein-HPMA copolymer conjugates. In this study a crude separation of immuno-conjugate 4 was made using protein-A affinity chromatography.

3.2.4 Protein-A Affinity Chromatography

Purified immuno-conjugate 4 was sub-divided into two broad groups by use of protein-A affinity chromatography; conjugate 4a was the fraction that passed through the column and was considered to have the Fc region of the antibody unavailable for interaction, that is, masked (Langone, 1982 stated that all rabbit IgG binds to protein A). Conjugate 4b bound to the protein-A column and was considered to have the Fc region of the antibody available for interaction with

either the protein-A column or, in later *in vivo* experiments, to cells of the RE system. It was assumed that conjugates 4a and 4b would have equal potential to bind antigen. The body distribution of these conjugates was investigated and results are shown in Chapter 8.

3.3 CONCLUSION

The HPMA copolymer preparations were characterised, as far as possible, in terms of purity, Mw, stoichiometry, and orientation of the antibody in immunoconjugate 4. There is however considerable inaccuracy in the determination of Mw and stoichiometry particularly in the case of conjugate 3. With this limitation in mind, the following study of cellular uptake (Chapter 4) and subcellular processing (Chapter 5) must be considered in some ways qualitative rather than quantitative. Protein concentration in each preparation was used as a means of standardising experiments, since exact molecular weights were not known. Therefore polymer concentration used was somewhat variable.

The possible stoichiometries of the conjugates show that 10-20 polymer molecules may be attached to each protein molecule. This may interfere with interaction of the protein with its specific cell-ssurface receptor, or antigen, and subsequent intracellular processing. This possibility has been investigated (Chapter 4 and 5). To optimise binding of protein to polymer, alternative methods of binding are being investigated at present in this laboratory. In the literature a number of methods are reported such as the periodate method (Arnon & Sela, 1982; Manabe, *et al.*, 1984), derivatisation of IgG with the heterobifunctional reagent N-succinimidyl-3,(2-pyridyldithio)propionate (SPDP ; Jung, *et al.*, 1981; Forrester, *et al.*, 1984) and the use of 1-ethyl-3-(3-dimethylaminopropyl)carbodiimide (ECDI; Kulkarni, *et al.*, 1981). An exciting advance towards the conjugation of

antibodies of defined orientation to a carrier has been made by Rodwell, et al., (1986) who employes covalent modification of antibody through the carbohydrate moiety (Fig. 1.4a) which has a limited defined location on the antibody molecule.

CHAPTER 4

The interaction and uptake of ^{125}I-labelled transferrin (apo and diferric), antibody (IgG and B3/25), HPMA copolymer and HPMA copolymer conjugated to these proteins by human fibroblasts

4.1 INTRODUCTION

An ideal drug-carrier (see Chapter 1, Fig. 1.18) should bind specifically to cell surfaces and, depending upon the constituent drug, either remain at the cell surface or gain access to the cell's interior.

HPMA copolymer containing a small amount of tyrosinamide residues (<1mol %) shows little, or no, non-specific binding to cell surfaces and a very slow rate of pinocytic uptake by cell types studied. For example, rat visceral yolk sacs (Duncan, et al. 1984; McCormick,et al.,1986) and hepatocytes (Duncan,et al., 1985) capture such HPMA copolymers at a rate consistent with uptake by fluid-phase pinocytosis.

Residues chosen to promote cell surface interaction, such as carbohydrates or proteins, bound via pendant oligopeptide side-chains, have shown a potential to enhance specific binding to target cells both in vitro and in vivo (Duncan,et al., 1985; Rihova & Kopecek, 1985).

In this Chapter, experiments have been carried out to investigate interaction and cellular processing of HPMA copolymer conjugates containing transferrin, IgG (non-specific), or anti-transferrin receptor monoclonal antibody B3/25 (McAb B3/25), using human fibroblasts as an in vitro model system. Radiolabelled substrates were used to study the binding, internalisation, and subsequent intracellular degradation of these protein-HPMA copolymer conjugates. Results were compared to those obtained with unconjugated protein and parent copolymer.

4.1.1 Methods

Cell culture methods used are given in Chapter 2 (2.2.5.3). However the nomenclature used in this Chapter is somewhat difficult and worthy of precise definition. The following terms are used

throughout:

Total Uptake (T.U.) was used to define the sum of trypsin-sensitive (bound) ^{125}I-labelled substrate, and trypsin-insensitive (internalised) ligand, including any internalised ligand subjected to intracellular degradation resulting in the liberation of low molecular weight degradation products from the cell.

Total uptake = trypsin-sensitive (bound) substrate
(T.U.) +
trypsin-insensitive (internalised) substrate
+
degraded substrate

Internalisation (In.) was used to define trypsin-insensitive ^{125}I-labelled ligand and any low molecular weight degradation products liberated from the cell

In. = trypsin-insensitive substrate
+
degraded substrate

4.1.2 Calculations

Calculations used in this Chapter are given in Chapter 2, Section 2.2.5.4.

4.2 RESULTS

4.2.1 Preliminary experiments to determine the optimum time course for measuring Total Uptake of ^{125}I-labelled HPMA, protein, and HPMA copolymer-protein conjugates.

The T.U. of HPMA-gly-gly-aminopropanol measured over 96h was very similar to that of PVP (Fig. 4.1). No low molecular weight ^{125}I-labelled degradation products were detected (G-25

Fig. 4.1 Total Uptake of ^{125}I-labelled HPMA copolymer and ^{125}I-labelled PVP by fibroblasts

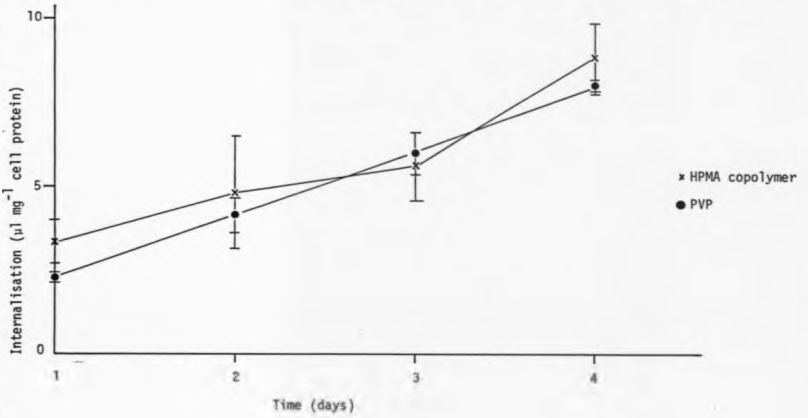

chromatography) in the culture medium during these experiments.

Trypsin-sensitive (surface bound) radioactivity associated with apotransferrin reached a plateau after 3h and degradation products were detected in the incubation medium and found to increase with time (Fig. 4.2). There was little change in the extent of binding or internalisation of transferrin after 3h. Therefore further experiments were carried out over a 3h time course.

In these further experiments (3h), ^{125}I-labelled ligands were added to Hank's balanced salt solution, instead of complete medium (Chapter 2, 2.2.5.3). Complete medium had the disadvantage of containing transferrin, immunoglobulins and many other unwanted proteins of unknown concentration, which could compete with ^{125}I-labelled substrate for binding sites on the fibroblast cell surface. The well defined balanced salt solution contained no unwanted protein. To ensure the integrity of apotransferrin (in terms of iron-loading) no iron was present in this solution (guaranteed by Suppliers, Flow Laboratories).

4.2.2 Comparison of T.U. and In. of ^{125}I-labelled IgG, McAb B3/25 and transferrin.

T.U. and In. of transferrin was independent of the iron loading of transferrin and little difference was found between the cell-associated radioactivity of apotransferrin and diferric transferrin (Fig. 4.3). The major contribution to both T.U. and In. was attributable to the levels of degradation products released into the extracellular medium (approximately 47µl mg^{-1} cell-protein after 3h). In relation to the total ^{125}I-labelled ligand processed very little cell-associated radioactivity was found to be trypsin-sensitive.

Because the processing of transferrin was shown to be independent of iron loading no routine attempt was made to determine

Fig. 4.2 Cell association of ^{125}I-labelled apotransferrin by fibroblasts in terms of total cell-associated and trypsin-insensitive radioactivity, together with released low molecular weight degradation products.

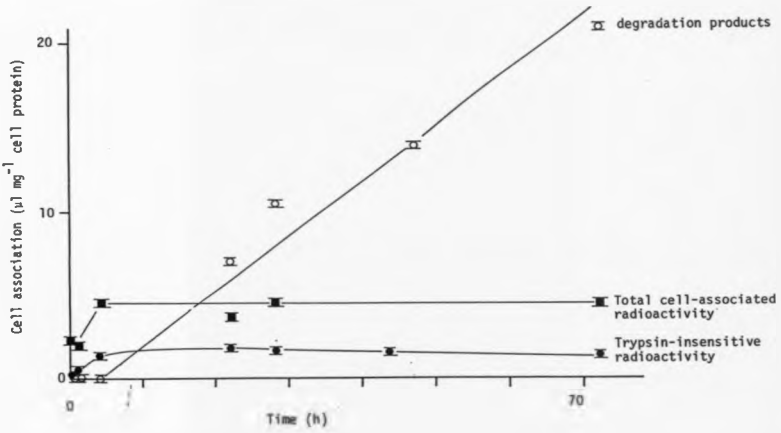

Fig. 4.3 Comparison of the Internalisation and Total Uptake of ^{125}I-labelled antibody (non-specific, IgG; specific, McAb B3/25) and ^{125}I-labelled transferrin (diferric and apo).

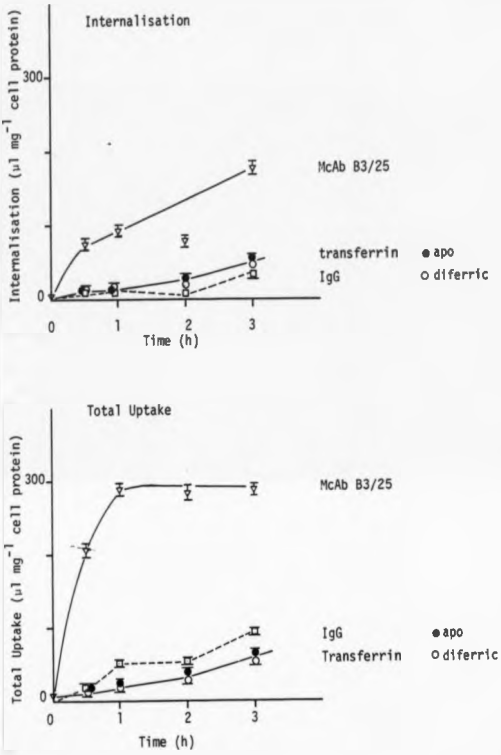

the iron loading of transferrin in the transferrin-HPMA copolymer conjugates.

T.U. of IgG was approximately 100% greater than T.U. of transferrin. In., however was approximately 20% lower than that of transferrin. More than 50% of the radioactivity was trypsin-sensitive (3h). Radioactivity attributable to degradation products of ^{125}I-labelled IgG was found to be equivalent to 30µlmg^{-1} cell-protein after 3h.

T.U. and In. of McAb B3/25 were much higher than those of either transferrin or non-specific IgG. T.U. reached a plateau at 295µlmg^{-1} cell protein after approximately 1h. This value corresponded to 1.68 pm mg^{-1} protein cell-associated radioactivity. In. of McAb B3/25 increased with time, with a significant contribution attributable to degradation (after 3h 100µlmg^{-1} cell-protein). Trypsin-sensitive surface-bound radioactivity decreased with time, contributing less than 50% of cell-associated radioactivity after 3h.

4.2.3 A comparison of T.U. and In. of ^{125}I-labelled IgG-HPMA copolymer (conjugate 3) preparations 1 and 2.

As described in Chapter 3 (3.2.3) two preparations of conjugate 3 were made and both were of very high molecular weight.

Incubation of the first preparation (which had the higher mean molecular weight; $\bar{M}w$>>2M Daltons) with fibroblasts gave rise to little cell-associated radioactivity (Fig. 4.4). T.U. was lower than that of HPMA copolymer after 3h and In. was negligible, the majority of cell-associated radioactivity being trypsin-sensitive.

In contrast, the second preparation of conjugate 3 (of lower mean molecular weight; $\bar{M}w$>2M Daltons) showed a 300% (3h) increase in T.U. when compared to that of HPMA copolymer, together with an enhanced In. (500% increase after 2h). The sharp decline of In. seen after 2h may be attributable to an inability to detect low levels of degradation products.

Fig. 4.4 Comparison of Total Uptake and Internalisation of the two preparations of ^{125}I-labelled HPMA copolymer conjugated to IgG

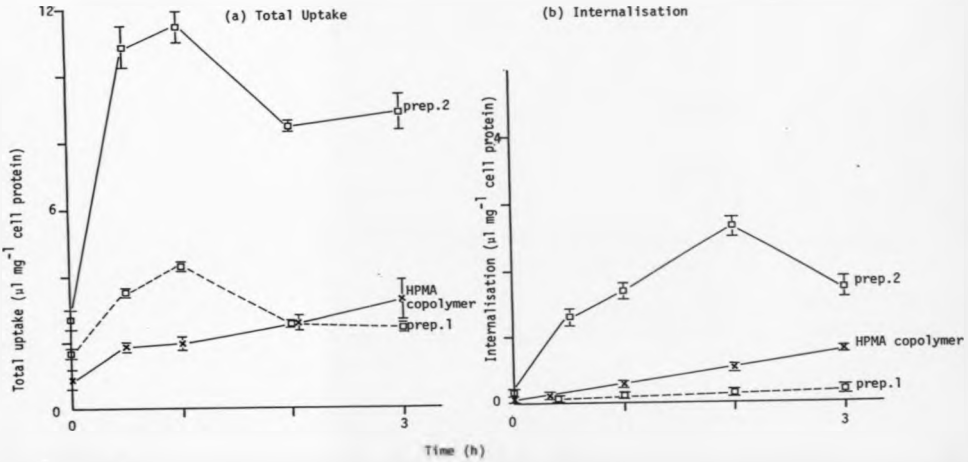

4.2.4 Comparison of T.U. and In. of HPMA copolymer conjugates 2 (containing transferrin), 3 (containing IgG) and 5 (containing McAb B3/25).

All three conjugates, and in particular those specific for the transferrin receptor, showed a higher T.U. than that of the parent HPMA copolymer (Fig. 4.5a,b; conjugate 2, 800% increase; conjugate 3 preparation 2, 300% increase) coupled with increased In. (conjugate 2, 350% increase; conjugate 5, 500% increase; conjugate 3, 100% increase). Trypsin-sensitive radioactivity varied from approximately 80% (conjugate 2, 3h) to approximately 10% (conjugate 5, 3h) of the total cell-associated radioactivity.

In contrast, there was a dramatic decline in both T.U. and In. of protein after conjugation to HPMA copolymer (Fig. 4.6, 4.7, 4.8), although in all cases the T.U. and In. were still higher than those of the parent copolymer.

4.3 DISCUSSION

The observed binding, internalisation and degradation of diferric transferrin was in accordance with published results (May & Cuatrecasas, 1985; Dautry-Varsat, 1986; Hunt, 1986). It has already been reported that the majority of receptor-bound transferrin recycles. However, the binding and subsequent intracellular processing of apotransferrin was, surprisingly, found to be very similar to that of diferric transferrin. Parallel experiments, to be presented in Chapter 6, indicated that the apotransferrin used in these experiments had not chelated iron, either in preparation or cell incubation. The iron-independent cell-association of transferrin was in agreement with the results of Young & Aisen (1979), and Ward (1982), but did not agree with the generally accepted model of transferrin recycling (May & Cuatrecasas, 1985;

Fig. 4.5a Comparison of the Total Uptake of HPMA copolymer and HPMA copolymer conjugates 2 (contains transferrin) 3 (contains IgG) and 5 (contains McAb B3/25). (All ligands were ^{125}I-labelled.)

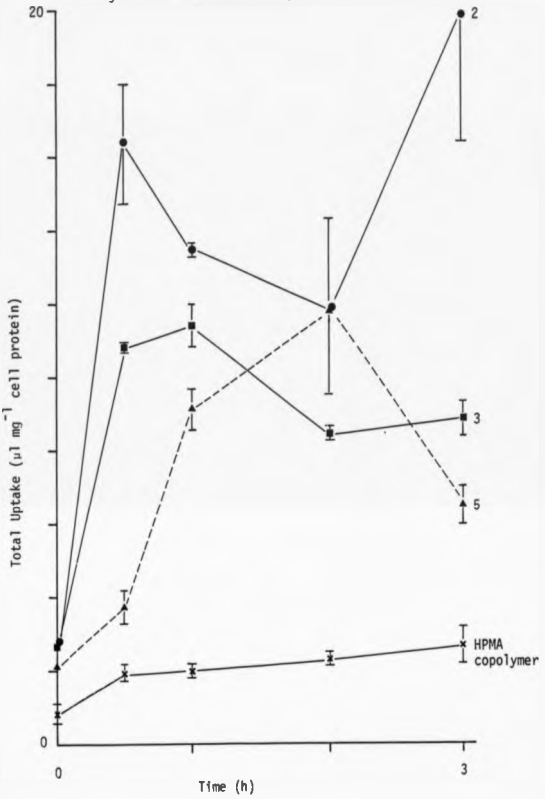

Fig. 4.5b Comparison of Internalisation of HPMA copolymer, HPMA copolymer conjugates 2 (contains transferrin), 3 (contains IgG) and 5 (contains McAb B3/25). (All ligands were ^{125}I-labelled.)

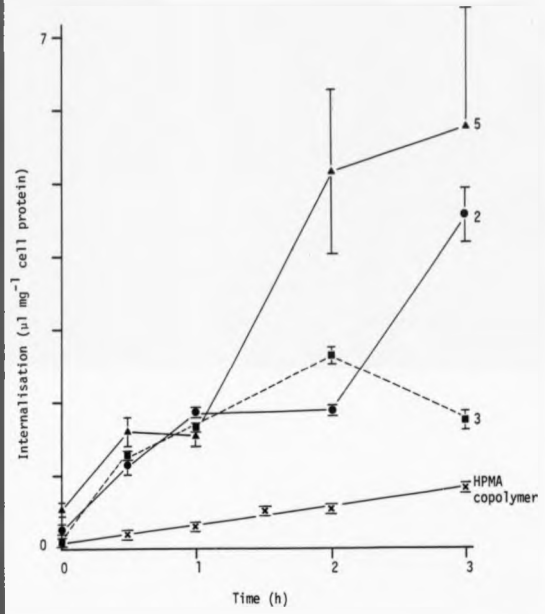

Fig. 4.6a Comparison of the Total Uptake of transferrin (apo and diferric), HPMA copolymer and HPMA copolymer conjugate 2 (containing transferrin). (All ligands were ^{125}I-labelled.)

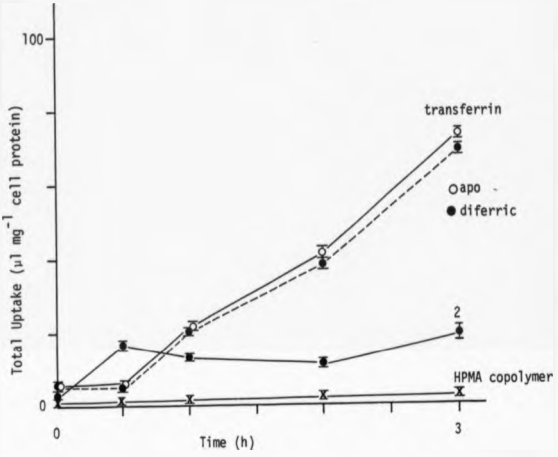

Fig. 4.6b Comparison of the Internalisation of transferrin (apo and diferric), HPMA copolymer and HPMA copolymer 2 (contains transferrin). (All ligands were ^{125}I-labelled.)

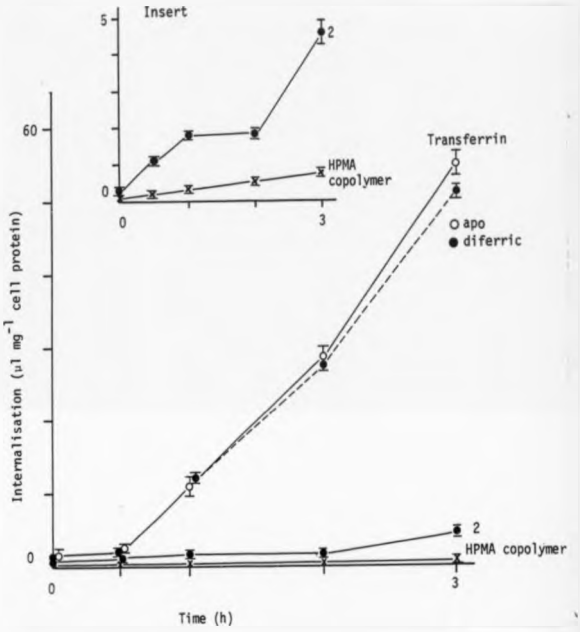

Fig. 4.7a Comparison of the Total Uptake of McAb B3/25, HPMA copolymer and HPMA copolymer conjugate 5 (contains McAb B3/25). (All ligands were ^{125}I-labelled).

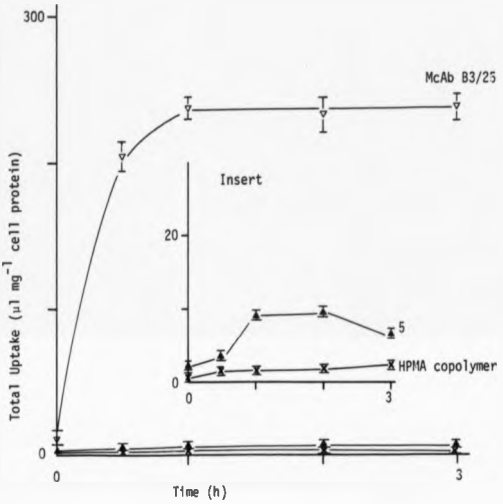

Fig. 4.7b Comparison of the Internalisation of McAb B3/25, HPMA copolymer and HPMA copolymer conjugate 5 (contains McAb B3/25). (All ligands were ^{125}I-labelled.)

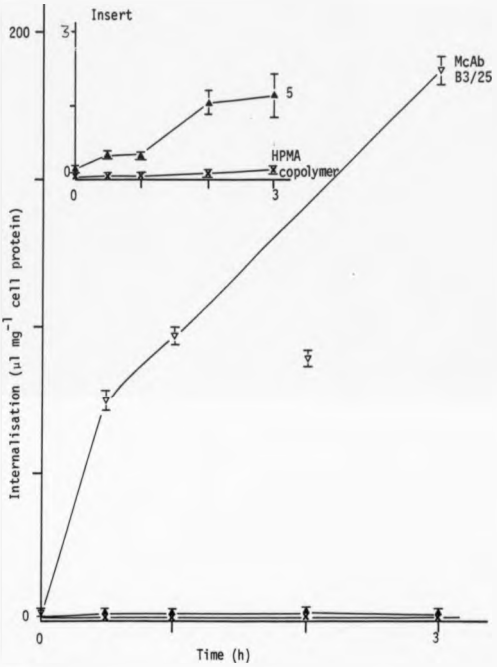

Fig. 4.8a Comparison of the Total Uptake of IgG, HPMA copolymer and HPMA copolymer conjugate 3 (contains IgG). (All ligands were ^{125}I-labelled.)

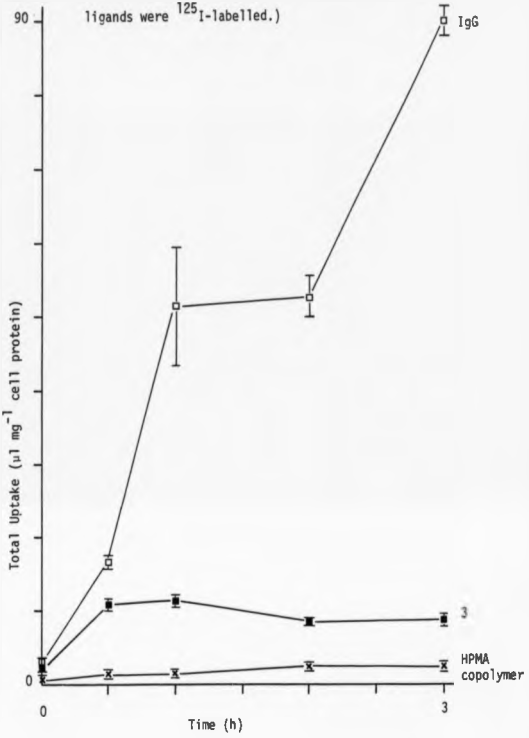

Fig. 4.8b Comparison of the Internalisation of IgG, HPMA copolymer and HPMA copolymer conjugate 3 (contains IgG). (All ligand were ^{125}I-labelled.)

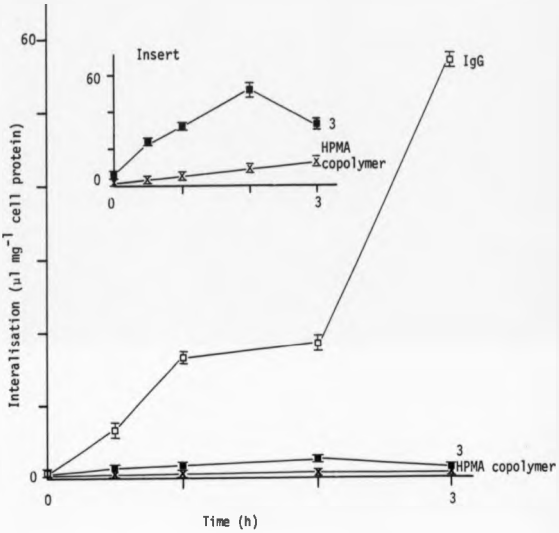

Dautry-Varsat, 1986; Hunt, 1986) in which the interaction of transferrin and its receptor is described as both iron and pH-dependent:- (i) at physiological pH the affinity of iron-loaded transferrin is two orders of magnitude greater than that of apotransferrin (ii) after endocytosis into the acidic environment of the endosome, iron is liberated from transferrin (Chapter 1, 1.4) to yield apotransferrin, which has a high affinity for the receptor at acidic pH (iii) the apotransferrin-receptor complex is recycled back to the plasma membrane where, under conditions of physiological pH, apotransferrin dissociates from the receptor. The inability of this model to explain the internalisation of the transferrin receptor in the absence of bound transferrin (Watts, 1985; Ajioka & Kaplan, 1986; Stein & Sussman,1986), and the demonstration of two distinct pathways of transferrin-receptor recycling (Golgi and non-Golgi mediated; Stein & Sussman, 1986) indicate that the recycling of transferrin is more complicated than this model implies.

The binding, internalisation and degradation of McAb B3/25 was in accordance with a transferrin-independent internalisation of the transferrin receptor. The shape and size of transferrin and McAb B3/25 are dissimilar (Chapter 1, 1.3; 1.4) and therefore it would not be expected that binding of McAb B3/25 to the transferrin receptor, at a site removed from the transferrin-binding site (Trowbridge & Omary,1981), would trigger a ligand-dependent internalisation of receptor. Results presented in this study indicated that, unlike a transferrin-receptor complex, receptor-bound McAb B3/25 did not recycle, but remained firmly attached to the transferrin receptor. Trypsin-sensitive radioactivity decreased with time, compared to a plateau of T.U., indicating that receptors were being internalised but not replaced at cell surface. This down-regulation of the transferrin receptor occurred after approximately 1.68 pm McAb bound

mg^{-1} cell protein. This value corresponded to approximately twice the calculated number of transferrin receptors $cell^{-1}$ (Chapter 6), and indicated that there had been some replacement of cell-surface receptors from the large intracellular pool (Ajioka & Kaplan, 1986). Down-regulation had probably occurred to prevent gross accumulation of receptor-McAb complex as a result of little, if any, recycling, together with the relatively slow degradation of antibody (approximately 30% of T.U. after 3h) in agreement with Ruud, et al. (1986).

As would be expected T.U. and In. of non-specific IgG was lower than that of either of the specific ligands (bearing in mind that the majority of cell-associated transferrin has recycled). After 3h approximately 50% of the IgG remained bound to the cell surface identifiable as trypsin-sensitive radioactivity. These results are in accordance with those of Schneider, et al. (1979, 1981), who reported that fibroblasts endocytose IgG (radiolabelled with acetate) very slowly followed by subsequent incomplete degradation within the lysosomes.

Conjugation of transferrin, McAb B3/25, or IgG to HPMA copolymer resulted in up to a 9-fold increase in T.U. and a 6-fold increase in In. when compared to the parent HPMA copolymer. There was, however, a disappointing decrease in the cell-surface interaction of the protein-HPMA copolymer when compared to unconjugated protein. A number of important points emerged from this study:-

1. The importance of conjugate size is clearly seen by comparison of T.U. and In. of the two preparations of conjugate 3 (Fig. 4.4). The limited cell-interaction of the first preparation was shown by its poor capacity to bind to the cell surface, together with an inability to gain access to the cell's interior. In fact the very high molecular weight of this preparation would probably mean that it

is better defined as a colloid rather than a soluble synthetic polymer (see Chapter 1, 1.2). Phagocytic uptake by macrophages, as indicated by Duncan,et al. (1981), would probably reduce the ability of such conjugates to reach any potential target tissue.

2. The T.U. and In. of the specific HPMA copolymer conjugates, containing transferrin or McAb B3/25, showed up to a 220% increase in T.U. and a 300% increase in In. compared with the non-specific conjugate containing IgG, and up to a 900% increase in T.U. and 600% increase in In. when compared to the parent HPMA copolymer. This indicated that these conjugates possessed some ability to bind specifically at the cell surface, although a much reduced ability than unconjugated protein. The probable explanation for this reduction in specificity has been discussed in Chapter 3 (3.2.3) where it was stated that there may be as many as 10-20 (conjugate 2, conjugate 5) HPMA copolymer molecules bound to the protein component. Such high ratios of polymer to protein may result in conjugates where protein is surrounded by HPMA, in a similar way to the shell of polyethylene glycol formed around albumin (Abuchowski,et al., 1979). The result of such a stoichiometry would mean that the protein cannot interact efficiently with its target antigen, or receptor. This would explain the dramatic decrease in T.U. and In. of protein after conjugation to HPMA copolymer. It is possible that the polymer shell is so effective at masking the protein component that the major contribution to the observed increase in T.U. and In., when compared to parent HPMA copolymer, was simply a result of an increased ability of a protein-polymer complex to interact non-specifically at the cell surface. Obviously it is critical that the targeting residue of an HPMA copolymer drug-carrier maintains its ability to interact specifically at the cell surface. The type of cell-surface interaction available to these particular conjugates, in terms of

specific or non-specific binding, was further investigated in Chapter 6.

3. A comparison of T.U. of transferrin before and after conjugation to HPMA copolymer (Fig. 4.6a) indicates that conjugate 2 (contains transferrin) has escaped futile recycling. The relatively high degree of specificity retained by the conjugated-protein (apparently 40% of unconjugated protein) is readily explained by the fact that most of the unconjugated protein has recycled and is not included in this data, in comparison to the conjugate, which has not recycled and is therefore totally accounted for. This alteration of intracellular routing is investigated further in Chapter 5. If transferrin is to be considered as a targeting-residue of a HPMA copolymer drug-carrier such a change in intracellular routing would be very important, since it would be a disadvantage for the majority of the drug carrier to be regurgitated before transfer into the secondary lysosomes.

These data describe the interaction of proteins, HPMA copolymer, and protein-HPMA copolymer conjugates in general terms of T.U. and In. In the following chapters the intracellular routing, and the ability of these conjugates to bind specifically to the cell surface is discussed.

CHAPTER 5

Subcellular fractionation of human fibroblasts after incubation with ^{125}I-labelled antibody (non-specific IgG and specific McAb B3/25), transferrin, HPMA copolymer and HPMA copolymer conjugated to these proteins

5.1 INTRODUCTION

An important consideration relating to the design of HPMA copolymers for use as drug-carriers is the pendant oligopeptide side-chain used to bind drug. These side-chains are used to facilitate controlled release of drug (Duncan, et al., 1983). Glycyl-phenyl-leucyl-glycine has been proposed as a useful biodegradable oligopeptide sequence allowing release of drug (for example, daunomycin) within the lysosomal compartment (Duncan, et al., 1987) and it is not cleaved in extracellular fluids.

In Chapter 4 it was shown that binding of HPMA copolymer conjugates (containing antibody (IgG or McAb B3/25), or transferrin) to the fibroblast surface was less efficient than binding of unconjugated protein. These conjugates were also internalised (and degraded) less effectively.

The following study has examined the subcellular localisation of these conjugates after incubation with fibroblasts. Tulkens, et al. (1974) showed that it is possible to homogenise fibroblasts and successfully separate intracellular organelles on a sucrose density gradient. In the following study Percoll was used, rather than sucrose, as a separation medium. It has several advantages over sucrose; (i) sterility (ii) low viscosity and therefore formed gradients rapidly (iii) impermeant to cells.

The presence of subcellular organelles on the gradient was identified by the presence of characteristic marker enzymes (Table 5.1). As yet there is no enzyme which has been identified as unique to the "endosome". This is probably attributable to the complex nature of this intracellular compartment, which has been identified as a network of tubules and/or vesicles (Geuze, et al. 1983; Hopkins, 1983; Harding, et al., 1985). In recent publications the endosome has been described as multivesicular (3 compartments demonstrated by Wall &

Hubbard, 1985 and multiple compartments described by Gorman & Poretz, 1987). Confusion concerning exact characterisation of the "endosome" may result from the suggestion that the "endosome" is not identical in all cell types (Stahl & Schwartz, 1986). In this study no attempt was made to identify the endosomal compartment specifically.

5.1.1 Methods

In this study fibroblasts which had been continuously incubated (2h, 5h, sometimes 24h) with ^{125}I-labelled antibody (IgG or McAb B3/25), transferrin, HPMA copolymer, or HPMA copolymer conjugates were homogenised and subsequently fractionated on a Percoll density gradient.

The data presented are representative of 3 separate, reproducible experiments (for each ligand for each time course). It was not possible to combine experimental results because of errors inherent in the method used to collect fractions (Chapter 2, 2.2.6.1.2). The number of fractions (250µl) collected varied between 30 and 32.

5.1.2 Calculations

Calculations used in this Chapter are given in Chapter 2, Section 2.2.6.3.

It is important to note that radioactivity detected in the lysosomal compartment is underestimated for all ligands. It was consistently found that incubation of fibroblasts, with any radiolabelled ligand, increased the fragility of the lysosomes during homogenisation. Hexosaminidase released during homogenisation of fibroblasts was not confined to fractions characteristic of the lysosomal compartment (fractions 21-30). but instead was detected throughout the density gradient. Burst lysosomes were calculated to account for 30% of the total hexosaminidase activity (this compared with <10% when fibroblasts had been incubated in medium alone). It

Table 5.1

Characteristic subcellular localisation of enzymes/proteins.

Subcellular localisation	enzyme
Plasma membrane	5'-nucleotidase
Endosomes	?
Lysosomes	hexosaminidase
Mitochondria	monoamine-oxidase
Nucleus	DNA
Cytosol	lactate-dehydrogenase

was therefore considered necessary to assay all fractions, in every separation, for the lysosomal enzyme hexosaminidase. (The other marker enzymes, Table 5.1, were assayed only three times since their buoyant densities were found to be consistent and reproducible).

Measurement of lysosomal enzymes in each fraction of every gradient allowed exact quantification of the extent of lysosomal breakage and the percentage of total hexosaminidase activity detected in fractions other than 21-30. To correct the radioactivity profiles measured on the gradient, radioactivity detected in fractions 21-30 was related to the percentage of intact lysosomes (for example there may be 1000 cpm recovered in 70% lysosomes). This relationship was then used to correct the radioactivity detected in fractions other than 21-30, by subtraction of radioactivity which was attributable to burst lysosomes (as measured by hexosaminidase release; see Fig. 5.1).

Lysosomal-associated radioactivity was not increased in parallel (since it was not possible to extrapolate the exact original density of these burst lysosomes).

5.2 RESULTS

5.2.1 Preliminary experiments to determine optimal conditions for homogenisation and subcellular fractionation of fibroblasts.

The number of strokes of a Dounce cell homogeniser were varied, and lysosomal integrity, together with the number of intact cells, were measured. These parameters were used as an indication of the appropriateness of the conditions used. It was found that 20 downward strokes of the big head of the homogeniser resulted in least damage to lysosomes (<10% burst) coupled with maximal cell breakage. It was surprising to find that the same conditions used to homogenise fibroblasts after incubation with radiolabelled ligand resulted in a

Fig. 5.1a Hexosaminidase profile on the Percoll gradient after subcellular fractionation of fibroblasts previously incubated with ^{125}I-labelled ligand.

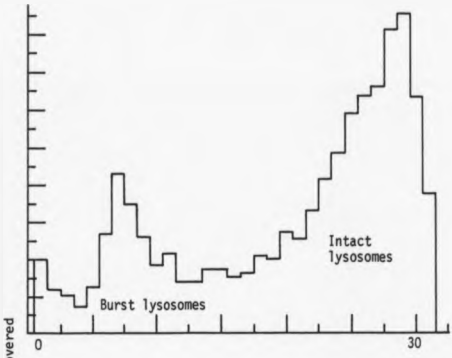

Fig. 5.1b ^{125}I-labelled ligand gradient profile corrected for radioactivity attributable to burst lysosomes.

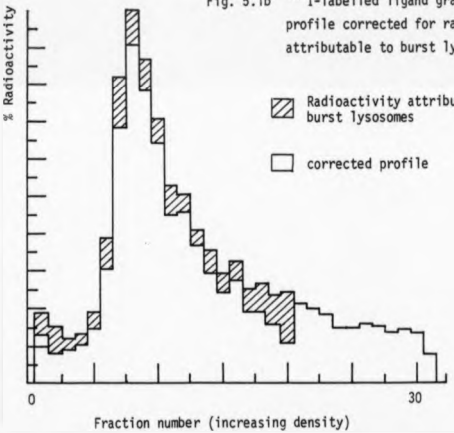

much higher percentage of burst lysosomes (approximately 30%). Intact cells were subsequently removed by centrifugation and the supernatant produced placed on the Percoll density gradient.

A range of Percoll gradients (5%-95% standard iso-osmotic Percoll SIP; Chapter 2, 2.2.6.1.1) were calibrated with density marker beads, under different centrifugation conditions (19-50g, 10-60min). A 30% SIP gradient, spun 40min x 19000g gave optimal separation between fractions containing plasma membrane and lysosomal enzyme markers, whilst maintaining a linear change in density over the majority of the gradient (Fig. 5.2). The shape of gradient was reproducible (n=30), and was calibrated using a number of fluorimetric enzyme assays:- 5'nucleotidase (plasma/membrane), monoamine oxidase (mitochondria), DNA (nucleus), lactate dehydrogenase (cytosol), and protein. It was not considered possible to identify the endosome because of the lack of a definitive marker enzyme (see Section 5.1). The horseradish peroxidase-diaminobenzidine density shift reaction (Courtoy, et al., 1984) has been used to locate the endosome, but use of this technique here was not possible with the small volume of gradient (8ml) and the small size of each fraction (250µl). Merion, et al. (1983) have reported densities of 1.04 and 1.051g ml^{-1} as characteristic of light and heavy endosomes and throughout this section reference will be made to a pre-lysosomal, or "endosomal" region corresponding to densities of approximately 1.04-1.065g ml^{-1}.

Occasionally, after homogenisation of fibroblasts which had been incubated in the presence of ^{125}I-labelled ligands radioactivity was detected at a density lower than that of plasma membrane (that is, at the top of gradient). This radioactivity was considered to be most probably associated with ligand which had sufficient affinity for the

Fig. 5.2 Profile of marker enzymes after subcellular fractionation of fibroblasts on a 30% SIP Percoll density gradient.

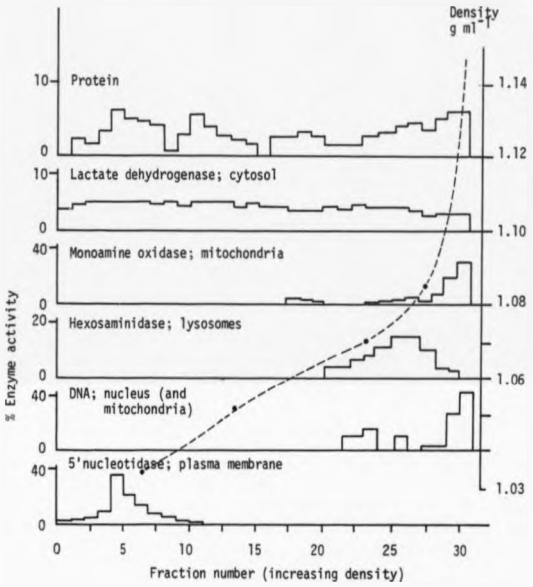

cell surface not to be removed during the washing procedure, but subsequently dissociated from the cell surface during homogenisation. It is also possible that this activity may have been associated with low molecular weight degradation products within the cytosol (LDH activity was also detected at very low densities) or, alternatively, burst endosomes (no characteristic enzyme marker to check this possibility).

5.2.2 Subcellular localisation of ^{125}I-labelled HPMA copolymer

After 2h ^{125}I-labelled HPMA copolymer was detected throughout the gradient (Fig. 5.3, Table 5.2) at densities corresponding to plasma membrane (5'-nucleotidase), the pre-lysosomal region of the gradient, and the density of the lysosomal compartment (31%). There was no difference in the percentage of HPMA copolymer detected in the lysosomes after 5h, although there was more radioactivity detected, with increasing fraction density, in the pre-lysosomal region of the gradient (see Fig. 5.3, Table 5.2).

5.2.3 Subcellular localisation of ^{125}I-labelled McAb B3/25 and ^{125}I-labelled HPMA copolymer 5 (contains McAb B3/25)

After 2h there was a high percentage of McAb B3/25-associated radioactivity recovered at a density equivalent to that of plasma membrane (55%) together with some radioactivity detected in fractions of higher density in the pre-lysosomal region of the gradient (37%) (Fig. 5.4, Table 5.2). After 5h the percentage of plasma membrane-associated radioactivity was proportionately lower as more McAb-associated radioactivity was detected at densities of the pre-lysosomal and lysosomal compartments.

The subcellular localisation of conjugate 5 (containing McAb B3/25) was difficult to interpret because of the high percentage of unconjugated HPMA present in this preparation. Due to the low amounts of radioactivity present in each fraction it was not

Fig. 5.3 Profile of radioactivity receoverd after subcellular fractionation of fibroblasts previously incubated for 2h or 5h in the presence of ^{125}I-labelled HPMA.

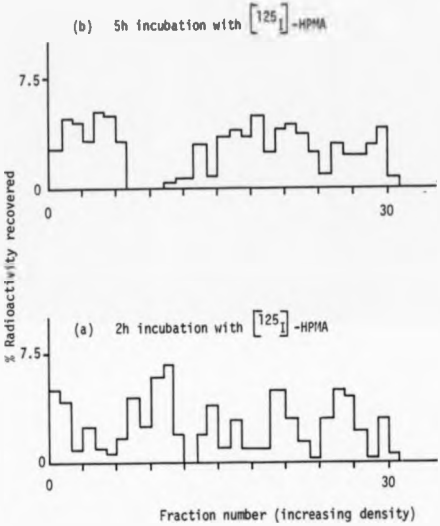

Fig. 5.4 Profile of radioactivity recoverd after subcellular fractionation of fibroblasts previously incubated for 2h or 5h in the presence of ^{125}I-labelled McAb B3/25 or HPMA copolymer conjugate 5 (contains McAb B3/25).

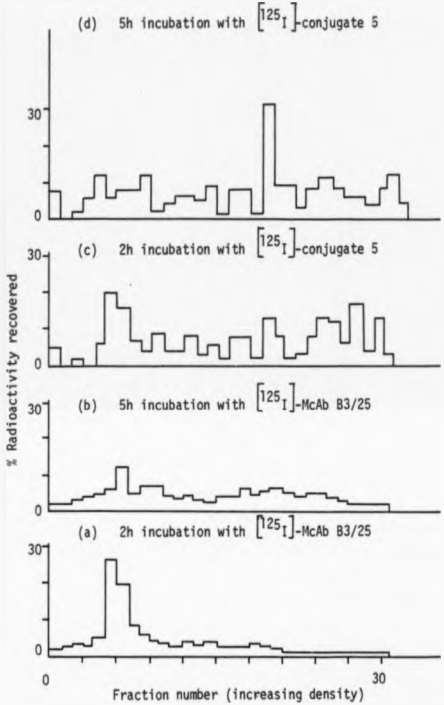

Table 5.2

Comparison of the percent of recovered ligand-associated radioactivity detected at the density of the lysosomal enzyme hexosaminidase.

^{125}I-labelled substrate	Percent of recovered radioactivity detected at the density of hexosaminidase[A]		
	2h	5h	24h
Tf	29	31	-
*IgG	51	55	-
McAb B3/25	13	41	-
HPMC copolymer	31	31	-
P-transferrin	37	59	-
P-IgG (prep. 1)	0	N.D.	6
P-IgG (prep. 2)	42	30	-
P-McAb B3/25	46	39	-

A These values take no account of either recycling via the endosome or degradation with subsequent exocytosis of degradation products.

* Including radioactivity detected at the density of mitochondria and nucleus

P = HPMA copolymer

considered to be acceptable to correct for the presence of HPMA-associated radioactivity. It is probable that the gradient profile is largely attributable to the subcellular processing of HPMA, however, there does appear to be a better localisation of conjugate within the lysosome than found with parent HPMA (Table 5.2) (no degradation products were detected for either conjugate 5 or HPMA after incubation with fibroblasts 3h, Chapter 4).

5.2.4 Subcellular localisation of ^{125}I-labelled IgG and ^{125}I-labelled HPMA copolymer conjugate 3 (contains IgG).

After 2h and 5h IgG-associated radioactivity was detected in all regions of the gradient (Fig. 5.5). Peaks of radioactivity were located at the density of plasma membrane (2h, 23%; 5h, 20%) and, surprisingly, at very high density (mitochondria and nucleus; 2h, 14%; 5h, 13%). Fig. 5.5l indicated that this peak of radioactivity at very high density is probably associated with the lysosomal compartment, since the hexosaminidase also gave an atypical distribution of activity.

Conjugation of HPMA copolymer to IgG altered the gradient profile of IgG (Fig. 5.5.2, 5.5.3). After 2h the majority of radioactivity associated with the first preparation of conjugate 3 ($\bar{M}w >> 2x10^6$ Daltons; Chapter 3) was detected at the density of plasma membrane. Even after 24h there was still approximately 55% of conjugate-associated radioactivity at the density of plasma membrane, together with 30% detected at the density of the pre-lysosomal compartment (1.04; 1.055; 1.06g ml^{-1}). It can be seen (Fig. 5.5.2) that after both 2h and 5h conjugate-associated radioactivity was detected at a density lower than that of plasma membrane (2h, 14%; 5h, 14%).

This pattern of subcellular localisation contrasted with the second preparation of conjugate 3 (Fig. 5.5.3) which, although still

Fig. 5.5.1 Profile of both hexosaminidase activity and radioactivity recovered after subcellular fractionation of fibroblasts previously incubated for 2h or 5h in the presence of ^{125}I-labelled IgG

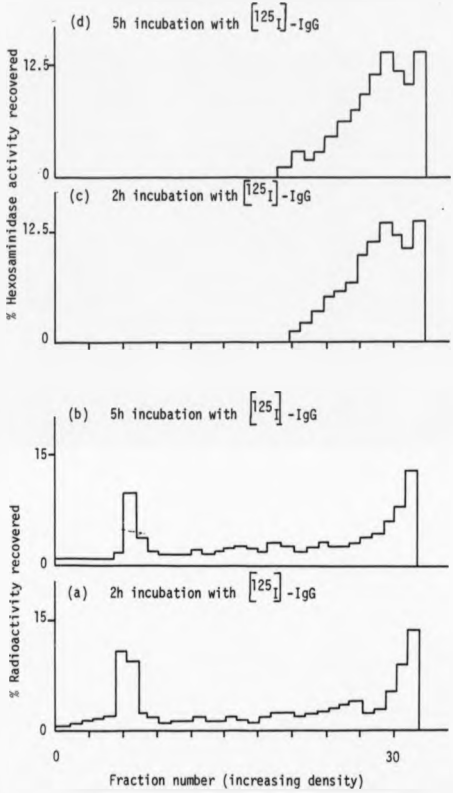

Fig. 5.5.3 Profile of radioactivity recovered after subcellular fractionation of fibroblasts previously incubated for 2h or 5h in the presence of ^{125}I-labelled HPMA copolymer conjugate 3, preparation 2.

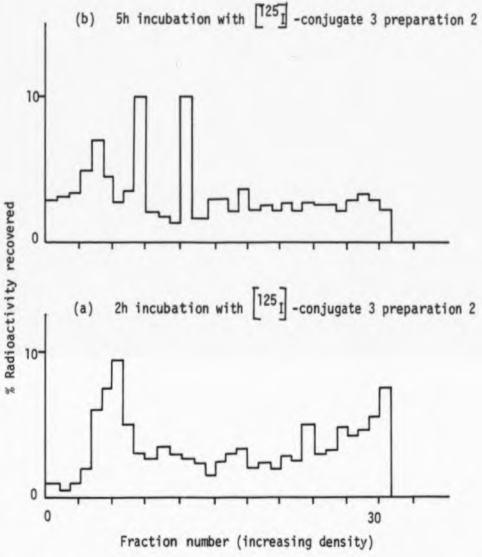

of high Mw, was of lower $\overline{M}w$ than the first preparation ($\overline{M}w > 2x10^5$ Daltons). After only 2h conjugate-associated radioactivity was detected at the density of lysosomes (42%, Table 5.2). After 5h only 30% of conjugate-associated radioactivity was detected at this density, together with an increased percentage of conjugate located in the pre-lysosomal region of the gradient (2h, 30%; 5h, 43%). It can be seen (Fig. 5.5.3) that there is a small percentage of radioactivity (9%) detected at a density lighter than that of plasma membrane.

5.2.5 Subcellular localisation of ^{125}I-labelled transferrin and ^{125}I-labelled HPMA copolymer 2(contains transferrin)

After 2h and 5h, transferrin-associated radioactivity was spread throughout the gradient with 20-26% (2h,5h) detected at the density of plasma membrane and 29-31% at the density of lysosomes Fig. 5.6; Table 5.2.

Conjugation of HPMA copolymer to transferrin altered this gradient profile (Fig. 5.6). After 2h 20% of conjugate-associated radioactivity was detected at a density lower than that of plasma membrane.

After 5h 59% of recovered radioactivity was detected at the density of lysosomes (Table 5.2) with approximately 15% still present at the density of plasma membrane.

5.3 DISCUSSION

The main aim of these studies, using subcellular fractionation as a tool, was to show that protein-HPMA copolymer conjugates, were able to reach the lysosomal compartment of the cell. This was demonstrated to be true for all conjugates (Table 5.2), despite the fact that the lysosomally-associated radioactivity given here cannot take into account the total amount of ligand which has reached the lysosome for a number of reasons. These include (i) as detailed

Fig. 5.6 Profile of radioactivity recovered after subcellular fractionation of fibroblasts previously incubated for 2h or 5h in the presence of ^{125}I-labelled diferric transferrin or HPMA copolymer conjugate 2 (contains transferrin).

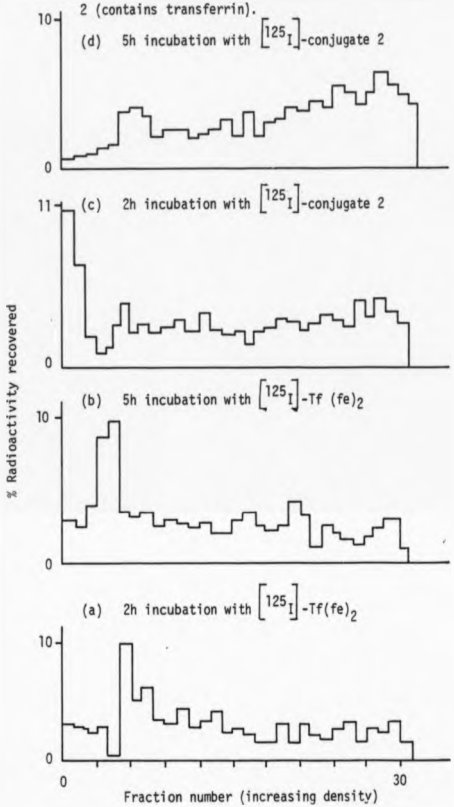

earlier (5.1.3) the lysosomal radioactivity is underestimated because of increased membrane fragility after incubation with radiolabelled ligands (ii) no account of degradation and subsequent exocytosis of degradation products was made, therefore the values given in Table 5.2 only reflect the ligand-associated radioactivity present within the lysosome at one instant in time. This would not dramatically alter the values given here for HPMA copolymer and HPMA copolymer conjugates, since no degradation products were detected after incubation of these ligands with fibroblasts (Chapter 4). However, there is a gross underestimation of lysosomal trafficking of all the proteins, which were shown to experience substantial degradation, followed by exocytosis of degradation products (Chapter 4).

The design of these subcellular fractionation experiments resulted in a number of inherent problems. Firstly, visualisation of the subcellular routing of ^{125}I-labelled substrates was difficult and could be improved by use of a pulse-chase incubation. Secondly, the problem of increased lysosomal fragility, resulting in approximately 30% lysosomal breakage, was not easily resolved. Less severe conditions of homogenisation resulted in a higher percentage of intact cells, which necessarily had to be removed from the homogenate prior to application to the gradient. The experimental conditions used here represent the best compromise which could be found. It was not considered acceptable to add radioactivity attributable to burst lysosomes to the radioactivity detected in fractions 21-30 (lysosomal density) since the original density of the burst lysosomes was not known. It was possible that the observed increase in membrane fragility was a result of loading the lysosomes with ligand, which was then only slowly degraded. This assumption is supported by the fact that <10% of the lysosomes of control fibroblasts (which had not

been incubated with ligand) burst. However, it cannot explain why increased lysosomal fragility was evident in experiments where little substrate was located within the lysosome. This is difficult to explain, but may result from the presence of a radiolabelled substrate within the lysosome affecting, in some unknown manner, the lysosomal membrane.

With these limitations in mind a number of interesting findings emerged:

(1) Conjugation of protein, in particular transferrin, to HPMA copolymer altered the sub-cellular processing of the constituent protein. The subcellular localisation of unconjugated transferrin has been studied at length elsewhere, and data presented here are in accordance with these published results (Harding, et al., 1984; Forsbeck, et al., 1986; Gorman & Poretz, 1987). This is true even though the composition, shape and starting density of the gradients used here were not identical to those used previously. There was little difference in the subcellular localisation of transferrin after 2h or 5h. This was in accordance with the accepted model of transferrin-receptor interaction (Chapter 4, 4.1), where it is proposed that the majority of transferrin recycles (thus at any one time very little is resident inside the cell) with the remainder entering the lysosomes (Neutra, et al., 1985; Hunt, et al., 1986; Gorman & Poretz, 1987; Stoorvogel, et al. 1987). Lack of any accumulation of transferrin in the lysosomes agreed with the results presented in Chapter 4 (Fig. 4.5) where degradation coupled with exocytosis of the degradation products of most of the transferrin which had entered the lysosome was shown.

After conjugation of transferrin to HPMA copolymer its subcellular localisation was altered. The presence of conjugate-associated radioactivity at a density lower than that of

plasma membrane was thought to be due to dissociated ligand. It is possible that the stoichiometry of protein to polymer (Chapter 3, $Tf(HPMA)_{10}$) is hindering the tight union of the HPMA-conjugated transferrin with its receptor, resulting in a less stable receptor-transferrin complex than is possible for unconjugated transferrin. This could result in removal of conjugate from the cell surface by the shearing action of homogenisation. Also, EDTA (1mM) was used in all solutions (to prevent clumping of organelles). This would remove Ca^{2+}, which could possibly influence the binding of transferrin and conjugate 2 differentially.

After internalisation it appeared that conjugate 2 was directed to the lysosome rather than regurgitated. In previous experiments (Chapter 4) no degradation products had been detected after a 3h incubation of fibroblasts with transferrin-HPMA copolymer. In accordance with these data a build up of conjugate at the density of the lysosomal compartment was detected between 2h and 5h.

(2) The importance of molecular weight on the subcellular localisation of an antibody-HPMA copolymer conjugate was clearly seen by a comparison of the distribution of radioactivity on the gradient after subcellular fractionation of the two preparations of IgG-HPMA copolymer conjugate. The first preparation of conjugate 3 ($\bar{M}w>>2x10^6$ Daltons; Chapter 3) was shown to have limited ability to gain access to the interior of the cell. After 24h only 6% of the total conjugate-associated radioactivity was found at the density equating with that of the lysosomal enzyme marker (Table 5.2). This contrasted with the second preparation ($\bar{M}w>2x10^6$ Daltons; Chapter 3) in which between 30% and 42% (5h, 2h; Table 5.2) of conjugate-associated radioactivity was detected at the density of the lysosomal enzyme marker. The observed decrease in the proportion of radioactivity detected in the lysosomal region of the gradient

between 2h and 5h may be due to some degradation of conjugate, coupled with release of degradation products, or it may simply reflect the build up of a higher proportion of radioactivity in the pre-lysosomal region of the gradient.

(3) The density of the lysosomal compartment was affected by the presence of certain ^{125}I-labelled substrates. In experiments investigating the subcellular localisation of IgG, a large percentage of radioactivity (13%, 5h) was detected at a density higher than that of the lysosomes, that is, at the bottom of the tube. This is difficult to explain, but could be due to lysosomes heavily loaded with IgG, since a profile of hexosaminidase in these fractions was similar (Fig. 5.5). This explanation is in accordance with the results of Schneider, et al. (1981), who found that after 24h fibroblasts accumulate $F(ab')_2$-type fragments in the lysosome due to incomplete degradation of IgG.

(4) The influence of a target antigen/receptor on intracellular routing was indicated by the different gradient profile of McAb B3/25 determined here, and that of anti-plasma membrane antibody described by Schneider, et al. (1979). Whereas here 41% of McAb B3/25 was detected at densities corresponding to the lysosomal compartment after 5h, Schneider, et al. (1979) detected little internalisation of bound anti-plasma membrane antibody after 36h. Such a contrast in the behaviour of antibodies, specific for cell-surface antigens, exemplifies the importance of choosing an antigen which offers a "gateway" to the cell's interior.

The subcellular localisation of conjugate 5 (containing McAb B3/25) could not be easily resolved, due to the high percentage of unconjugated HPMA copolymer (as discussed previously Chapter 3; 3.2). In Chapter 4 it was shown that no degradation products could be detected for HPMA copolymer or conjugate 5 (containing McAb B3/25)

after incubation with fibroblasts. This allows a comparison of the percentage lysosomal-associated radioactivity of these ligands to be made using Table 5.2, where it can be seen that proportionally more of the conjugate is localised within the lysosome than parent HPMA copolymer.

The results presented here show that all the HPMA copolymer conjugates, with all their inherent problems, such as inappropriate $\bar{M}w$, stoichiometry, and undefined orientation of the protein residue (see Chapter 3), are internalised by fibroblasts and eventually localise within the lysosome. This was true even for the very heavy conjugate containing IgG. This route of intracellular processing is central to the design of any lysosomotropic drug-carrier.

CHAPTER 6

Determination of the transferrin receptor density and ligand affinity using ^{125}I-labelled transferrin (both apo and diferric), McAb B3/25, HPMA copolymer conjugated to IgG or transferrin, and a number of different cell lines

6.1 INTRODUCTION

The transferrin receptor is not a tumour-specific antigen, indeed a number of cell types express the receptor (Tables 6.2 and 6.3). It is, however, a tumour-associated antigen (Gatter, et al., 1983; Trowbridge, 1985). Recent evidence has shown that the transferrin receptor may be composed of a family of antigenically similar molecules and that the density of the receptor is related to the rate of cell growth, or differentiation of tumour cells (Gatter, et al., 1987). Indeed Trowbridge, et al. (1981) have reported selective inhibition of human melanoma growth in nude mice using anti-transferrin receptor antibody.

There have been conflicting reports in the literature concerning the differential ability of transferrin, in its iron loaded and unloaded forms, to bind to the transferrin receptor. Hamilton, et al. (1979), Ward, et al. (1982) and Hopkins & Trowbridge (1983) have reported that the degree of iron saturation did not affect the binding of transferrin to its receptor. This conflicted with a reported lack of affinity of apotransferrin for the receptor at physiological pH (reviewed Hunt, 1986). The work presented in Chapter 4 indicated that there was little difference in the uptake and degradation of transferrin in its iron loaded and unloaded forms. Scatchard analysis of transferrin binding allowed the nature of this interaction to be determined in terms of non-specific and specific binding.

In the area of targeted drug-delivery choice of a potential targeting residue, be it monoclonal antibody or a protein specific for a receptor, will be influenced by the affinity of the target residue for its target antigen/receptor. In this Chapter a comparative study has been made of the number of binding sites available to, and the affinity of McAb B3/25 and transferrin for

these sites. Since it has been reported (Trowbridge & Omary, 1981; Gatter, et al., 1983) that the density of the transferrin receptor is dependent upon both cell type and state of differentiation, a number of cell lines were used, and also CCRF/CEM subcultured at two different frequencies.

In Chapter 4 it was shown that uptake of HPMA was increased following conjugation to McAb B3/25, IgG, or transferrin. In the work which follows, the nature of the interaction between HPMA copolymer-protein conjugates and fibroblasts was determined in terms of specificity and affinity of binding. Unfortunately, because of the difficulty in purification of conjugate 5 (Chapter 3), it was not possible to characterise the cell surface interaction of HPMA copolymer conjugated to McAb B3/25.

6.1.1 Methods

A description of the cell lines used is given in Table 6.1.

Graphical representation of the data is given only for the interaction of transferrin, McAb B3/25 and protein-HPMA copoymer conjugates with fibroblasts, otherwise results are summarised in Tables 6.2, 6.3, 6.4.

In this study "specific binding" was used to define cell surface-bound ^{125}I-labelled ligand which could not be removed by a large excess (usually 1000-fold) of unlabelled ligand and which was shown (Scatchard analysis) to have a high affinity for its target antigen/receptor.

"Non-specific/low affinity binding" was used to define cell surface bound ^{125}I-labelled ligand which was readily removed by an excess of unlabelled ligand and which was shown (Scatchard analysis) to have a low affinity for its binding site.

Table 6.1

Details of cell lines.

Name of cell line	Characteristics	*Cells mg^{-1} protein
Human skin fibroblasts	normal	2.2×10^6
CCRF/CEM	human T-cell leukaemia, transformed at pre-T cell stage	2.2×10^6
Hep G_2	human hepatoma	2.14×10^6
Alexander	human hepatoma	2.14×10^6
Clone M_3	murine melanoma	2.14×10^6

* determined by relating cell counts (haemocytometer) to protein content (Lowry)

6.1.2 Calculations

Calculations used in this Chapter are given in Chapter 2, Section 2.2.7.1.

6.2 RESULTS

6.2.1 Density of the transferrin receptor on the cell surface of fibroblasts determined by ^{125}I-labelled transferrin or McAb B3/25.

(i) Diferric transferrin

At low concentrations (0-50pm ml^{-1}) a plateau of specific-binding was seen (Fig. 6.1a) at 0.6pm ligand bound mg^{-1} cell protein. Above 50pm $Tf(Fe)_2 ml^{-1}$ an additional low-affinity/non-specific interaction was seen, which itself plateaued at 1.45pm of ligand bound per mg cell protein (Fig. 6.1b).

Competitive binding of ^{125}I-labelled $Tf(Fe)_2$ with $Tf(Fe)_2$ showed that in the concentration range of ligand subsequently used for Scatchard analysis, low-affinity/non-specific binding accounted for only 8% of the total binding (Fig. 6.1c).

Scatchard analysis of binding (Fig. 6.1d) gave a $Tf(Fe)_2$-receptor interaction which was 92% specific, with a calculated receptor density of 2.26×10^5 receptors $cell^{-1}$, and a calculated affinity of $8.18 \times 10^7 M^{-1}$.

(ii) Apotransferrin

At low concentrations (0-50pm ml^{-1}) a specific component of binding was seen (Fig. 6.2a) which plateaued at approximately 0.9pm apotransferrin bound mg^{-1} cell protein. At higher concentrations this specific-binding was masked by an excess of low-affinity/non-specific binding (Fig. 6.2b) which reached a plateau at approximately 8pm apotransferrin bound mg^{-1} cell protein. Competitive binding of ^{125}I-labelled apotransferrin with unlabelled apotransferrin (graph not shown) showed that this low-affinity/non-specific component contributed 50% of the total

Fig. 6.1 Binding of diferric transferrin to human fibroblasts.

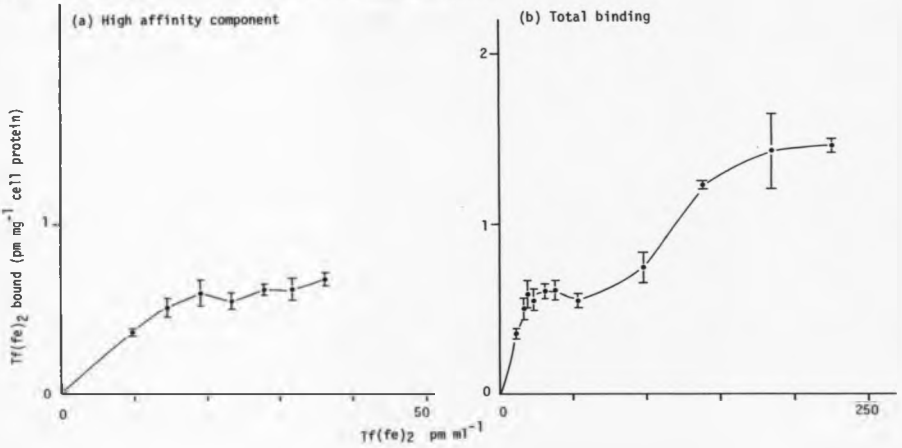

Fig. 6.1 contd...

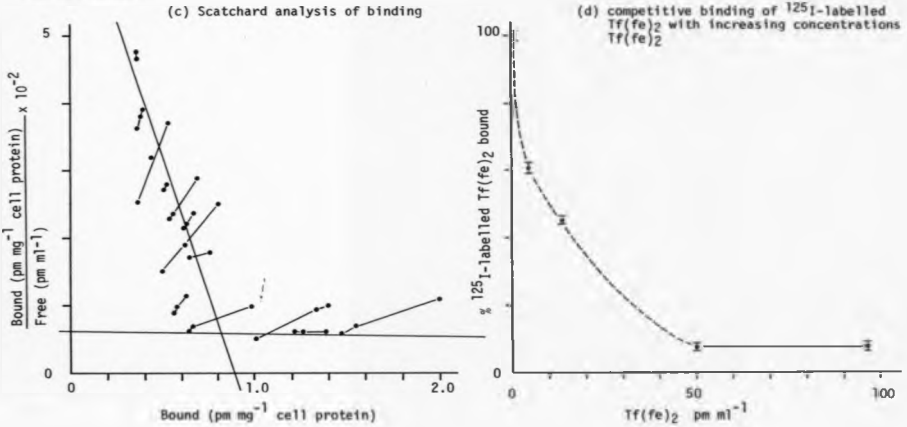
(c) Scatchard analysis of binding
Bound (pm mg-1 cell protein) / Free (pm ml-1) x 10-2
5
0
0
1.0
2.0
Bound (pm mg-1 cell protein)
(d) competitive binding of 125I-labelled Tf(fe)2 with increasing concentrations Tf(fe)2
% 125I-labelled Tf(fe)2 bound
100
0
0
50
100
Tf(fe)2 pm ml-1

Fig. 6.2 Binding of apotransferrin to human fibroblasts.

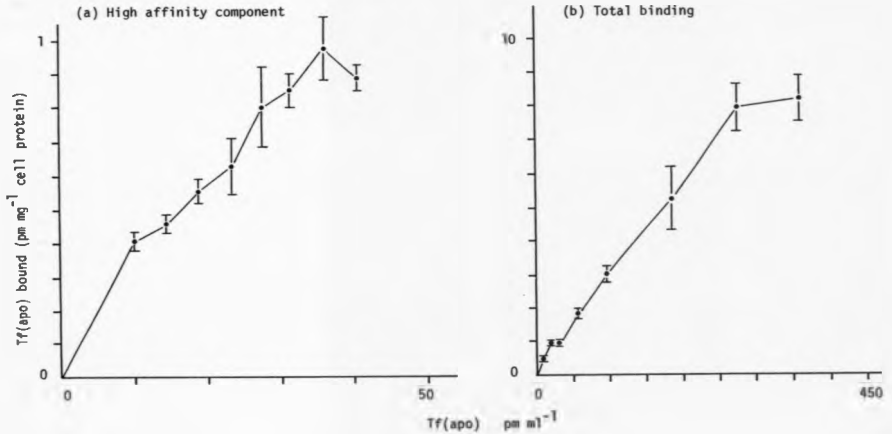

Fig. 6.2 contd...

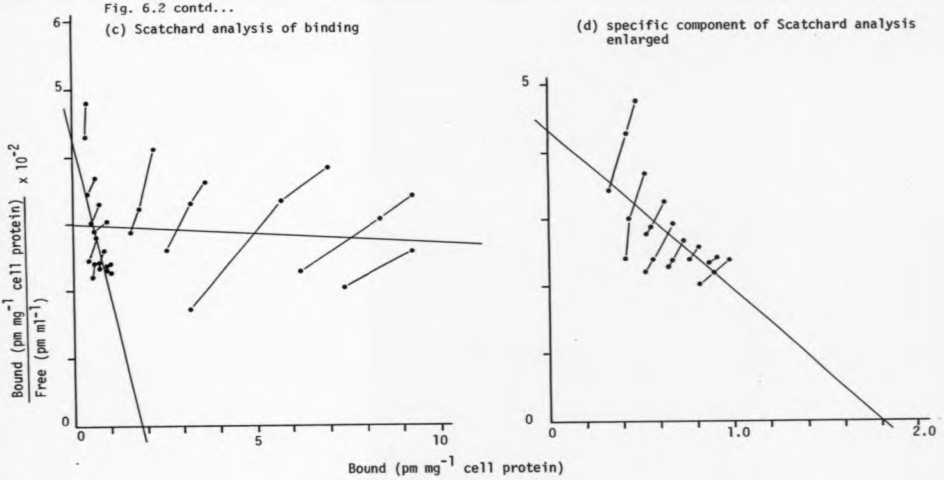
(c) Scatchard analysis of binding
(d) specific component of Scatchard analysis enlarged
Bound (pm mg^{-1} cell protein) / Free (pm ml^{-1}) x 10^{-2}
Bound (pm mg^{-1} cell protein)
0
5
10
1.0
2.0
6

binding in concentration range subsequently used for the Scatchard analysis.

Scatchard analysis of binding gave an apotransferrin-receptor interaction which was 50% specific (Fig. 6.2c), with a calculated receptor density of 2.47×10^5 receptors $cell^{-1}$ and a calculated affinity of $2.76 \times 10^7 M^{-1}$.

(iii) Monoclonal antibody B3/25

At low concentrations (0-20pm ml^{-1}) a plateau of specific binding was seen (Fig. 6.3a) at 0.75pm McAb B3/25 bound mg^{-1} cell protein. At higher concentrations binding seemed to level slightly at approximately 1.25pm antibody bound mg $cell^{-1}$ protein (possibly Fc interaction) followed by a non-saturated non-specific binding (Fig. 6.3b).

Competitive binding of labelled and unlabelled McAb B3/25 (graph not shown) showed a 0.68% non-specific component of binding in the concentration range of antibody to be used in the Scatchard analysis.

Scatchard analysis of binding (Fig. 6.3c) gave a McAb B3/25-transferrin receptor interaction which was >99% specific with a calculated 2.4×10^5 binding sites $cell^{-1}$ and a calculated affinity of $3.9 \times 10^8 M^{-1}$.

A comparison of binding of transferrin and McAb B3/25 is given in Table 6.2. It can be seen that the calculated receptor density was independent of the ligand used. Also, the affinity of McAb B3/25 for the receptor was highest with apotransferrin having the least affinity.

6.2.2 Density of the transferrin receptor on the cell surface of CCRF/CEM cells sub-cultured at two different frequencies

Scatchard analysis of CCRF/CEM subcultured every 5 days gave a calculated receptor density of 1.71×10^7 $cell^{-1}$ with a Ka $1.37 \times 10^8 M^{-1}$ (binding of McAb B3/25) and 1.87×10^7 receptor $cell^{-1}$ with Ka 3.09×10^7

Fig. 6.3 Binding of monoclonal antibody B3/25 (specific for the transferrin receptor) to human fibroblasts.

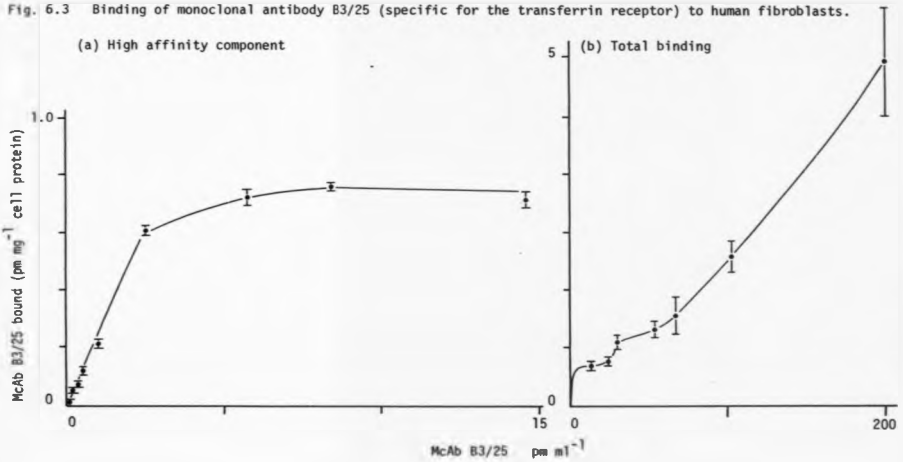

Fig. 6.3 contd...

(c) Scatchard analysis of binding

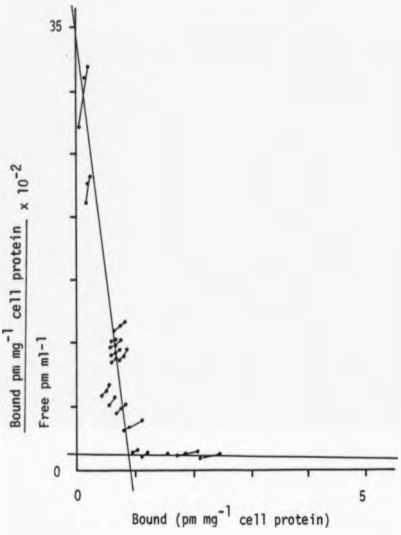

Table 6.2

A summary of transferrin receptor density and ligand affinity.

Ligand	Density transferrin receptor $cell^{-1}$	Ka (M^{-1})
(a) Human skin fibroblast cells		
$Tf(Fe)_2$	2.26×10^5	8.18×10^7
Tf(apo)	2.47×10^5	2.78×10^7
B3/25	2.44×10^5	3.9×10^8
(b) CCRF/CEM) (i) subcultured every 5 days		
$Tf(Fe)_2$	1.86×10^7	3.09×10^7
B3/25	1.71×10^7	1.37×10^8
(ii) subcultured every 8 days		
$Tf(Fe)_2$	1.54×10^6	2.45×10^8

(binding of $Tf(fe)_2$) (Table 6.2). This compared with $1.54x10^5$ receptors $cell^{-1}$ with a Ka of $2.45x10^8 M^{-1}$ determined (binding of $Tf(fe)_2$) using CCRF/CEM subcultured every 8 days. Competitive binding of labelled with non-labelled ligand (data not shown) showed that in addition to this specific component of binding there was a 28% low-affinity/non-specific contribution to $Tf(fe)_2$ binding and 0.7% to McAb B3/25 binding.

6.2.3 Density of the transferrin receptor on the cell surface of a variety of different cell lines

All cell lines (Table 6.1) were grown to confluence or equivalent.

Receptor densities and affinities are summarised in Table 6.3. By comparing Tables 6.2 and 6.3 it can be seen that the affinity of McAb B3/25 for the transferrin receptor is usually higher than that of $Tf(fe)_2$. Also, if a comparison is made between the different cell lines it appears that an inverse relationship exists between the density of the transferrin receptor and the affinity of $Tf(fe)_2$ for its receptor. That is, the affinity of $Tf(fe)_2$ for its receptor is lower (Clone M_3, $4.97x10^7$, fibroblasts $8.18x10^7$) when cells have a higher density of receptor (for example Clone M_2, $5.4x10^4$ compared with fibroblasts, $2.4x10^5$). This relationship was also seen when CCRF were subcultured at different frequencies. However, such a pronounced relationship between receptor number and affinity is not seen with the binding of McAb B3/25 (Table 6.3; compare Hep G_2, receptor density $7.17x10^4$ $cell^{-1}$, Ka $3.91x10^8$; CCRF, receptor density $1.71x10^7$ cell, Ka $1.37x10^8$).

6.2.4 The density of fibroblast cell surface binding-sites available to HPMA copolymer conjugate 2 (contains transferrin) and conjugate 3 (contains IgG), and the affinity of binding of conjugates for these sites.

Table 6.3

Transferrin receptor density and ligand affinity on a number of cell lines.

cell type	Ligand	Transferrin receptor density $cell^{-1}$	Ka (M^{-1})
Hep G_2	McAb B3/25	7.17×10^4	2.91×10^8
Alexander	$Tf(fe)_2$	8.30×10^4	1.41×10^8
Clone M_3	$Tf(fe)_2$	5.40×10^4	4.97×10^7

HPMA copolymer conjugated to IgG (preparation 1) showed limited ability to bind to the cell surface of fibroblasts (Chapter 4). However, Scatchard analysis showed that a large percentage of this binding was specific (Fig. 6.4a,b) as defined by the high binding affinity of conjugate for the fibroblast cell surface (Table 6.4). Unfortunately, due to the limited supply of conjugate it was not possible to perform the competitive binding experiments necessary to quantitate the percentage of non-specific binding. However, with this limitation in mind there was found to be maximum binding of 2.17×10^{-15} moles of conjugate mg^{-1} cell protein (assuming that one mole of conjugate bound to one mole of binding sites), or 5.94×10^{2} binding sites $cell^{-1}$. Surprisingly the affinity of binding was very high, 4.76×10^{13} M^{-1}, but this is probably due to avidity rather than affinity (see Discussion 6.3).

In Chapter 4 it was shown that the uptake of transferrin was independent of iron-loading. Here it was shown that both apotransferrin and diferric transferrin are able to bind specifically to the transferrin receptor. For these reasons no attempt was made to determine the degree of iron loading of conjugated transferrin.

Transferrin bound to HPMA copolymer retained its ability to bind specifically to the cell surface (Fig. 6.5a,b) with maximum binding of 2.08×10^{-11} moles mg^{-1} cell protein, or 5.96×10^{6} binding sites per cell (assuming 1 mole conjugate bound to 1 mole of binding sites). Again it was not possible to assess the non-specific contribution to this figure, although the Scatchard plot (Fig. 6.6b) indicates that it will not be very large. The affinity of the HPMA copolymer-transferrin conjugate was found to be 1.25×10^{6} M^{-1}, which was 22-times lower than that of apotransferrin (Table 6.4).

Fig. 6.4 Binding of HPMA copolymer conjugate 3 (contains IgG) to human fibroblasts.

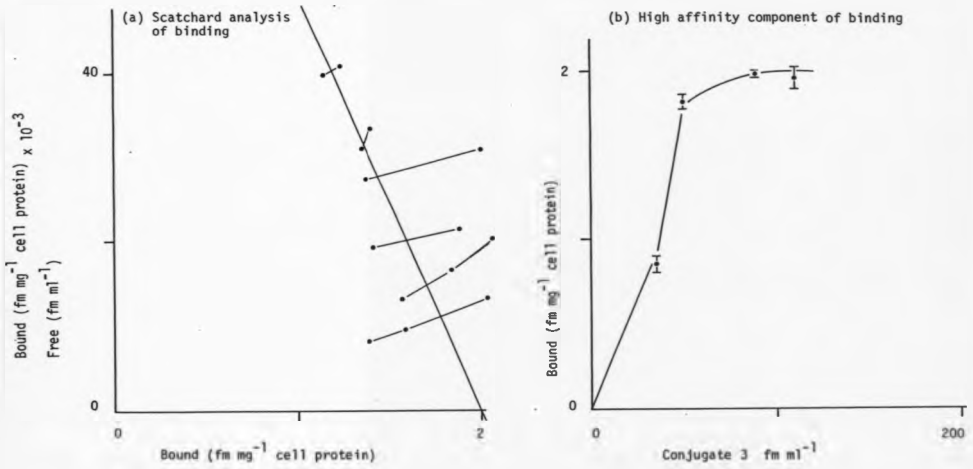

Fig. 6.5 Binding of HPMA copolymer conjugate 2 (contains transferrin) to human fibroblasts.

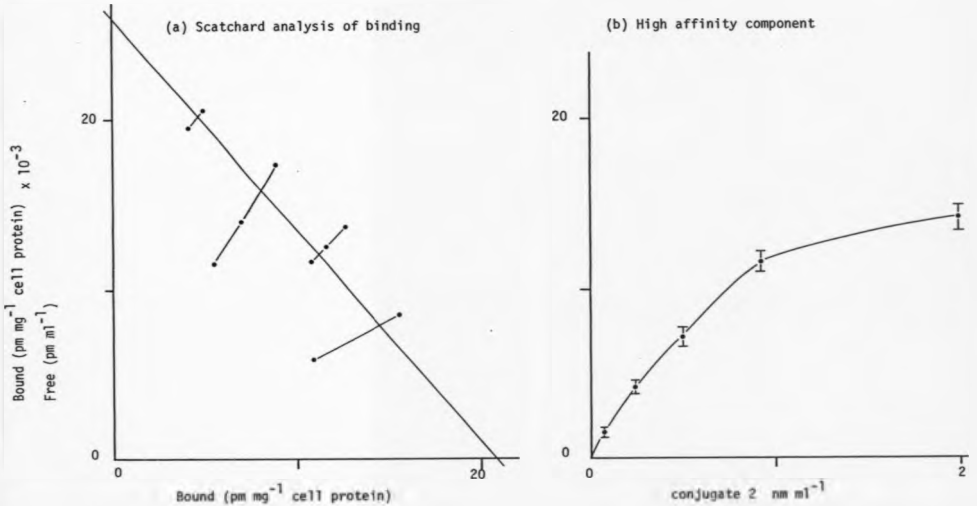

Table 6.4

Comparison of the number of binding sites* on the fibroblast cell surface recognised by HPMA copolymer conjugates 2 (contains transferrin) and 3 (contains IgG).

conjugate	binding sites mg^{-1} cell protein	$Ka^{+}(M^{-1})$
2	5.96×10^{6}	1.25×10^{6}
3	5.94×10^{2}	4.76×10^{10}

*Assuming a 1:1 binding ratio of conjugate to binding site.

+See Discussion

6.3 DISCUSSION

The most important conclusion to be drawn from this study relates to the ability of the HPMA copolymer-protein conjugates to bind to the fibroblast cell surface. It cannot be said with certainty that the transferrin-HPMA copolymer conjugate is still recognising the transferrin receptor, particularly if a comparison is made between the calculated number of transferrin receptors (2.4×10^5 $cell^{-1}$) and the number of binding sites recognised by this conjuate (59.6×10^5). It was very encouraging, however, to find that the conjugate had an affinity for the cell surface, which was only 22-times less than that of the unconjugated protein. Given that this conjugate probably has a stoichiometry of $Tf_1(HPMA)_{10}$ (Chapter 3, 3.2.3) it was not expected that such a high affinity (1.25×10^6 M^{-1}) would be seen. With future improvements in the preparation of this conjugate (see General Discussion) it will be possible to increase dramatically the specificity of HPMA-copolymer bound transferrin for its target receptor.

The large IgG-HPMA copolymer conjugate (Chapter 3; Mw>>2M Daltons) seemed to bind specifically to a large number of binding sites (5.94×10^2). This degree of specific binding had not been expected for a conjugate which was so removed from an ideal molecular weight and stoichiometry. Interestingly, the calculated affinity of this conjugate was very high (4.76×10^{13} M^{-1}). Given that this conjugate probably contained at least 10 antibody molecules (Chapter 3, 3.2.3), and with the resulting possibility of more than one antibody molecule having the ability to recognise the cell surface at any one time, it is possible that the calculated affinity constant is a measure of avidity rather than affinity. That is, the binding of this conjugate to the fibroblast cell surface is a multivalent phenomenon, whereas affinity is used to define a monovalent

interaction between antibody and antigen. As a result the calculated Ka is in fact attributable to the summation of the affinities of these monovalent interactions (see Thompson & Jackson,1984) and as a consequence, the calculated number of binding sites will be underestimated since there was not a 1:1 binding ratio of conjugate to binding site. A consideration of avidity rather than affinity will be important in the future development of antibody-targeted drug-carriers, particularly if consideration is made of the possibility of using combinations of $F(ab')_2$ fragments of different specificity attached to HPMA copolymer as potential targeting residues (see General Discussion).

The affinity and specificity of a targeting residue for its target antigen/receptor is of obvious importance in targeted drug-delivery. In this Chapter it was shown that although apotransferrin was able to bind to the same number of receptors as diferric transferrin, there was an additional large (50%) component of non-specific binding inappropriate to targeted drug-delivery. This view, however, may be too naive since in vivo the drug-carrier will experience a far more complicated environment, where there are many factors, such as transferrin recycling in the absence of bound ligand (Ajioka & Kaplan, 1986; Stein & Sussman, 1986), local falls in pH (apotransferrin is reported to have a higher affinity for the transferrin receptor a low pH; reviewed Dautry-Varsat, 1986) which could give apotransferrin some advantage as a targeting residue.

The affinity of McAb B3/25 for the transferrin receptor was consistently higher than that of transferrin, and importantly this affinity was not inversely related to transferrin receptor density (as was found for transferrin). This observation together with the calculated >99% specificity of binding of McAb B3/25 indicates that McAb B3/25 is a more appropriate targeting residue for HPMA copolymer

conjugates directed to the transferrin receptor than transferrin per se. Unfortunately it was not possible to determine the effect of conjugation of McAb B3/25 to HPMA copolymer on binding to the fibroblast cell surface. Results presented previously (Chapter 4) indicate that there is interference with cell surface interaction of the antibody following conjugation to HPMA (Chapter 3, stoichiometry probably $Ab(HPMA)_{20}$).

If the transferrin receptor is to be used as a potential targeting site, it would be an advantage if the target cells expressed a higher density of receptor. Oudermans, et al. (1986) have shown that the transferrin receptor density on B-lymphoma is increased when cells are encouraged to proliferate (Concanavalin A), Testa, et al. (1986) have found that the erythroleukaemic cell lines (K562 & HEL) synthesize transferrin at an enhanced rate after subculture, at low density, into fresh medium. In agreement with these published results transferrin receptor density was found here to be higher on CCRF/CEM which had been encouraged to proliferate rapidly. Also, a positive relationship between transferrin receptor density and malignancy was indicated by the 5-fold higher density of receptor on CCRF/CEM (subcultured every 8 days) than fibroblasts (subcultured every 7 days). However, the data presented in this Chapter and also the published work of Oudermans (1986), and Testa (1986) indicated that a direct comparison of the transferrin receptor density between different cell lines, grown in different laboratories, under different conditions, may be difficult. Table 6.2 shows that simply varying the frequency of subculturing made a dramatic difference to the density of receptor measured on CCRF/CEM.

Rapidly proliferating cancer cells will be targets for HPMA copolymer-antibody conjugates. A problem when using the transferrin receptor as the target antigen/receptor is the amount of these

conjugates which will localize at normal, rapidly dividing cells (Table 6.5). For this reason the body distribution of these conjugates, was investigated in mice. Tsavaler (1986) had shown the ability of transferrin to bind interspecies and this observation, together with the ability of human transferrin to bind to murine Clone M_3 (Table 6.3) and the reported high degree of sequence homology between the human and mouse transferrin receptor (Schneider & Williams, 1985) supported the feasibility of testing the conjugates used here in DBA_2 mice (Chapter 8).

Table 6.5

A summary of published values for the transferrin receptor density and its affinity for diferric transferrin.

Cell type	density of transferrin receptor $cell^{-1}$	Ka (M^{-1})	Reference
Be Wo; choriocarcinoma	$3.7x10^5$	$4.2\ 2.1x10^8$	Hamilton, et al, 1979
K562; erythroleukaemic	$1.2x10^5$	$1.5x10^8$	Besancon, et al, 1985
	$2.65\text{-}5.9x10^5$	$1.1x10^8$	Lazarus, et al, 1985
	$2x10^5$	$1x10^9$	van Renswoude, et al, 1982
HeLa; cervical carcinoma	$1.8\text{-}3.7x10^6$	$2.7x10^8$	Ward, et al, 1982
Daudi; Burkitt lymphoma	$7.5x10^4$	$2.5x10^8$	Besancon, et al, 1985
A431; human carcinoma	$5x10^4$	N.D.	Hopkins & Trowbridge, 1983
PMC-22B; melanoma	$6.9x10^4$	$1.4x10^9$	Musgrove, et al, 1984
Rat liver	$2.7x10^5$	$5.2x10^6$	Morgan, et al, 1986
Rat brain	ND	$1.0x10^9$	Hill, et al, 1985
Rat hepatocytes	$4\text{-}6x10^4$	N.D.	Bomford & Munro, 1985
Rat embryo fibroblasts	$6\text{-}10x10^4$	$1.1x10^7$	Octave, et al, 1981
Hep G2 (Table 6.1)	$5.1x10^4$	N.D.	Wu & Wu, 1986
CCRF (Table 6.1)	$1.9x10^5$	$1.20x10^9$	Musgrove, et al, 1984

(Details of first isolation of these cell lines can be found in the "Flow catalogue").

CHAPTER 7

Body distribution of ^{125}I-labelled diferric transferrin, McAb B3/25, HPMA copolymer and HPMA copolymer conjugated to these proteins, after intravenous administration to DBA_2 male mice

7.1 INTRODUCTION

The ability of HPMA-copolymer conjugates, containing McAb B3/25 or transferrin, to bind to cell-surface transferrin receptors and undergo subsequent internalisation, has been described in Chapters 4 and 5. However, the *in vitro* evaluation of these conjugates gives only a basic indication of their potential for use in targeted drug delivery. Therefore, it was considered necessary to examine the distribution of these conjugates in the more complicated *in vivo* milieu. HPMA copolymer conjugates used in this study contained human transferrin, or anti-human transferrin-receptor antibody. The feasibility of using these conjugates to determine body distribution in mice was supported by the ability of transferrin to bind interspecies (Chapter 6; Tsavaler, *et al.*, 1986), together with the large percentage of homology between the mouse and human transferrin receptor (Schneider & Williams, 1985).

The transferrin receptor is present on most, if not all, nucleated cells, in particular cells which are rapidly dividing (see Chapter 1, 1.4.1; reviewed by May and Cuatrecasas, 1985). This indicates that, like the Thy-1 antigen, (Chapter 8) the transferrin receptor may be far from ideal as an antigen for use in targeted drug-delivery (see Chapter 1, 1.3.3). However, Omary, *et al.* (1980) have shown that the transferrin receptor is an important immunodominant surface-antigen on cultured human tumour cells, and this observation, together with data from Gatter, *et al.* (1983) who showed that transferrin receptors have a restricted distribution *in vivo* indicate that this receptor may indeed be useful in promoting targeted drug-delivery. The efficiency of targeting *in vivo*, however, remains unclear. Gatter, *et al.* (1983) have shown that in normal cells the transferrin receptor is localised mainly in the basal epidermis (skin, tongue, tonsil, oesophagus, cervix), the

endocrine pancreas, liver (hepatocytes and Kupffer cells), testes, kidney, stomach and the pituitary. In contrast, a wide distribution of the receptor was found in carcinomas and sarcomas. Antibodies against the transferrin receptor (which were known to block receptor function, that is, unlike B3/25) have been shown to inhibit growth of transplanted syngeneic AKR/J SL-2 leukaemic cells in AKR/J male mice (Sauvage, et al., 1987).

Experiments carried out in this Chapter set out to determine the body distribution of transferrin, anti-transferrin receptor antibody (McAb B3/25) and polymer conjugates containing these proteins, to assess the possibility of using these conjugates to accomplish an altered body distribution of drug. The body distribution of ^{125}I-labelled HPMA copolymer, McAb B3/25, diferric transferrin, and HPMA copolymer bound to either B3/25 (conjugate 5) or transferrin (conjugate 2) was determined 5h after iv administration to DBA_2 male mice (approximate age 16 weeks). No attempt was made to determine the iron saturation of the transferrin since the receptor-binding of apotransferrin and diferric transferrin have been shown to be very similar (Chapter 4 and 6).

7.1.1 Calculations

Calculations used in this Chapter are as given in Chapter 2 Section 2.2.8.1.

7.2 RESULTS

The body distributions of ^{125}I-labelled proteins, (McAb B3/25 and $Tf(fe)_2$) HPMA copolymer, and HPMA copolymer conjugated to either of these proteins (including the data extrapolated for conjugate 5) are summarised in Table 7.1.

The body distribution of ^{125}I-labelled HPMA copolymer was quite different from that observed for both the proteins (McAb B3/25 and $Tf(fe)_2$). There was obviously much more radioactivity in the urine

Table 7.1

Body distribution (% administered dose) of ^{125}I-labelled HPMA copolymer, McAb B3/25, $Tf(fe)_2$ and HPMA copolymer conjugates 2 (contains transferrin) and 5 (contains McAb B3/25) 5h after i.v. administration to male DBA_2 mice (approximate age 16 weeks).

organ	HPMA copolymer (I)	B3/25	conjugate 5	$Tf(Fe)_2$	conjugate 2
Heart	0.03±0.002	0.93±0.17	0.41±0.08	0.34±0.07	0.76±0.13
Liver	0.5±0.3	5.01±0.72	3.81±1.17	8.03±0.48	5.58±0.22
Lung	0.14±0.05	1.07±0.18	1.0±0.09	0.56±0.11	0.63±0.25
Kidney	0.44±0.03	2.43±0.51	1.27±0.2	1.08±0.06	2.44±0.25
Spleen	0.02±0	0.3±0.04	0.3±0.02	0.14±0.02	0.36±0.04
Thymus	0.006±0.001	0.073±0.002	0.05±0.01	0.05±0.001	0.1±0.02
Lymph	0.08±0.007	0.5±0.04	0.68±0.2	0.46±0.06	0.53±0.04
Stomach	1.06±0.69	1.32±0.2	5.44±0.9	2.54±0.55	1.79±0.18
Intestine	5.44±2.8	4.42±0.44	4.58±2.73	2.94±0.19	4.6±0.6
Skin	1.81±0.04	5.16±0.4	4.92±2.73	4.50±0.14	5.18±0.58
Bone	1.18±0.26	10.28±1.61	5.72±0.6	5.32±0.28	8.36±0.36
Urine	49.37±6.44	5.48±0.79	-	15.23±3.58	6.54±1.47
Faeces	3.73±1.78	0.14±0.07	0.27±0.2	0.53±0.27	1.07±0.4
Blood	2.51±0.19	36.32±2.46	54.83±2.3	12.63±1.45	57.71±2.49
Recovery	66.31±1.5	74.36±2.3	96.38±0.5	56.35±3.1	95.67±0.9

after administration of HPMA copolymer (that is, 49.4% for polymer; 5.5-15.2% for proteins). Second, there was a much higher percentage (administered dose) of protein-associated radioactivity in the blood (that is, 12.7-36.3% proteins; 2.5% polymer). The level of radioactivity detected in the bloodstream (5h) after administration of antibody was 3-times higher than that observed with transferrin.

Conjugation of HPMA copolymer to either transferrin, or McAb B3/25, resulted in a marked alteration in body distribution. The distribution of conjugates was closer to that seen previously for the radiolabelled-proteins than that of radiolabelled-HPMA copolymer. The HPMA-copolymer conjugates were retained in the bloodstream (2.5%, HPMA; 57.5% conjugate 2; 54.8% conjugate 5) and showed a parallel decrease in the radioactivity detected in the urine (49.4%, HPMA; 6.5% conjugate 2; 0% extrapolated for conjugate 5). In most organs (heart, liver, kidney, thymus, submaxillary glands plus attached lymph nodes, bone marrow) the percentage (administered dose) localisation of conjugate was comparable to that measured for unconjugated protein, but was approximately 10-times higher than that seen for HPMA copolymer.

After administration of radiolabelled proteins, and both the HPMA copolymer-protein conjugates, radioactivity was principally found in the liver, stomach, intestine, skin and bone marrow. Uptake of protein by the liver was slightly reduced after conjugation of the protein to HPMA copolymer.

It is interesting to note that >95% of the administered dose of conjugates 2 and 5 was recovered from the organs selected for analysis. In comparison this fell to between 56-74% when using $Tf(Fe)_2$ or McAb.

7.3 DISCUSSION

The body distributions of unconjugated protein (anti-human transferrin receptor McAb B3/25, human transferrin) and the HPMA copolymer conjugates 2 (containing transferrin) and 5 (containing McAb B3/25), described in this Chapter were consistent with binding of these ligands to the mouse transferrin receptor, and with accumulation by rapidly dividing cells known to be the natural target for transferrin. Body distributions for DBA_2 mice are consistent with the findings of Sauvage, et al. (1987) who administered McAb R17 207 and REM 17.2 (which are both specific for, and block the function of, the transferrin receptor) intraperitoneally to 6-8 week old AKRJ mice. The experiments described in this Chapter, however, followed the distribution of administered ligand over a 5h period (in contrast with the 24h used by Sauvage, et al. (1987)) to allow direct comparison of the results with those of HPMA conjugated to the anti-Thy 1.2 antibody (Chapter 8). Also, the proteins and conjugates were all administered intravenously, which was considered to have more relevance to a clinical situation. For this reason larger, 16-week old mice were used rather than 6-8 week old mice used by Sauvage.

The 56-74% recovery (of administered dose) of $Tf(Fe)_2$ and McAb B3/25 implied that these proteins were also present in tissues other than those chosen for study in this chapter, perhaps the brain. This would be consistent with the known existence of transferrin receptors, with a high affinity for transferrin, in rat brain (Hill et al., 1985). Recovery of both HPMA copolymer conjugates was much higher (>95%). The high molecular weights (Chapter 3, 3.2.3) of these conjugates would probably interfere with extravasation. This assumption was in accordance with the high percentage of conjugate remaining in the bloodstream after 5h. Also, a comparison of

urine-associated radioactivity resulting from low molecular weight degradation products (Table 7.1) indicated that the conjugates were not able to reach target tissues, and undergo subsequent intracellular processing as efficiently as the unconjugated proteins.

In general, it was found that the body distribution of the HPMA copolymer conjugates was independent of the protein targeting-residue used (transferrin, McAb B3/25, or anti-Thy 1.2, see following Chapter 8). These results suggested that either the specificity of the protein was being masked by conjugated HPMA copolymer (Chapter 3, 3.2.3; Chapter 4, 4.3), or that the three conjugates were targeting to the same tissues, but not necessarily the same cells. The latter explanation is in accordance with the similar body distributions of unconjugated antibodies B3/25 (Table 7.1) and anti-Thy-1.2 (Chapter 8, Table 8.4) 5h after i.v. administration to mice aged approximately 16 weeks.

It has been repeatedly cited in the literature that the density of the transferrin receptor is higher on tumour cells than normal cells (reviewed May & Cuatrecasas, 1985; Trowbridge, 1985). There is already evidence that the apparent tumour-associated distribution of the transferrin receptor may be of diagnostic value (Gatter, et al., 1983; see Section 7.1). In fact, it has been proposed that selective tumour cell death, brought about by the natural killer (NK) cells, is related to a high density of the transferrin receptor on the target cells (Herberman & Holden, 1978; Herberman, 1980; Borysiewicz, et al., 1986). This relationship, however, has not been proven, and has been disputed by Bridges & Smith (1985) and Reiber, et al. (1986). It would be interesting to see if there was a preferential tumour localisation of either HPMA copolymer conjugate 2 or 5 after administration to mice bearing tumours, in comparison to the DBA_2 mice used in this chapter. It has been reported that after

conjugation of anti-transferrin receptor antibody to ricin-A chain (Trowbridge & Domingo, 1981) selective cell death of M21 cells in nude mice was achieved. This suggested that there was indeed preferential localisation of antibody at a target tumour. In contrast, however, it has been reported (Trowbridge, 1985) that in some cell lines with equal ability to bind the anti-transferrin receptor antibody, there were differences in response of the cells to the antibody. Such resistance to antibody alone would not be a problem when using HPMA copolymer conjugates specific for the transferrin receptor, since the antibody, or transferrin, would simply be used to facilitate binding of HPMA copolymer conjugate to the cell surface. Cell death would be achieved by the incorporation of drug into the carrier.

The natural targets for transferrin are all rapidly dividing cells. However, these are also the non-specific targets of many chemotherapeutic agents used at present in patients (see Chapter 1, 1.1). Although Sauvage,et al. (1987) have reported no evidence of acute toxicity in normal tissues after administration of anti-transferrin receptor antibody, there could be problems after administration of HPMA copolymer conjugates 2 or 5 containing drug. Rihova,et al. (1985; 1986) have reported pharmacological effects after administration of HPMA copolymer containing both druq (DNM) and targeting residue (anti-Thy-1.2). The data presented in Chapter 8, 8.3) indicated that these pharmacological effects were attributable to localisation of a low percentage (<1% administered dose) of conjugate at the target-organ. The results presented in Chapter 8 and those presented here suggest that the localisation of HPMA copolymer conjugates, "targeted" to the transferrin receptor, present on normal tissues may be sufficiently high to deliver a cytotoxic quantity of drug to those rapidly dividing cells that are already the

non-specific target of drug.

Although the transferrin receptor was considered an ideal *in vitro* model antigen for reasons detailed in Chapter 1 (1.4.1) the clinical relevance of this antigen may be more limited. The transferrin receptor is not a tumour-specific antigen, but it is certainly considered to be a tumour-associated antigen (Trowbridge, 1985). Due to the presence of the receptor on normal cells it may be necessary to use anti-transferrin receptor McAb in combination with other McAbs. Sauvage, *et al.* (1987) used a combination of the anti-Thy-1 antibody (19E12) and the anti-transferrin receptor antibody (R17 208) against Sc-2 leukaemia. An increased survival time of mice receiving combination therapy was shown when compared to mice receiving either antibody alone. The possibility that the anti-transferrin receptor antibody and anti-Thy 1.2 are localising in the same tissues has already been mentioned in relation to the HPMA copolymer conjugates. The relevance of combination therapy to the HPMA copolymer conjugates will be discussed in the General Discussion.

CHAPTER 8

Body distribution of HPMA copolymer conjugates containing anti-Thy-1.2 polyclonal antibody as a potential targeting residue

8.1 INTRODUCTION

Thy-1 is a cell-surface glycoprotein present on mouse thymocytes (Williams & Gagnon, 1982). Molecular weights of 17,800, 18,700 (Williams & Gagnon, 1982) and 25,000 Daltons (Kroczek et al. 1986) have been reported for this glycoprotein. The antigen exist in two allotypic forms, Thy 1.1 and Thy 1.2. The latter form is used as a target antigen in this study.

The structure of Thy-1 is not typical of plasma membrane proteins. Low & Kincade (1985) have shown that the glycoprotein is anchored in the plasma membrane via the lipid, phosphatidylinositol. This observation was supported by Ishihara et al. (1987) who found that the Thy-1 antigen exhibits a lateral diffusion coefficient in the plasma membrane which is similar to that of lipids embedded within the same membrane, but more than 10-times greater than membrane proteins.

The function of the Thy-1 glycoprotein is thought to be that of a "signal transduction molecule". Krozcek et al. (1986) showed that crosslinking of Thy-1, using monoclonal antibodies, resulted in a rapid rise in the level of cytoplasmic free Ca^{2+}. The Thy-1 glycoprotein is not readily internalised (Hopkins, 1986), but crosslinking of Thy-1 by divalent antibodies inhibits lateral flow of the glycoprotein resulting in membrane patching and then capping, eventually followed by internalization (Hopkins, 1986). The subsequent intracellular routing of Thy-1 ligand complexes has not been studied, but will probably involve the lysosomal compartment of the cell. Understanding of such intracellular routing is important if this antigen is considered as a target antigen for antibody-HPMA copolymer drug-carriers.

The Thy-1 antigen has been used as a model target antigen for antibody-HPMA copolymer conjugates (Rihova & Kopecek, 1985; Rihova et

al., 1986). HPMA copolymer was conjugated to anti-Thy-1.2 (both polyclonal and monoclonal) and pharmacologically active groups (daunomycin (DNM), or quaternary ammonium groups). Conjugates containing both anti-Thy-1.2 and a cytotoxic group resulted in a significant increase in T-lymphocyte killing (both in vitro and in vivo) than was observed using similar HPMA copolymer conjugates containing a non-specific antibody. In vitro evaluation was carried out by incubating spleen cells, isolated from 12-week old female A/J mice, with appropriate conjugates. To discriminate between cytotoxicity due to the pharmacologically active group and that due to the antibody alone, tests were carried out either in the presence, or absence, of complement. Rihova, et al. (1986) found that HPMA copolymer conjugated to anti-Thy-1.2 was up to 70-times more toxic against target T-lymphocytes than a similar HPMA copolymer-conjugate containing non-specific antibody.

In vivo evaluation of the activity of such conjugates involved enumeration of antibody (IgG and IgM) secreting cells (plaque forming cells, PFC) present in the spleen of 8-week old, A/J female mice previously injected intraperitoneally (i.p.) with the HPMA copolymer bound to both anti-Thy-1.2 and DNM, on day 4, 3, 2 and 1 before stimulation with sheep red blood cells (SRBC; i.p. $1x10^8$ cells). On day 5 after immunisation with SRBC the spleen was removed and PFC could then be counted. Rihova, et al. (1986) reported that a 97.9% reduction in the number of PFC was seen after pre-immunisation of mice with HPMA copolymer conjugated to anti-Thy 1.2 and DNM, compared to a 67% reduction using similar conjugates containing no drug.

The published cellular distribution of Thy-1 in different species, is given in Table 8.1. It can be seen that T-lymphocytes are not unique in displaying the anti-Thy-1.2 antigen, therefore, cytotoxic HPMA copolymer-drug conjugates, targeted to the Thy-1

Table 8.1

Cellular distribution of Thy-1 glycoprotein in different species

Species	Common Name	Distribution	References
Man	Thy-1	neurones thymocytes (few %)	Kroczek, et.al. (1986) Williams & Gagnon (1982)
Rat	Thy-1	neurones thymocytes peripheral T-cells	Williams & Gagnon (1982)
Mouse	Thy-1	mouse thymocytes peripheral T-cells neurones fibroblasts	Kroczek, et al. (1986)

antigen, will probably exhibit a more widespread effect than the reduction in PFC reported. In the following study the body distribution of ^{125}I-labelled antibody-HPMA copolymer conjugates has been determined using Thy-1 as a model antigen. In particular the following factors were investigated:-

1. The body distribution of HPMA copolymer, unconjugated anti-Thy-1.2 antibody, and antibody-HPMA copolymer conjugates.
2. The body distribution of anti-Thy-1.2 antibody-HPMA copolymer conjugates conjugates in which the antibody is (a) Fc not available or (b) Fc available for interaction with the cell surface (Chapter 3, 3.2.4).
3. The effect of route of administration on body distribution.
4. The effect of age on the body distribution of unconjugated anti-Thy-1.2, and HPMA conjugated to anti-Thy-1.2.

8.1.1 Calculations

Calculations used in this Chapter are as detailed in Chapter 2, Section 2.2.8.1.

8.2 RESULTS

Materials used in this study were described in Chapter 3 (Table 3.1) and Appendices (1 & 2).

8.2.1 Effect of time after administration on the body distribution of ^{125}I-labelled anti-Thy-1.2 antibody-HPMA copolymer conjugates.

All mice were 16-20 weeks of age unless otherwise stated.

This preliminary experiment was designed to determine the optimal time course for monitoring the body distribution of HPMA-copolymer antibody conjugates. All conjugates were administered intraperitoneally (see Chapter 2, 2.9) and the radioactivity recovered in each organ expressed as a percentage of the total radioactivity recovered from the animal. This method of data analysis was not used in subsequent experiments because it was found

that the total radioactivity recovered, as a percentage of administered dose, was unacceptably low (50%) and the radioactivity unaccounted for could perhaps bias the data.

Over a 24h period most of the radioactivity recovered was located in one, or more, of the following tissues/compartments: peritoneal cavity, blood, urine and liver. Fig. 8.1 shows the radioactivity (% recovered dose) at 1, 5 and 24h.

From Fig. 8.1 it can be seen that more than 90% of the recovered radioactivity associated with the conjugate had left the peritoneal cavity after 5h. In parallel, the radioactivity recovered in the blood and liver reach a maximum after 5h (within the limits of the time points chosen). There was a steady increase with time of radioactivity detected in the urine to a maximum of approximately 50% recovered radioactivity after 24h.

In subsequent experiments it was considered desirable to use a time course over which there was maximal transfer of conjugate out of the peritoneal cavity to give the greatest possibility for cell-specific "targeting", coupled with a minimal amount of conjugate degradation, avoiding the complicating factor of low molecular weight ^{125}I-labelled degradation products. A time course of 5h was chosen for further experiments.

8.2.2 The body distribution of ^{125}I-labelled HPMA copolymer, anti-Thy-1.2 polyclonal antibody, and antibody-HPMA conjugates (containing either non-specific IgG, or anti-Thy-1.2) after i.p. administration.

All experiments were carried out over 5h. As described in the methods (Chapter 2, 2.9), fifteen body compartments were routinely assayed for radioactivity. These organs constitute approximately 42% of the total body weight of a mouse (Appendix 7). The radioactivity recovered in these compartments was found to be dependent on the

Fig. 8.1 Body distribution of ^{125}I-labelled anti-Thy-1.2-HPMA copolymer conjugate 1h, 5h and 24h after intraperitoneal administration to DBA_2 male mice (approximate age 16 weeks).

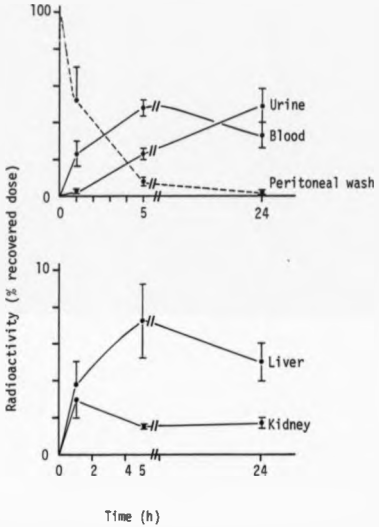

individual conjugates used, varying between 53-70% (Table 8.2).

The body distribution of ^{125}I-labelled HPMA and antibody-HPMA copolymer conjugates (% administered dose and % administered dose gm^{-1} organ) are shown in Table 8.3. It can be seen that HPMA copolymer conjugated to antibody (conjugate 3 containing non-specific IgG; conjugate 4 containing anti-Thy-1.2) left the peritoneal cavity more slowly than either the parent HPMA copolymer or unconjugated anti-Thy-1.2. In addition there was a much higher recovery of radioactivity in the blood (approximately 28% antibody-HPMA copolymer conjugates; 5% HPMA copolymer) together with a lower recovery of radioactivity in the urine (4-7% antibody-HPMA copolymer conjugates; 49% HPMA). As expected, uptake of HPMA copolymer by the liver was increased up to 3-fold after conjugation to antibody.

In general, radioactivity detected in the organs was higher after conjugation of HPMA copolymer to anti-Thy-1.2 than to non-specific IgG and, with the exception of the intestine, always higher than that of the parent HPMA copolymer. In particular, localisation in the thymus of conjugate 4 (containing anti-Thy-1.2) was 3-5 times greater than either anti-Thy-1.2 unconjugated antibody, or conjugate 3 (containing IgG), and 2-3 times greater than HPMA copolymer alone (Fig. 8.2). In the skin a 1.4-fold increase in the localisation of conjugate 4 over conjugate 3 was seen (Table 8.3).

When the results were expressed in terms of the percentage of administered dose recovered gm^{-1} organ (Table 8.3 and Fig. 8.2) it seemed that no additional information was obtained. Further results were presented only in terms of percentage administered dose.

8.2.3 The body distribution, after i.p. administration, of ^{125}I-labelled HPMA copolymer-anti-Thy-1.2 antibody conjugates in which the antibody was (a) Fc not available or (b) Fc available.

The mean molecular weights of HPMA copolymer conjugates 4a and

Fig. 8.2 The percent (administered dose) of HPMA (1) polyclonal anti-Thy 1.2 antibody, and HPMA copolymer conjugates 3 (contain IgG) and 4 (contain anti-Thy-1.2) in the thymus 5h after i.p. administration to DBA_2 male mice (approximate age 16 weeks).
(All ligands were ^{125}I-labelled.)

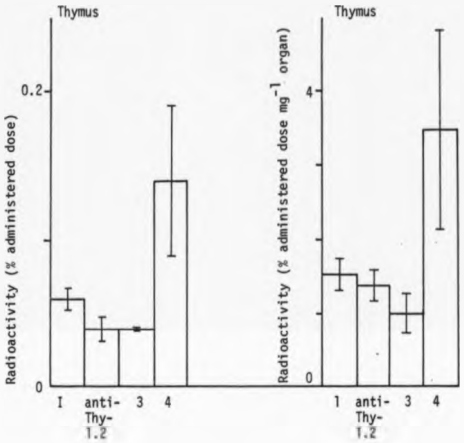

Table 8.2

The percentage of administered dose recovered after administration of ^{125}I-labelled HPMA, unconjugated anti Thy 1.2 and antibody-HPMA copolymer conjugates

^{125}I-labelled substrate	Code number	% of administered dose recovered *	
		i.p. administration	i.v. administration
HPMA +	1	64.6 ± 2.6	N.D.
anti-Thy-1.2		70.1 ± 4.4	81.1 ± 1.2
HPMA-IgG	3	52.6 ± 1.4	N.D.
HPMA-anti-Thy-1.2	4	67.7 ± 5.5	66.2 ± 1.3
	4a	58.9 ± 10	78.2 ± 6.4
	4b	69.5 ± 3.6	81.4 ± 5

* see Appendix 7

Body weight recovered = 40-43% of total mouse weight

+ Body weight recovered = 23% of total mouse weight

Table 8.3

Body distribution (percentage of administered dose) of ^{125}I-labelled HPMA copolymer, unconjugated anti-Thy-1.2 antibody and HPMA copolymer-antibody conjugates, in 16 week old DBA$_2$ male mice 5h after i.p. administration.

Organ	^{125}I-labelled substrate CODE NUMBER			
	1	Anti-Thy-1.2	3	4
Heart	A 0.13 ± 0.02 B 0.9 ± 0.1	0.42 ± 0.04 2.76 ± 0.21	0.31 ± 0.05 1.87 ± 0.36	0.43 ± 0.05 2.8 ± 0.3
Liver	1.3 ± 0.9 0.9 ± 0.32	3.72 ± 0.37 2.88 ± 0.3	2.8 ± 0.39 1.87 ± 0.27	3.82 ± 0.5 2.5 ± 0.3
Lung	0.19 ± 0.04 1.4 ± 0.13	0.59 ± 0.03 3.86 ± 0.16	0.37 ± 0.07 2.29 ± 0.4	0.65 ± 0.06 4.40 ± 0.4
Kidney	0.98 ± 0.09 1.84 ± 0.12	1.34 ± 0.11 3.08 ± 0.22	1.11 ± 0.2 1.99 ± 0.49	1.41 ± 0.3 2.6 ± 0.65
Spleen	0.21 ± 0.07 1.88 ± 0.5	0.37 ± 0.04 4.18 ± 0.57	0.44 ± 0.15 5.87 ± 2.6	0.34 ± 0.08 3.23 ± 0.7
Thymus	0.06 ± 0.007 1.54 ± 0.17	0.04 ± 0.008 1.38 ± 0.19	0.04 ± 0 0.99 ± 0.2	0.14 ± 0.05 3.49 ± 1.3
Submaxillary	0.15 ± 0.018 0.65 ± 0.07	0.43 ± 0.6 2.07 ± 0.2	0.3 ±0.06 1.27 ± 0.17	0.38 ± 0.05 1.56 ± 0.2
Stomach	0.49 ± 0.04 0.61 ± 0.06	2.43 ± 0.16 5.18 ± 0.12	1.29 ± 0.17 1.8 ± 0.52	1.69 ± 0.54 2.1 ± 0.6
Intestine	4.0 ± 0.6 1.06 ± 0.27	5.63 ± 0.44 2.40 ± 0.07	2.58 ± 0.4 2.71 ± 1.5	3.29 ± 0.72 1.01 ± 0.2
Skin	N/D	5.29 ± 0.4 2.55 ± 1.02	4.19 ± 0.73 0.98 ± 0.2	6.1 ± 1.24 1.63 ± 0.3
Bone	N/D	9.18 ± 0.42 5.73 ± 0.35	6.35 ± 2.71 3.71 ± 0.17	7.1 ± 0.8 4.19 ± 0.1
Urine	48.8 2.7	7.3 ± 2.96	4.78 ± 1.3	4.32 ± 0.8
Faeces	0.32 ± 0.2	-	0.14 ± 0.02	-
Blood	5 ± 0.55	25.93 ± 1.13	28.2 ± 4.96	29.0 ± 2.4
Peritoneal wash	2.8 ± 1.2	2.06 ± 0.46	5.1 ± 0.28	5.72 ± 1

1 HPMA

3 HPMA-IgG

4 HPMA-anti-Thy-1.2

A = percentage of administered dose ± S.E. (n= 3-8 mice)

B = percentage of administered dose g^{-1} organ

N/D = Not determined

4b were shown to be approximately equal, but slightly lower than that of parent conjugate 4 (Chapter 3; 251K Daltons, conjugates 4a, 4b; 301K Daltons, parent conjugate 4). Purification of conjugate 4 and subsequent separation by protein-A affinity chromatography into conjugates 4a and 4b, did not result in the detection of degradation products (a problem experienced in the purification of conjugates 3 and 5).

The rate of clearance of conjugates 4a, and in particular 4b, from the peritoneal cavity was faster than that of parent conjugate 4 (Fig. 8.3a). This difference in behaviour of the three related preparations was again evident in the amount of blood-associated radioactivity (% administered dose) (Fig. 8.3b) where both conjugates 4a and 4b were present to a lesser extent than parent conjugate 4, and in the urine (Fig. 8.3c) where more than twice as much urine-associated radioactivity was detected after administration of conjugate 4a than either conjugates 4, 4b, or, in fact, unconjugated anti-Thy-1.2 (Table 8.4).

In general organ-associated radioactivity was lower after administration of conjugates 4a and 4b when compared to the parent copolymer (Table 8.4). Surprisingly, this reduction in tissue-localisation was seen in the spleen, thymus, and bone marrow (Fig. 8.4), but not in the skin, where up to a 2-fold increase in the localisation of 4b, when compared to conjugates 4 or 4a, was seen. Little difference was seen between the levels of liver-associated radioactivity after administration of either conjugates 4, 4a, or 4b (Fig. 8.5). There were however, differences seen in faecal-associated radioactivity (Fig. 8.5), (0%, conjugate 4; 0.3-0.45%, 4b, 4a).

Fig. 8.3 Comparison of the percent (administered dose) of HPMA copolymer conjugates 4 (contains anti-Thy-1.2), 4a (Fc not available) and 4b (Fc available) localised in the peritoneal cavity, blood and urine 5h after i.p. administration to DBA_2 male mice (approximate age 16 weeks). (All ligands were ^{125}I-labelled.)

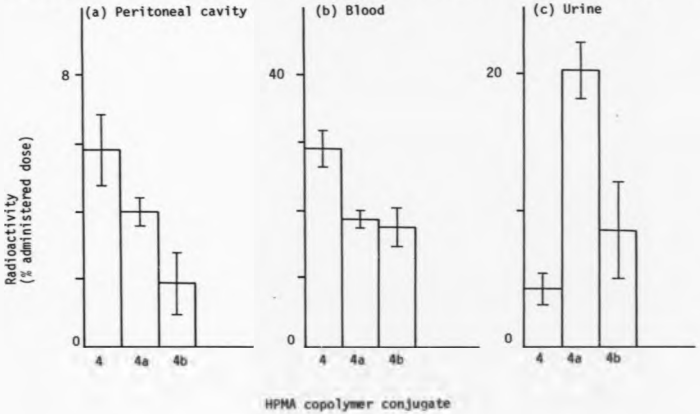

Fig. 8.4 Comparison of the percent (administered dose) of HPMA copolymer conjugates 4, 4a and 4b localised in the spleen, thymus, HPMA skin and bone marrow 5h after i.p. administration to DBA_2 male mice (approximate age 16 weeks). (All ligands were ^{125}I-labelled.)

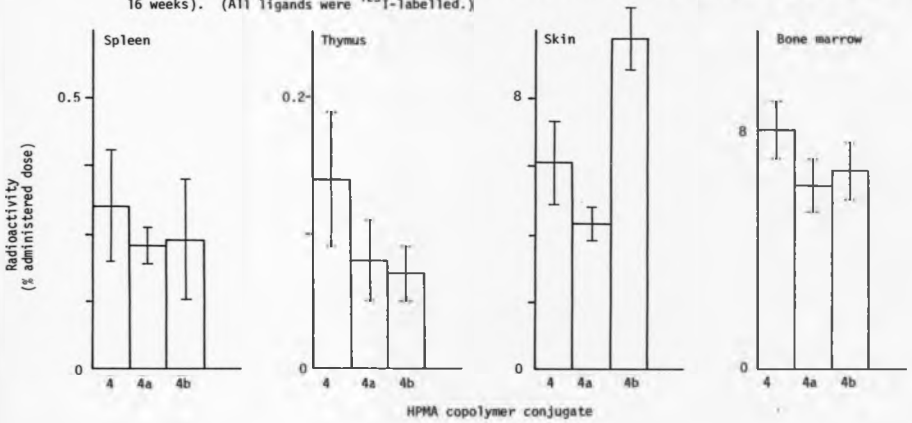

Fig. 8.5 Comparison of the percent (administered dose) of HPMA copolymer conjugates 4, 4a and 4b localised in the liver and faeces 5h after i.p. administration to DBA_2 male mice (approximate age 16 weeks). (All ligands were ^{125}I-labelled.)

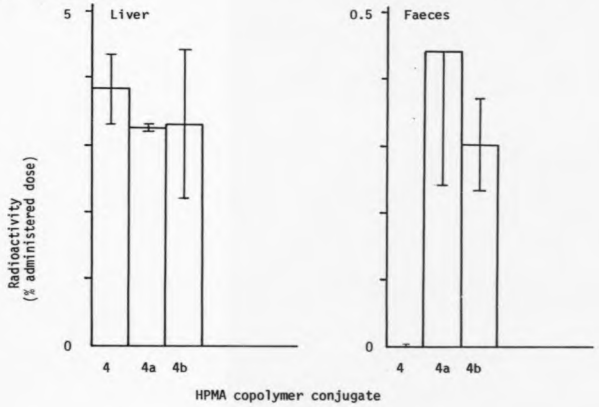

Table 8.4

Body distribution (percentage of administered dose) of anti-Thy-1.2 antibody-HPMA copolymer conjugates 4, 4a and 4b, in 16 week old male* DBA_2 mice, 5h after i.p. administration.

Organ	conjugate 4	4a	4b
Heart	0.43 ± 0.05	0.35 ± 0.08	0.24 ± 0.05
Liver	3.82 ± 0.5	3.26 ± 0.3	3.28 ± 1.1
Lung	0.65 ± 0.06	0.41 ± 0.06	0.42 ± 0.1
Kidney	1.41 ± 0.3	1.4 ± 0.14	1.23 ± 0.4
Spleen	0.34 ± 0.08	0.28 ± 0.03	0.29 ± 0.09
Thymus	0.14 ± 0.05	0.08 ± 0.03	0.07 ± 0.02
Submaxillary gland**	0.38 ± 0.05	0.39 ± 0.06	0.39 ± 0.04
Stomach	1.69 ± 0.54	1.63 ± 0.43	2.74 ± 0.85
Intestine	3.29 ± 0.12	2.98 ± 0.73	2.7 ± 0.5
Skin	6.1 ± 1.24	4.25 ± 0.5	9.67 ± 0.9
Bone	7.1 ± 0.8	4.43 ± 0.8	5.83 ± 0.9
Urine	4.32 ± 0.8	20.4 ± 1.96	8.6 ± 3.6
Faeces	-	0.44 ± 0.2	0.3 ± 0.07
Blood	29 ± 2.4	18.4 ± 1.54	17.5 ± 3.9
Peritoneal wash	5.74 ± 1	3.95 ± 0.42	1.8 ± 0.9

* = approximate age

** = plus attached lymph nodes

4 = parent HPMA copolymer-anti-Thy-1.2

4a = Fc region of antibody not available

4b = Fc available

8.2.4 The body distribution of ^{125}I-labelled antibody-HPMA copolymer conjugates compared after either intraperitoneal or intravenous administration.

The percentage of administered dose recovered after intravenous (i.v.) injection was generally higher (66-84%) than after i.p. administration (58-70%) (Table 8.2).

A comparison of Tables 8.4 and 8.5 shows that the pattern of tissue/organ distribution was dependent upon the route of administration. Administration directly into the bloodstream resulted in a higher recovery of radioactivity in the blood, than seen following i.p. administration, for all substrates investigated (Table 8.5; Fig. 8.6). Also radioactivity recovered in the urine for conjugates 4, 4a and 4b, but not for unconjugated anti-Thy-1.2, was higher after i.v. administration (Fig. 8.6). Both unconjugated anti-Thy-1.2 and HPMA copolymer conjugate 4b (Fc presenting) showed an increase in liver-associated radioactivity (Fig. 8.7a) together with considerable radioactivity recovered in the faeces (Table 8.5; Fig. 8.7b) and increased localisation in the spleen and intestine. This differed from the body distribution of conjugate 4a (Fc masked), which showed greater association (than after i.p. administration) with lungs, stomach, intestine, and significantly higher levels of radioactivity in the bone marrow.

8.2.5 The effect of mouse age (3 week or 16 weeks of age) on the body distribution of ^{125}I-labelled anti-Thy-1.2 and anti-Thy-1.2 antibody-HPMA copolymer conjugates.

Unconjugated ^{125}I-labelled anti-Thy-1.2 antibody was administered to 3-week old DBA_2 male mice by either the i.v. or i.p. route and the body distribution of radioactivity compared with that described earlier for 16 week old mice. The data obtained are shown in Fig. 8.8a,b and Table 8.6.

Fig. 8.6 Comparison of the body distribution (% administered dose) of anti-Thy-1.2, and HPMA copolymer conjugates 4, 4a and 4b 5h after either i.p. (▨) or i.v. (▭) administration to DBA_2 male mice (approximate age 16 weeks). (All ligands were ^{125}I-labelled.)

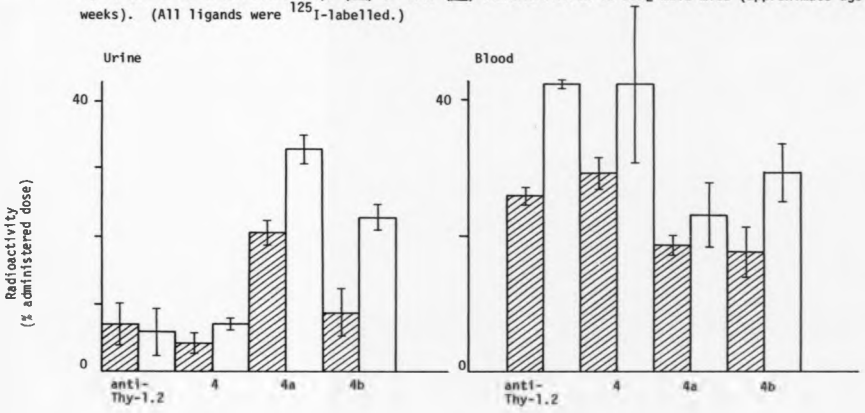

Fig. 8.7 Comparison of the percent (administered dose) of anti-Thy-1.2 and HPMA copolymer conjugates 4, 4a and 4b localised in the liver and faeces 5h after administration to DBA_2 male mice (approximate age 16 weeks). (All ligands were ^{125}I-labelled.)

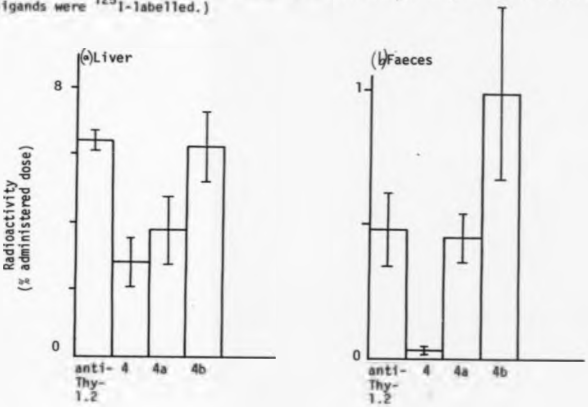

Fig. 8.8a Comparison of the body distribution of anti-Thy-1.2 antibody 5h after i.p. administration to either 3-week (▨) or 16-week (□) old male DBA_2 male mice. (All ligands were ^{125}I-labelled.)

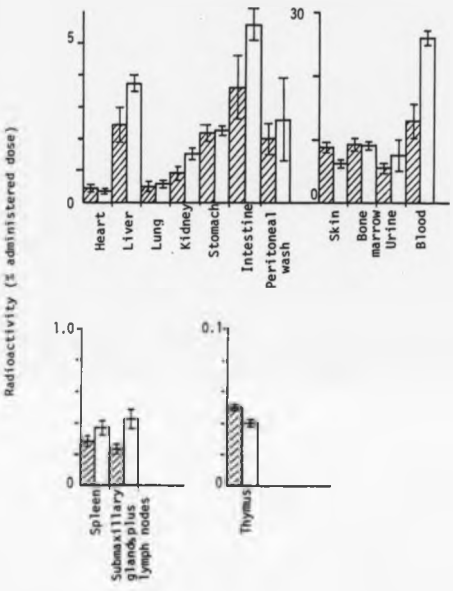

Fig. 8.8b Comparison of the body distribution of anti-Thy-1.2 antibody 5h after i.v. administration to either 3-week (▨) or 16-week (□) old DBA_2 male mice. (All ligands were ^{125}I-labelled.)

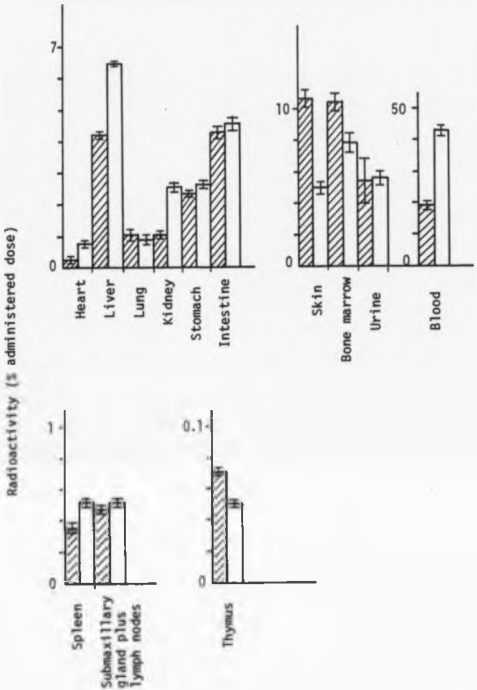

Table 8.5

Body distribution (percentage of administered dose) of anti-Thy-1.2 antibody and HPMA copolymer-anti-Thy-1.2 antibody conjugates in *16 week old DBA_2 male mice, 5h after i.v. administration.

Organ	1	Anti-Thy-1.2	4	4a	4b
Heart	0.03 ± 0.003	0.79 ± 0.09	0.32 ± 0.07	0.24 ± 0.04	0.43 ± 0.1
Liver	0.5 ± 0.03	6.45 ± 0.18	2.78 ± 0.75	3.74 ± 0.97	6.23 ± 0.95
Lung	0.14 ± 0.05	0.95 ± 0.07	0.55 ± 0.14	0.72 ± 0.28	0.56 ± 0.05
Kidney	0.44 ± 0.03	2.6 ± 0.17	1.21 ± 0.3	1.24 ± 0.16	1.28 ± 0.21
Spleen	0.02 ± 0	0.52 ± 0.01	0.27 ± 0.04	0.24 ± 0.07	0.49 ± 0.07
Thymus	0.006± 0.001	0.05 ± 0.001	0.11 ± 0.03	0.03 ± 0.005	0.06 ± 0.02
Submaxillary	0.08 ± 0.007	0.52 ± 0.04	0.29 ± 0.06	0.67 ± 0.15	0.52 ± 0.08
Stomach	1.06 ± 0.069	2.68 ± 0.1	0.34 ± 0.45	2.96 ± 0.54	2.35 ± 0.48
Intestine	5.44 ± 2.8	5.07 ± 0.33	2.38 ± 0.55	3.79 ± 0.66	4.19 ± 0.64
Skin	1.81 ± 0.04	5.03 ± 0.13	3.08 ± 0.4	4.58 ± 0.8	4.52 ± 1.1
Bone	1.18 ± 0.26	7.86 ± 0.51	5.2 ± 2.6	9.9 ± 2.9	4.3 ± 0.5
Urine	49.37 ± 6.44	5.62 ± 0.39	7.01 ± 0.42	32.72 ± 2.3	22.75 ± 1.65
Faeces	3.73 ± 1.78	0.45 ± 0.28	0.06 ± 0.05	0.4 ± 0.17	0.97 ± 0.36
Blood	2.51 ± 0.19	42.45 ± 0.5	42.5 ±11.9	22.78 ± 4.4	28.9 ± 4.4

*approximate age

Table 8.6

Body distribution (percentage of administered dose) of anti-Thy-1.2 antibody, and HPMA copolymer-anti-Thy-1.2 conjugates in 3 week old DBA_2 male mice (5h) after either i.p. or i.v. administration.

Organ/ compartment	Anti-Thy-1.2 i.p.	Anti-Thy-1.2 i.v.	4a i.p.	4b i.p.
Heart	0.37 ± 0.05	0.28 ± 0.04	0.118± 0.004	0.09 ± 0.005
Liver	2.45 ± 0.54	4.41 ± 0.38	1.41 ± 0.01	1.6 ± 0.08
Lung	0.5 ± 0.13	1.04 ± 0.22	0.26 ± 0.07	0.23 ± 0.03
Kidney	0.92 ± 0.22	1.04 ± 0.12	1.14 ± 0.03	1.4 ± 0.07
Spleen	0.24 ± 0.07	0.36 ± 0.03	0.09 ± 0.008	0.008± 0.08
Thymus	0.05 ± 0.07	0.07 ± 0.002	0.03 ± 0.004	0.01 ± 0.003
Submaxillary	0.24 ± 0.05	0.48 ± 0.02	0.2 ± 0.02	0.16 ± 0.02
Stomach	2.37 ± 0.52	2.37 ± 0.11	1.09 ± 0.17	2.78 ± 0.23
Intestine	3.61 ± 1.1	4.25 ± 0.6	1.94 ± 0.16	2.46 ± 0.14
Skin	8.58 ± 1.96	10.69 ± 0.5	2.12 ± 0.15	3.54 ± 0.89
Bone	9.13 ± 1.2	10.43 ± 0.74	9.21 ± 3.38	9.33 ± 2.9
Urine	5.25 ± 1.61	5.46 ± 1.52	9.9 ± 0.57	17.57 ± 2.9
Faeces	-	-	0.61 ± 0.03	0.69 ± 0.23
Blood	12.91 ± 2.35	19.79 ± 1.89	6.3 ± 0.51	25.26 ± 1.41
Peritoneal wash	2.61 ± 1.39	-	0.55 ± 0.19	0.88 ± 0.33

In general, the body distribution seen was similar after either route of administration. However, there did seem to be a difference in body distribution related to the age of the animals used (Fig. 8.8a,b). An increased localisation of anti-Thy-1.2 unconjugated antibody in the skin (31% i.p.; 44% i.v.), bone marrow (25% i.v. only) and thymus (20% i.p.; 29% i.v.) of 3-week old DBA_2 mice was seen when compared to the distribution seen in 16-week old mice (compare Tables 8.3 and 8.6; Fig. 8.8a,b). Also, a decrease in the radioactivity detected in blood, liver and spleen was seen following i.p. and i.v. administration to 3-week old mice when compared to the 16-week old mice.

In a second series of experiments, to determine the body distribution of conjugates 4a and 4b in 3-week old DBA_2 male mice, it was impossible to carry out i.v. injections due to the small size (approximately 6g) of the animals supplied (guaranteed as 3-weeks of age). Therefore, these animals could only be used to examine the body distribution of ^{125}I-labelled HPMA copolymer conjugates after i.p. administration. It was shown (Fig. 8.9a,b) that the body distribution of conjugates 4a and 4b was dependent upon the age of the mice used. In contrast to the data obtained using anti-Thy-1.2 unconjugated antibody there was shown to be a decreased localisation of both conjugates 4a and 4b in the thymus (4a, 63% decrease; 4b, 86% decrease), skin (4a, 45%; 4b, 70.5%) and an increased localisation in the bone marrow (4a, 33% increase; 4b, 81% increase) of 3-week old mice when compared to 16-week old mice.

The body distribution of HPMA copolymer conjugates 4a and 4b in 3-week old mice are compared in Fig. 8.10, where it can be seen that conjugate 4b (Fc available) is cleared from the bloodstream more slowly than 4a (Fc not available), and is localised to a greater extent in the skin and urine than conjugate 4a. In contrast, there

Fig. 8.9a Comparison of the body distributions (% administered dose) of HPMA copolymer conjugate 4a (Fc not available) 5h after i.p. administration to DBA_2 male mice aged either 3 weeks (▨) or 16 weeks (□). (All ligands were ^{125}I-labelled).

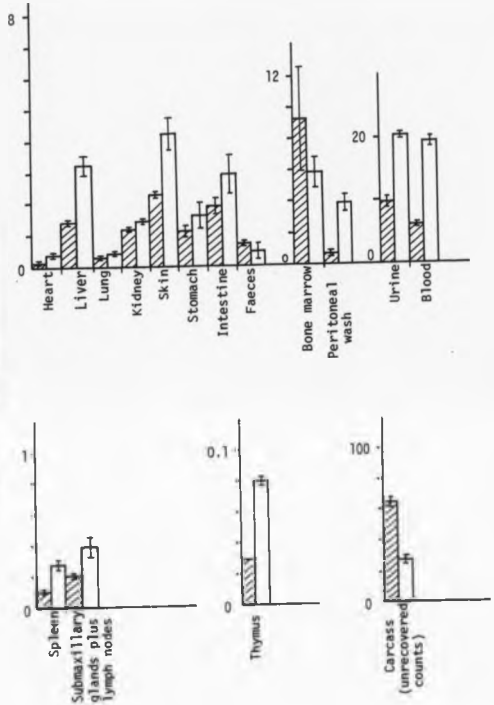

Fig. 8.9b Comparison of the body distributions (% administered dose) of HPMA copolymer conjugate 4b (Fc available) 5h after i.p. administration to DBA_2 male mice aged either 3-weeks (▨) or 16 weeks (□). (All ligands were ^{125}I-labelled).

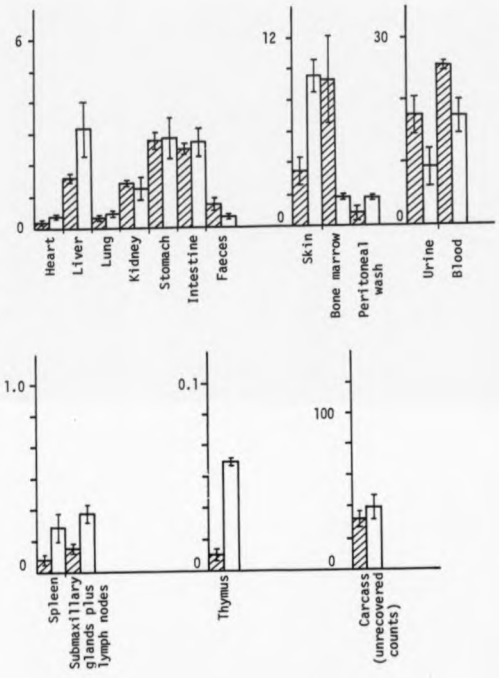

Fig. 8.10 Comparison of the body distribution (% administered dose) of HPMA copolymer conjugates 4a (▨) and 4b (□) 5h after i.p. administration to 3-week old DBA_2 male mice. (All ligands were ^{125}I-labelled.)

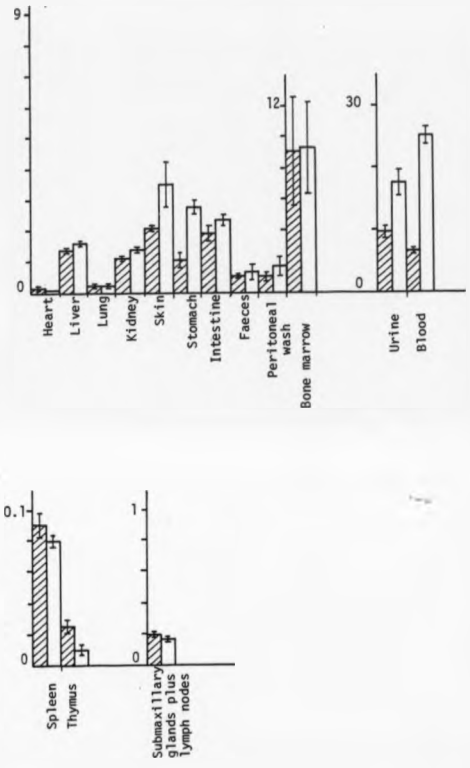

is 2.4-times as much thymus-associated radioactivity after administration of conjugate 4a than 4b.

8.3 DISCUSSION

It is hoped that antibody-HPMA copolymer conjugates can be designed to achieve "targeted" drug-delivery, that is, to preferentially localise in a target tissue and effect cell death.

Cartlidge, et al. (1986) have shown that HPMA copolymer conjugates are able to cross compartmental barriers in vivo. Duncan, et al. (1986), and Seymour, et al. (1986) have shown that the rapid clearance by the RE system, found after in vivo administration of colloidal carriers, was not typical of the HPMA copolymer carrier. The experimental data presented in this chapter show that conjugation of HPMA copolymer to antibody results in an altered body distribution which is closer to that of the unconjugated anti-Thy-1.2 antibody than that of the unmodified HPMA copolymer. Furthermore tissue/organ localisation was dependent upon the route of administration, the orientation of the antibody within the conjugate, and the age of mice used. In particular an increased liver uptake of both unconjugated anti-Thy-1.2 and conjugate 4b, plus an increased bone marrow localisation of conjugate 4a were observed after i.v. administration to 16-week old mice.

As detailed in Chapter 3 there are still many problems to be solved in the synthesis and characterisation of these conjugates, including a a precise definition of molecular weight, stoichiometry, and orientation of protein in the conjugates. Due to these problems of synthesis, repeated preparations of a protein-HPMA copolymer-protein conjugate will never be identical. Bearing this limitation in mind, it has been shown by Rihova & Kopecek (1985) and Rihova, et al. (1986), using similar HPMA copolymer conjugates bound to both anti-Thy-1.2 and DNM, that after i.p. administration, a

pharmacological effect is observed in terms of a reduction in the number of PFC in the spleen of immunised mice. Data presented in this chapter show a 350% increase in the amount of HPMA copolymer found in the thymus after conjugation of HPMA copolyer to anti-Thy-1.2, than after conjugation to a non-specific antibody, an observation consistent with the therapeutic effect observed previously.

Rihova & Kopecek (1985) have also used a skin transplantation model to investigate the effect of HPMA copolymer, bound to both anti-Thy-1.2 and quaternary ammonium groups, on the survival time of a skin allograft in mice. Recipient mice were injected with the conjugate 2, and 1 day before and 1, 2, 3, 5 and 7 days following skin grafting. These workers found that the ability of the antibody-conjugate to increase survival time of the graft was significantly less than antibody alone. These published results are consistent with the assumption made in Chapter 3, that the orientation of the antibody in the antibody-HPMA copolymer conjugates has not been optimised to effect maximal antigen binding. Also, the data presented in this Chapter indicate that an Fc interaction may be important in determining the body distribution of antibody-HPMA copolymer conjugates containing whole antibody molecules, since there is a relatively large localisation in the skin of conjugates targeted by both anti-Thy-1.2 and non-specific IgG. This assumption is further supported by greater skin-localisation of conjugate 4b (Fc presenting) than either 4a, or 4. Some form of Fc interaction is also indicated in the thymus and stomach, but surprisingly not the liver.

Localisation of the anti-Thy-1.2 containing conjugates at the thymus, a major target organ, was relatively low (<1%). A possible explanation for this relatively poor localisation was degeneration of

thymus with age. The mice used in this study may have been too old to demonstrate optimal targeting to thymus (Rihova, 1987). For this reason the body distribution of anti-Thy-1.2 antibody-HPMA copolymer conjugates was determined in 3-week old DBA_2 male mice. Unconjugated antibody did localise more efficiently in the thymus of the younger mice. However, there was a dramatic decrease in the thymus localisation of both conjugates 4a and 4b, together with an increased localisation in the bone marrow. This difference in body distribution of unconjugated antibody and antibody-HPMA copolymer conjugate may be due to the size of the conjugate (Chapter 3, 3.2.3) becoming a limiting factor in animals which are so small (6g), an effect which did not show itself in 30g mice.

Although the amount of anti-Thy-1.2 antibody-HPMA copolymer conjugate which reached the thymus was very low (<1%), Rihova, et al. (1986) have reported a dramatic effect on the immune system of A/J mice (8-week old, female) using similar conjugates. Obvious problems in directly comparing the results of this study with those of Rihova, et al. (1986) are the difference in strain of mice used and the fact that the two preparations of antibody-HPMA copolymer conjugates used cannot be guaranteed identical. Ideally, it is necessary to look at both body distributions and determine the number of PFC in the DBA_2 mice, using the same immunoconjugate preparation. As an initial estimation of pharmacological potential, however, the results seem promising, and are consistent with the work of others; Baldwin & Byers (1986) estimate that optimal localisation of 791T/36 antibody, after administration to patients with colorectal cancer, is only 0.002% g^{-1} tissue; Hazra & Dass (1984) reports 0.1% (administered dose) tumour localisation of ^{131}I-labelled anti-CEA antibody (whole, or fragments); Munz, et al. (1986) who achieved 0.45% (administered dose) tumour localisation gm^{-1} tissue 5 days after injection of antibody

fragments. The reported results of Munz, et al. (1986) indicated that, in the field of radioimmunoimaging, a mixture of McAb gives optimal tumour localisation. Low percentage tumour localisation is a common problem in the field of immunotargeting (Cobb & Humm, 1986). However, the published pharmacological effects achieved by such poor localisation (Baldwin & Byers, 1986; Rihova, et al. 1986) suggest that more well-defined immunoconjugates, in terms of molecular weight, stoichiometry, and orientation of the antibody within the conjugate, could increase tumour localisation. This may consequently result in the need to administer only minute quantities of the conjugates to patients, and so minimise the potential of an immune response towards the conjugates now seen by some workers (Duncan, 1987; Embleton, 1987).

The low levels of target-cell localisation of administered HPMA copolymer, and other solutes (after i.v. and i.p. administration) can be readily explained by reference to Fig. 8.11. After i.p. administration, a route which is becoming increasingly important in chemotherapy (Flessner, et al. 1983; 1985a,b), such large molecules as HPMA copolymer conjugates (Chapter 3) would not be expected to gain direct entry into capillaries (due to the properties of the capillary basement membrane and endothelial layer) but instead would be drained into the lymphatic circulation. Once inside the lymphatic circulation conjugates would have access to extravascular target cells such as the T-cells of the lymphatic system (Freitas, et al., 1986) and possibly become incorporated into the interstitial fluids bathing organs. The thymus, spleen and liver are all intimately involved in the lymphatic system (Andrews, 1979); in the data presented in this chapter the highest localisation of anti-Thy-1.2 antibody-HPMA copolymer conjugates in the thymus was found after i.p. administration.

Fig. 8.11 A schematic diagram to summarise the fate of a HPMA copolymer-antibody conjugates after either i.p. or i.v. administration.

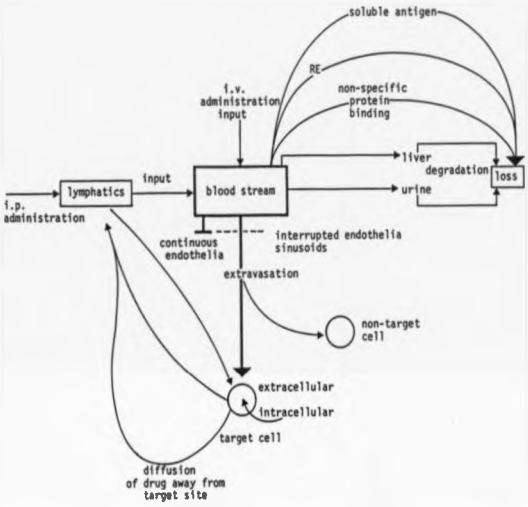

Drainage into the bloodstream occurs via the thoracic duct and other lymphatic venous connections (Weinstein, *et al.*, 1986). Once inside the bloodstream, either after drainage from the lymphatics or after i.v. injection, conjugate will have differential access to organs depending upon the ability of the conjugate to cross endothelial barrier or penetrate capillary pores. The results presented here show that direct administration into the bloodstream of 16-week old DBA_2 mice (as compared to i.p. administration) resulted in a consistently higher percentage (administered dose) of the conjugate remaining within the circulation. These results agree with those of Patel (1984) who found that after i.v. administration of liposomes (not engulfed by the RE system) they could not extravasate and remained in the bloodstream (24h). An additional complication in the interpretation of the data presented in this Chapter is the presence of target T-cells in the bloodstream which may bind the anti-Thy-1.2 antibody-HPMA copolymer conjugates and subsequently migrate.

The most accessible organs to the HPMA copolymer-antibody conjugate are the liver, spleen and bone marrow, where fenestrated endothelia (30-80nm gaps) and sinusoidal endothelia (150nm gaps) allow delivery to the parenchymal cells of these organs (Wisse & de Leeuw, 1984). Data presented in this Chapter show an increased localisation of copolymer 4b (Fc available) in the liver (together with a large increase in faecal radioactivity indicative of degradation), spleen, and an increased localisation of 4a (Fc not available) in the bone marrow after i.v. injection (than after i.p. administration). This difference in localisation of conjugates 4a and 4b indicates that the antibody is able to recognise its target antigen, although data presented in Chapter 4 and 6 using conjugates 2 (containing transferrin) and 3(containing IgG) show that there will probably be interference in antigen-antibody interaction by bound

HPMA copolymer.

When the target antigen is directly accessible to the vasculature (Fig. 8.11) effective targeting should be a relatively easy task. Wolf & Gregoriadis (1984) have used McAb anti-Thy-1 to target liposomes to AKRA cells after i.v. administration of both cells and targeted liposomes. The decreased amount of radioactivity present in the bloodstream after administration of conjugate 4a (when compared to conjugates 4 and 4b) paralleled by a dramatic increase in radioactivity detected in the urine may be due to uptake and processing by target T-cells in the vasculature, with subsequent loss of degradation products in the urine.

It will be more difficult to target effectively to extravascular target cells (Fig. 8.11). Inevitably, only a small percentage of the administered dose is likely to have the potential to reach a target cell-surface antigen and then maintain sufficiently high concentration of drug to effect cell death. For example after administration of antibody-HPMA copolymer conjugate, there is potential loss attributable to removal by the liver, uptake by the RE system, non-specific binding to serum proteins, or specific binding to soluble antigen shed by the target cell. Remaining conjugate must be able to extravasate (a problem seen here by the high percentage of blood-associated radioactivity remaining after 5h), find its target cells, bind to the target cell-surface antigen, undergo internalisation and routing to the lysosomes where finally drug is released to effect cell death. Duncan, *et al.* (1986) have achieved effective tumour cell death in DBA_2 male mice injected i.p. with L1210 leukaemia, using HPMA copolymer bound to DNM and using fucosylamine as a targeting moiety. With the ever increasing list of antibodies available for immunotargeting and the technology to manipulate the antibody molecule structure, (Nishimura, *et al.*, 1987

Hamblin, et al. 1987) and define the orientation of an antibody molecule in immunoconjugates (Rodwell, et al. 1986) it should be possible to effect tumour localisation of more than 1%.

The characteristics of antibody-HPMA copolymer which make it a suitable candidate to play an important role in the field of immunotargeting will be discussed in detail in the General Discussion.

CHAPTER 9

Immunogenicity of protein-HPMA copolymer conjugates; preliminary results

9.1 INTRODUCTION

Protein-HPMA copolymer conjugates can only fulfil their potential as targeted drug-carriers if they have limited, or ideally no, immunogenicity *in vivo*.

Immunogenicity is already regarded as a major problem when administering antibodies for diagnostic purposes (Courtenay-Luck, *et al.*, 1986) or as antibody conjugates for chemotherapy (Duncan, 1987; Embleton, 1987). Certain experiments have shown that binding protein to a soluble synthetic polymer (polyethylene glycol, PEG) can reduce its immunogenicity (Abuchowski, *et al.*, 1977,a,b; Savoca, *et al.*, 1979; Davis, *et al.*, 1980). Likewise, it was considered possible that conjugation of HPMA copolymers to proteins, in particular antibodies, might produce conjugates with reduced immunogenicity.

The immunogenicity of HPMA homopolymer and a number of HPMA copolymers have previously been investigated (Rihova, *et al.*, 1983; 1984; 1985; Rihova & Riha, 1986) using a variety of techniques; (1) determination of the number of antibody-producing cells in the spleens of immunised mice (2) demonstration of serum antibody using one of two methods (a) a passive haemagglutination assay or (b) an ELISA test.

Rihova, *et al.* (1983;1985) have demonstrated several important characteristics of the immune response directed against HPMA homopolymer and HPMA copolymers;

1. There was no antibody response to HPMA homopolymer
2. Modification of the homopolymer to incorporate oligopeptide side-chains and model drugs (fluorescein isothiocyanate, FITC; 2,4-dinitrophenol, DNP; arsanilic acid, ARS) resulted in an immune response which was dependent upon the structure of the incorporated groups. Using side-chains composed of different amino acids, the relative order of immunogenicity was found to be glycyl-glycl-OH>

aminocaproyl-leucyl-hexamethylene diamine >

aminocaproyl-phenylalanyl-OH > glycyl-phenyl-leucyl-glycyl-OH. Antibodies were raised mainly against the oligopeptide side-chains and model drugs.

3. The magnitude of the antibody response was not affected by the number of side-chains per HPMA copolymer molecule.

4. The immune response was dependent upon the mean molecular weight of the HPMA copolymer. After injection of mice with HPMA copolymer of different mean molecular weight, the number of antibody-producing cells detected in the spleens of these mice was found to be 2-5 fold greater after injection of HPMA copolymers with a mean molecular weight 150-200K Daltons, than after injection of similar HPMA copolymer conjugates of mean molecular weight 5K Daltons.

5. Also, the immune response was dependent upon the dose of antigen given to mice. Using a dose range 1-100μg Rihova, et al. (1985) found the optimal dose of polymer was 10μg. Higher doses were thought to be tolerogenic.

6. The genetic background of the mice was found to be very important in determining the immune response. Rihova, et al. (1985) found, for example, that only one of five strains of mice responded to HPMA copolymer-glycyl-ARS.

It was considered extremely important to try to determine the immunogenicity of the antibody-HPMA copolymer conjugates described in this study. For this reason a short collaborative study was undertaken in the laboratory of Dr. B. Rihova, Institute of Microbiology, Prague. AJ, or B10, mice were immunised with human serum albumin (HSA), IgG, HPMA aminolysed homopolymer (conjugate 1) or HPMA conjugated to either transferrin (conjugate 2) or IgG (conjugate 3). Substrate was administered either in complete Freund's adjuvant (to stimulate antibody production), or in solution

(more appropriate to the clinical situation). Subsequently the serum antibody titre was determined using the ELISA technique.

9.1.1 Calculations

Calculations used in this Chapter are as detailed in Chapter 2, Section 2.2.9.4.

9.2 RESULTS

Optimal interaction between antibody and antigen requires that each well of the ELISA plate is coated with a monolayer of antigen. In the short time available to perform these experiments it was not possible to determine the concentration of each substrate necessary to achieve a monolayer. For this reason wells were coated at one of two concentrations, $500\mu gml^{-1}$ or $2mgml^{-1}$ irrespective of the molecular weight of the substrate (Dr. Rihova had found generally that $500\mu gml^{-1}$ was an ideal concentration for other HPMA copolymer antigens).

A summary of the doses used for immunisation is given in Table 9.1. All groups of mice (n=6 per group) were injected with 100µg of substrate in either CFA or in solution (for protocol see Chapter 2, 2.2.9.1).

When carrying out an ELISA assay serum samples are diluted serially into microtitre plates. It is important to understand the consequences of this ongoing serial dilution of antibody. For example it can be seen (Table 9.2) that after diluting 12-times the reduction in antibody level would be approximately $4x10^3$ fold and likewise after a 24-times dilution the reduction would be $1.6x10^7$ fold. It is usual in such experiments to identify the highest dilution producing a definite antibody-antigen reaction. The reciprocal of this antibody dilution-factor is termed the antibody titre.

A summary of the highest antibody dilution (HAD) at which an

Table 9.1

Summary of Immunisation Protocol

Substrate	Dose per immunisation	Method of Immunisation	Strain of Mouse
Human Serum Albumin	100 µg 100 µg	CFA SOL	AJ; B10
Human Gamma Globulin (IgG)	100 µg 100 µg	CFA SOL	AJ; B10
Human Transferrin (TF)	100 µg	SOL SOL	AJ; B10
*HPMA-gly-gly-Tf	100 µg	CFA SOL	AJ; B10
HPMA-gly-gly-IgG	100 µg	CFA SOL	AJ; B10

*HPMA poly-N-(2-hydroxypropyl)-methacrylamide

CFA complete Freunds adjuvant

SOL In solution

Table 9.2

Serial dilution of serum

well row number	1	2	3	4	5	6	7	8	9	10	11	12
antibody dilution	2	4	8	16	32	64	128	256	512	1024	2048	4096

well row number	13	14	15	16	17	18	19	20	21	22	23	24
antibody dilution	8.2×10^3	1.6×10^4	3.3×10^4	6.6×10^4	1.3×10^5	2.6×10^5	5×10^5	1×10^6	2×10^6	4×10^6	$8. \times 10^6$	1.6×10^7

antigen-antibody interaction could be detected, using the ELISA technique, is given in Table 9.3 and Figures 9.1 a-f. For ease of interpretation these graphs show the microtitre well row number equivalent to HAD. This can be converted to an antibody titre by using Table 9.3.

Differences in antibody titre obtained when coating the plates with $500\mu gml^{-1}$ or $2mgml^{-1}$ indicated that these results would benefit from a calibration of the number of molecules of substrate necessary to cover the well. With this limitation in mind, it can be seen from Fig. 9 a-f that the observed titre was always higher after administration of substrate in CFA.

Generally, there was a higher antibody response in AJ mice than was found in B10 mice, although this did not always hold true when using plates coated with $2mgml^{-1}$ substrate (possibly due to the formation of multilayers of substrate in the wells thus interfering with the antibody-antigen interaction).

Under all conditions HPMA-gly-gly-aminopropanol was the least immunogenic substrate. The HAD corresponded to a 512-fold dilution of serum. It should be stressed that this response was very low indeed, but it was not possible to convert this to a concentration of antibody since no calibration curves were constructed.

The most immunogenic substrate in AJ mice was IgG (HAD $1.6x10^7$; Fig. 9.1e; Tables 9.2 and 9.3) and in B10 mice was transferrin (HAD $2.4x10^6$; Fig. 9.1c; Table 9.2 and 9.3). It is interesting to note that the highest antibody titre detected in any experiment was against IgG after administration to AJ mice in CFA.

Conjugation of IgG to HPMA copolymer resulted in a much reduced antibody titre (Fig. 9.1e,f) when compared to unconjugated IgG in both AJ and B10 mice, particularly after administration in CFA. Ratios of antibody titres measured against protein, and the

Fig. 9.1 Highest antibody dilution at which a positive antibody-antigen reaction could be detected in ELISA plate wells coated with two concentrations of antigen and using antisera from mice that had been immunised by antigen in either complete Freund's adjuvant (□) or in solution (▨).

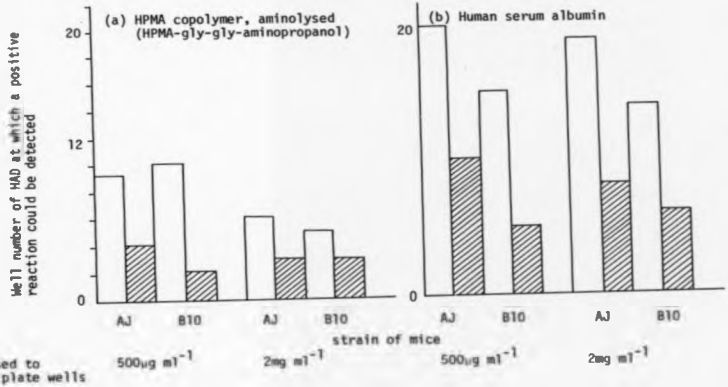

Fig. 9.1 contd...

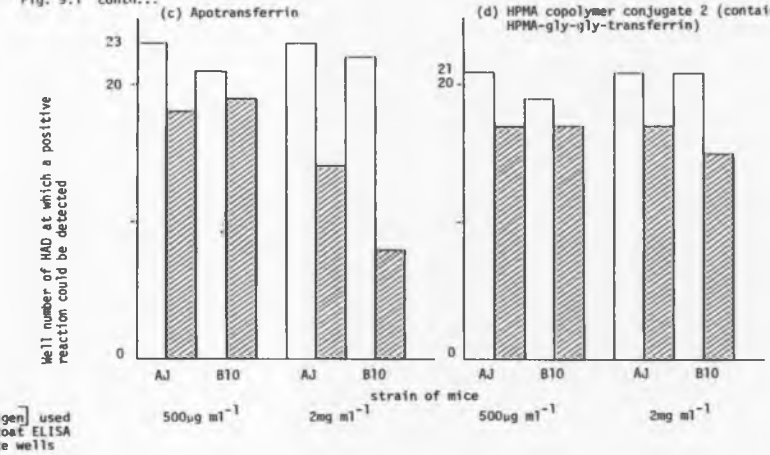
(c) Apotransferrin
(d) HPMA copolymer conjugate 2 (contains transferrin; HPMA-gly-gly-transferrin)
Well number of HAD at which a positive reaction could be detected
23
20
0
21
20
0
AJ
B10
AJ
B10
AJ
B10
AJ
B10
strain of mice
[antigen] used to coat ELISA plate wells
500μg ml-1
2mg ml-1
500μg ml-1
2mg ml-1

Fig. 9.1 contd...

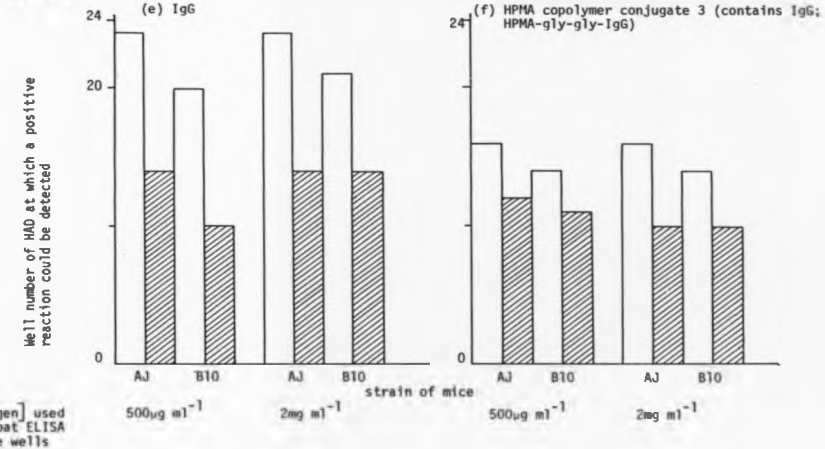
(e) IgG
(f) HPMA copolymer conjugate 3 (contains IgG; HPMA-gly-gly-IgG)
Well number of HAD at which a positive reaction could be detected
24
20
0
AJ
B10
strain of mice
[antigen] used to coat ELISA plate wells
500μg ml-1
2mg ml-1

Table 9.3 Summary of the highest antibody dilutions at which a positive antibody-antigen interaction was detected.

concentration of antigen used to coat wells of ELISA plate	Strain of Mouse	Type of Immunisation	Antibody Dilution					
			HPMA	HSA	Tf	IgG	conjugate 2	conjugate 3
500μgml	AJ	CFA	$5x10^2$	10^6	$8x10^6$	$1.6x10^7$	$2x10^6$	$6.5x10^4$
		SOL	16	10^3	$2.6x10^5$	$1.6x10^4$	$1.3x10^5$	$4x10^3$
	B10	CFA	$8x10^3$	$3.3x10^4$	$2x10^6$	$1x10^6$	$5x10^5$	$1.6x10^4$
		SOL	4	32	$5x10^5$	$1x10^3$	$1.3x10^5$	$2x10^3$
2mg ml^{-1}	AJ	CFA	64	$5x10^5$	$8x10^6$	$1.6x10^7$	$2x10^6$	$6.5x10^4$
		SOL	8	$2.5x10^2$	$1.6x10^4$	$1.6x10^4$	$1.3x10^5$	$1x10^3$
	B10	CFA	32	$1.6x10^4$	$1x10^6$	$2x10^6$	$5x10^5$	$1.6x10^4$
		SOL	8	64	256	$1.6x10^4$	$3.2x10^4$	$1x10^3$

corresponding protein-HPMA copolymer conjugate, are given in Table 9.4. A 250-fold decrease in antibody titre was found after conjugation of IgG to HPMA copolymer (independent of the concentration of antigen coating the microtitre plate wells) when administered in CFA to AJ mice. Similarly a 63-125-fold decrease was found after administration in CFA to B10 mice. The reduction in antibody titre was much less pronounced after administration as solute (4-16-fold).

Conjugation of transferrin to HPMA copolymer resulted in a slight reduction in antibody titre (approximately 2-4 fold) under all conditions,

9.3 DISCUSSION

In these experiments comparison of antibody titre against substrate given in solution or in CFA, showed that CFA, as expected, potentiates the immune response. With the time scale of these experiments the stimulation of an antibody response by administration of conjugate in CFA was probably the most useful experimental model with which to make a comparison of proteins and protein polymer conjugates.

Conjugation of HPMA copolymer (low immunogenicity) to protein (highly immunogenic) produced protein-polymer conjugate whose immunogenicity was up to 250-fold lower than that of the parent protein but higher than that of HPMA-gly-gly-aminopropanol.

In accordance with the results of Rihova, et al. 1983; 1985) HPMA-glycyl-glycyl-aminopropanol was found to elicit a very low immune response in both AJ and B10 mice. Also, in agreement with the earlier studies, an increase in molecular complexity, in this case by incorporation of antibody or transferrin, resulted in a dramatic increase in the immunogenicity of the conjugate as a whole. It was probable that antibodies against polymer conjugates were raised

Table 9.4

Ratios of the antibody titers against protein to those against protein after conjugation to HPMA copolymer.

concentration substrate	Strain of mice	type of immunisation	$Tf(Fe)_2$: HPMA copolymer 2	IgG: HPMA copolymer 3
500µg ml^{-1}	AJ	CFA	4:1	250:1
		SOL	2:1	4:1
	B10	CFA	4:1	63:1
		SOL	4:1	1:2
2mg ml^{-1}	AJ	CFA	4:1	250:1
		SOL	1:8	16:1
	B10	CFA	2:1	125:1
		SOL	1:125	16:1

against the protein component of the conjugate, since it had previously been found that antibodies raised against more simple HPMA copolymer conjugates were predominantly specific for the oligopeptide side-chains and certain incorporated model drugs (Rihova, et al., 1983; 1984).

The 250-fold reduction of antibody titre against IgG after conjugation to HPMA implies that HPMA has the potential to mask the immunogenicity of proteins, in a similar fashion to the ability of PEG to reduce the immunogenicity of bovine serum albumin (Abuchowski, et al. 1977). This ability of PEG to alter immunological properties of a protein has been attributed to PEG (and its bound water) forming a shell around the protein, thus masking antigenic determinants. The possible stoichiometries of the conjugates 2 and 3 (Chapter 3, 3.2.3) would suggest that HPMA may be acting in a similar manner, that is, there could be up to 20 HPMA copolymer molecules bound to each protein molecule. With the increasing use of antibodies (particularly murine) in patients, this ability of HPMA to reduce immunogenicity of antibodies, or other proteins may have important clinical implications. The problems of an anti-mouse immunoglobulin response have already been reported (Courtenay-Luck, et al., 1986).

The immunogenicities of unconjugated transferrin and IgG were found to be quite similar. However, after conjugation of HPMA copolymer to transferrin, there was a much lower reduction in immunogenicity (2-4 fold) than that seen after conjugation of HPMA copolymer to IgG (250-fold).

In the complicated in vivo milieu the reasons for these observed differences in behaviour of the immunocompetent cells towards these two conjugates may be several-fold:-

1. The dose regime of immunisation was based upon the weight (g) of protein irrespective of the molecular weight of the conjugate. The molecular weight of conjugate 3 (contains IgG) is approximately 5-times higher than that of conjugate 2 (contains transferrin) (Chapter 3, 3.2.3). This would mean that approximately 5-times more molecules of conjugate 2 were administered to each mouse.

However, using the same logic in each dose the number of molecules of either conjugate 2 or 3 was much lower than the number of molecules of unconjugated protein. The observation that there was little difference in the antibody titre against transferrin and conjugate 2 (contains transferrin) implies that the number of molecules administered is not the only relevant factor.

2. The high molecular weight of conjugate 3 ($>2x10^6$ Daltons) may promote phagocytosis by macrophages. This would be consistent with a molecular weight-dependent uptake of polymers described *in vitro* (Duncan, *et al.* 1981) (see Chapter 1, 1.2).

In comparison the smaller conjugate 2 (280K Daltons) would not be expected to be removed as readily by macrophages.

Phagocytosis by macrophages, the number of molecules per dose, and relatively slow rates of extravasation of conjugates 2 and 3 (Chapters 7, 8) may all contribute to prolonging contact of conjugate 2 with the immunocompetent cells when compared with conjugate 3.

Interestingly, the extravasation of transferrin (Chapter 7) was much greater than that of conjugate 2 (contains transferrin). Therefore, conjugate 2 would have greater exposure to immunocompetent cells than transferrin. All of these factors may explain why the observed 2-4-fold reduction in antibody titre against transferrin after conjugation to HPMA copolymer is not more pronounced, or equivalent, to that seen for IgG.

3. However, if conjugate 3 is not readily removed by macrophages and if, over the time scale of these experiments (6 weeks) there was limited ability of these conjugates to extravasate (conjugate 2 > conjugate 3) then it is possible that conjugate 3 could induce immunotolerance. Rihova, et al. (1983, 1985) found that a 100μg dose of high molecular weight HPMA copolymers (approximately 200K Daltons induced immunotolerance.

All these points need clarification and their interrelationships determined. It is possible that in vivo all of these factors play some role. These observations, however, do suggest that conjugation of HPMA copolymer to protein may not necessarily reduce immunogenicity of all proteins.

Further experiments are needed to determine (1) an appropriate dose regime of immunisation (2) relationship between molecular weight of antigen and the amount needed to coat an ELISA plate well with a monolayer (3) antibody titre, in terms of moles of antibody produced (4) if the antibody produced is IgG or IgM. However, the limited control of molecular weight, stoichiometry and orientation of protein, particularly antibody, in these conjugates (Chapter 3) means that no two preparations of a single conjugate will ever be identical. Necessarily, further experiments will therefore be able to characterise only single batches of antigen with integral controls.

CHAPTER 10

General Discussion

As a drug-carrier HPMA-copolymer with its pendant, oligopeptide side-chains, specifically designed for release of drug within the lysosomal compartment (Duncan, et al.,1983), offers an ideal means of delivering optimal concentration of drug to a target cell (see Chapter 1, 1.2). It has already been shown that incorporation of carbohydrate residues can effect selective uptake of these conjugates (galactosamine, specific for hepatocytes, Duncan,et al. 1985; fucosylamine, specific for L1210 cells, Duncan, et al., 1987). This study has evaluated the potential use of HPMA copolymer conjugates containing protein, in particular antibody, for targeted drug-delivery.

The HPMA-copolymer conjugates used in this study were among the first to be prepared. As might be expected, biological evaluation has revealed a number of "teething" problems inherent in their preparation.

1. High molecular weight (with particular reference to the conjugates containing IgG) was shown to decrease dramatically the ability of conjugate to bind to cell surfaces, and subsequently gain access to the interior of the cell (Chapters 4, 5). The major contribution to the $\bar{M}w$ of a protein (in particular antibody)-containing conjugate is attributable to the protein component (150k Daltons, antibody; 80k Daltons, transferrin; approximately 15k Daltons HPMA copolymer). An immediate reduction in the molecular weight of an antibody-containing conjugate can be achieved using $F(ab)_2$ fragments, rather than whole antibody molecules (see Chapter 1, Fig. 1.4). This would also have the added advantage of reducing the potential immunogenicity of these conjugates, since a large proportion of any immune response seen in patients is thought to be raised against the Fc region of the antibody (Courtenay-Luck, et al., 1986).

2. The stoichiometry of all conjugates was shown to be far from an ideal ratio of approaching 1:1, antibody:copolymer. In Chapter 3 it was proposed that up to 20 HPMA copolymer molecules may be bound to the protein component. Such stoichiometries are in accordance with the results presented in Chapter 4, where it was shown that conjugation of HPMA copolymer to protein dramatically decreased cell-surface interaction. However, it was shown (Chapter 6) that the conjugates did retain some specificity of binding. A high ratio of polymer to protein, in particular antibody, was also in accordance with the 250-fold reduction in the immunogenicity of IgG seen after conjugation to HPMA copolymer (Chapter 9).

The problems of both stoichiometry and the orientation of a protein within HPMA copolymer-protein conjugates are a consequence of the simple nucleophilic substitution reaction used in their preparation (see Chapter 1, 1.2). When the targeting residue consisted of a sugar molecule, modified at carbon-2 to contain a primary amino-group the resulting conjugates were well defined, containing a known mol %, or weight %, of sugar (for example the fucosylamine-HPMA copolymer conjugates used by Duncan, et al. 1987 contained 8-11 mol % of fucosylamine). This study has shown, however, that a simple nucleophilic substitution reaction is unsuitable for the conjugation of protein to HPMA copolymer. The reason for this is, in comparison to a modified sugar which contains only one amino group, a protein contains many amino groups. Inevitably there is limited control over the degree of substitution and no control over protein orientation in the conjugate. It will be necessary to use alternative methods of conjugation if protein is ever to act as targeting residue to its full potential.

There are a variety of methods available for conjugation of drug to antibody (reviewed Ghose & Blair, 1978). More recent examples

include (1) formation of amide bonds between drug and antibody using water soluble carbodiimides; for example, Kulkarni, et al. (1981) bound methotrexate to IgG via 1-ethyl-3,(3'-dimethylaminopropyl)carbodiimide (2) modification of drug prior to conjugation; for example, Gallego, et al. (1984) modified the sugar amino-group of daunomycin (DNM) by reaction with cis aconitic anhydride. The modified drug was subsequently coupled to IgG using a carbodiimide reaction (3) modification of both antibody and drug prior to conjugation; for example, Gallego, et al. (1984) have modifed IgG by introduction of free thiol groups using N-succinimidyl-3(2-pyridyl-dithio)propionate. Modified antibody was subsequently bound to 14-bromo-DNM. All these examples resulted in the formation of conjugates which retained some antibody specificity. Methods used for conjugation of drug to antibody may not, however, be appropriate for the conjugation of HPMA to antibody. With particular reference to the carbodiimide reaction, where coupling of antibody and drug occurs via activated carboxyl groups of the antibody molecule (of which the antibody molecule has many) there is still the problem of reaction between two multifunctional groups. More appropriate methods of conjugation of HPMA copolymer to protein, in particular antibody, will involve immobilisation of the protein during synthesis, using for example an affinity column, or an antigen matrix (Pressman, 1980). Alternatively, conjugation of HPMA copolymer to antibody via the carbohydrate component of the antibody (see Chapter 1, Fig. 1.4; Rodwell, et al., 1986) may be a more suitable method of preparation.

Once the basic chemistry of conjugation of IgG to HPMA copolymer has been perfected the potential of these conjugates for use in targeted drug-delivery will be greatly increased. It should then be possible to bind IgG of any desired specificity to HPMA copolymer or,

alternatively, to use modified IgG. Although the structure of IgG is ideally suited for its role *in vivo*, it is not so ideally suited for its role as a targeting residue for HPMA copolymer conjugates. There are a number of possibilities available now to modify IgG (1) Enzyme-cleavage to produce $F(ab)_2$ fragments (see Chapter 1, Fig. 1.5), these were mentioned above (2) Chimeric antibodies; gene splicing techniques allow human and mouse genes to be joined, for example genes coding for the variable region of a mouse antibody can be joined to genes coding for the constant region of a human antibody (Boulianne,*et al.* 1984; Golding,*et al.* 1985; Stevenson, *et al.*, 1985; Nishimura, *et al.*, 1987). These modified antibody molecules should be less immunogenic in patients since they contain a human Fc region, and as stated earlier, a major component of the immune response raised in patients against murine antibodies was thought to be raised against the Fc region (3) Hybrid antibodies; chemical reconstitution, or cell fusion techniques can produce antibodies with two different binding specificities (reviewed Milstein & Cuello, 1984; Brennan, *et al.*. 1985; Staerz, *et al.* 1985). These antibodies will retain the benefits of bivalent binding (higher affinity than univalent binding) and in addition be able to cross-link two different antigens. Hybrid antibodies, and possibly $F(ab)_2$ hybrid fragments may play an important role in the future development of antibody-HPMA copolymer conjugates. The reasons for this are several-fold;

(1) There may not exist a tumour-specific antigen, but instead a tumour may express a characteristic set of antigens. Conjugation of possibly 2 $F(ab)_2$ hybrid fragments to HPMA copolymer would effectively give the conjugate the ability to recognise a set, or combination, of up to four different antigens. For example, let us consider use of a hybrid specific for both the Thy-1 antigen and the transferrin receptor; the data presented in Chapters 7 and 8

indicated that these antigens were present on the same cells. Also, Sauvage, et al., (1987) have shown an increased survival time of mice, previously innoculated with SL-2 leukaemia, after administration of a combination of both anti-transferrin receptor and anti-Thy-1.2 antibodies than after administration of either antibody alone. In order to minimise molecular weight it seems a logical step to have both these antigen-binding sites within the same antibody molecule.

(2) The consideration of avidity (interaction of antibody with antigen as a whole; multivalent antibodies will have a higher avidity than monovalent antibodies. See Chapter 6, 6.3) versus affinity (interaction between an antigen and the binding site of one F(ab) arm of an antibody) will always mean that HPMA copolymer conjugate bound to at least two antigen-binding sites will have an increased stability (in terms of Ka) at the cell surface than a similar conjugate containing only one antigen-binding site. The data presented in Chapter 6 suggested that the high calculated "affinity" of the HPMA copolymer conjugate containing IgG was probably due to the presence of at least 10 antibody molecules in this excessively large conjugate. The fact that such a large conjugate could bind to the cell surface, with such a high calculated affinity ($Ka, 4.76 \times 10^{13} M^{-1}$) indicates that conjugates approaching a more ideal molecular weight (approximately 200k Daltons) and bound to at least 2 F(ab) fragments of different specificities (possibly in the form of a hybrid $F(ab)_2$) will have great potential in targeted drug-delivery.

There is obviously a great deal more work to be done before these conjugates are ready for use in patients. In particular the results obtained in Chapter 9, where up to a 250-fold reduction in immune response towards conjugated protein was seen, are very encouraging but need to be expanded to determine the immunogenicity

of all conjugates used. The fact that the preparation of these conjugates has not yet been optimised for use in targeted drug-delivery has been discussed throughout this study. Despite this fact however, it has been shown that the conjugates are able to bind with some specificity to cell surfaces (Chapters 4 and 6), to undergo internalisation and reach the lysosomal compartment (Chapter 5). *In vivo* evaluation has shown that these conjugates can reach target organs in amounts comparable with those of others working in this field (Chapter 7 and 8). If such results can be achieved with these conjugates, then the future potential of more precisely controlled conjugates is phenomenal!

REFERENCES

Aasa, R., Malmstrom, P. & Varingard, T. (1963). Biochem. Biophys. Acta 75, 203-226.
Abuchowski, A., van Es, T., Palczuk, & Davis, F.F. (1977). J. Biol. Chem. 252(11), 3578-3581.
Abuchowski, A., Karp, D. & Davis, F.F. (1981). J. Pharmacol. & Expt. Therapeutics 219(2), 352-354.
Aisen, P. (1980). Iron in Biochem. and Med. London Academic Press, 89-129.
Aisen, P. & Listowsky, I. (1980). Annu. Rev. Biochem. 49, 357-393.
Ajioka, R.S. & Kaplan, J. (1986). Proc. Natl. Acad. Sci. USA 83, 6445-6449.
Ajioka, R.S. & Kaplan, J. (1987). J. Cell Biol. 104, 77-85.
Alberts, B., Bray, D., Lewis, J., Raff, M., Roberts, K. & Watson, J.D. (1983). Molecular Biology of the Cell Garland Publishing Inc., (N.Y.)
Amazel, L.M., Poljak, R.J., Saul, F., Varga, J.M. & Richards, F.F. (1974). Proc. Natl. Acad. Sci. USA 71(4), 1427-1430.
Amazel, L.M. & Poljak, R.J. (1979). Ann. Rev. Biochem. 48, 961-997.
Anderson, R.G.W., Brown, M.S. & Goldstein, J.L. (1976). Proc. Natl. Acad. Sci. USA 73, 2434-2450.
Andrews, W.H.H. (1979). Studies in Biology 105, Liver.
Arnon, R. & Sela, M. (1982). Immunolog. Rev. 62, 5-27.
Ashwell, G. & Harford, J. (1982). Annu. Rev. Biochem. 51, 531-554.
Avruch, J. & Wallach, D.F.H. (1971). Biochim. Biophys. Acta 233, 334-347.
Baldwin, R.W. (1985). Eur. J. Cancer Clin. Oncol. 21(11), 1281-1285.
Baldwin, R.W. & Byers, V.S. (1985). Monoclonal antibodies for cancer detection and therapy (Baldwin & Byers eds.). Academic Press, London.
Baldwin, R.W. & Byers, V.S. (1986). Springer Semin. Immunopathol. 9, 39-50.
Barrett, A.J. (1969). Properties of lysosomal enzymes. Lysosomes in Biology and Pathology Vol. 2. Ed. Dingle, J.T. & Fell, H.B. North-Holland, Amsterdam, 245-275.
Batzer, H. & Lohse, F. (1979). Introduction to Macromolecular Chemistry, 2nd Edition. J. Wiley & Son Ltd.
Benjamin, D.C., Berzofsky, J.A., East, I.J., Crurd, F.N.N., Hannum, C., Leach, S.J., Margoliash, L., Michael, J.G., Miller, A., Prayer, E.M., Reichlin, M., Sercarz, E.E., Smith-Crill, S.J., Todd, P.E. & Wilson, A.C. (1984). Annu. Rev. Immunol. 2, 67-101.
Benner, R., von Oudenarten, A. & Koch, G. (1981). Immunol. Methods (ed. Lefkovitis, I. & Pernis, B.) 2 p247-253.
Besancan, F., Bourgeade, M-F. & Testa, U. (1985). J. Biol. Chem. 260(4), 13074-13080.
Besterman, J.M., Airhart, J.A., Woodworth, R.C. & Low, R.B. (1981). J. Cell Biol. 91, 716-727.
Besterman, J.M. & Low, R.B. (1983). Biochem. J. 210, 1-13.
Blakey, D.C., Watson, G.J., Knowles, P.P. & Thorpe, P.E. (1987). Cancer Res. 47, 947-952.
Bomford, A.B. & Munro, H.N. (1985). Hepatology 5(5), 870-875.
Borysiewicz, L.K., Graham, S. & Sissons, J.G.P. (1986). Eur. J. Immunol. 16, 405-411.
Boulianne, G.L., Hozumi, N. & Schulman, M.J. (1984). Nature 312, 643-646.
Bradwell, A.R., Fairweather, D.S., Dykes, P.W., Keeling, A., Vaughan, A. & Taylor, J. (1985). Immunol. Today 6(5), 163-171.
Brennan, M., Davison, P.F. & Paulus, H. (1985). Science 229, 81-83.
Bretscher, M.S., Thomson, J.N. & Pearse, B.M.F. (1980). Proc. Natl. Acad. Sci. USA. 77, 4156-4159.

Bridges, K.R. & Smith, B.R. (1985). J. Clin. Invest. 76(9), 913-918.
Capra, J.D. & Edmundson, A.B. (1977). Sci. Am. 223(2), 34-42.
Cartlidge, S.A., Dunca, R., Lloyd, J.B., Kopeckova-Rejmanova, P., & Kopecek, J. (1986). J. Cont. Rel. 3, 55-66.
Cheng, T.P-O. (1986). Cell Tissue Res. 244, 613-619.
Cheng, T.W. (1985). Immunol. Today 6(8), 245-249.
Cobb, L.M. & Humm, J.L. (1986). Br. J. Cancer 54, 863-870.
Courtenay, N.S., Epenetos, A.A., Moore, R., Larche, M., Pectasides, D., Dhokia, B. & Ritter, M.A. (1986). Cancer Res. 46, 6489-6493.
Courtoy, P.J., Quintart, J. & Baudhuin, P. (1984). J. Cell Biol. 98, 870-876.
Dautry-Varsat, A. (1986). Biochimie 68, 375-381.
Davies, M.M. (1980). Nature 283, 733-739.
Davies, R.O. and Metzger, H. (1983). Ann. Rev. Immunol. 1, 87-111.
Davis, F.F., Abuchowski, A., van Es, T., Palczuk, N.C., Savoca, K., Chen, R. H-L. & Pyatak, P. (1980). Biomed. Polymers Academic Press Inc. 441-452.
Davis, S.S. (1984). Optimisation of Drug Delivery (ed. Bungaard, H., Bagger-Hansen, A., Kofod, H.) Munkggard, Copenhagen, 198-208.
Davis, S.S., Frier, M. & Illum, L. (1986). Polymeric Nanoparticles and Microspherse (ed. Guiot, P. & Couvreur, P.) CRC Press Boca Raton, 175-197.
Davis, S.S. & Illum, L. (1986). Site Specific Drug Delivery (ed. Tomlinson, E. & Davis, S.S.) J. Wiley & Sons Ltd. 93-110.
Dean, R.T. (1977). Lysosomes. Studies in Biology 84. Edward Arnold, London.
Dean, R. (1985). Personal communication.
Dickson, R.W. (1981). J. Biol. Chem. 256, 3454-3470.
Dickson, R.B., Hanover, J.A., Willingham, M.C. & Pastan, I. (1983). Biochem. 22, 5667-5674.
Dillman, R.O., Johnson, D.E., Shawler, D.L., Halpern, S.E., Leonard, J.E. & Hagan, P.L. (1985). Cancer Res. 45, 5632-5636.
Dreyer, G. & Ray, W. (1910). Philos. Trans. R. Soc. London Ser. 201, 133-137.
Dreyer, W.J. & Bennett, J.C. (1965). Proc. Natl. Acad. Sci. USA. 54, 864-869.
Duncan, R., Pratten, M.E. & Lloyd, J.B. (1979). Biochim. Biophys Acta 574, 463-475.
Duncan, R. & Lloyd, J.B. (1980). Biochem. Biophys. Res. Comm. 94(11), 284-290.
Duncan, R., Pratten, M.K., Cable, H., Lloyd, J.B. (1980). Cell Biol. Int. Rep. 4(8), 786-787.
Duncan, R., Pratten, M.K., Cable, H.C., Ringsdorf, H. & Lloyd, J.B. (1981). Biochem. J. 196, 49-55.
Duncan, R. (1982). Biochim Biophys. Acta 717, 248-268.
Duncan, R., Cable, H.C., Lloyd, J.B., Rejmanova, P. & Kopecek, J. (1983). Makromol. Chem. 184, 1997-2008.
Duncan, R., Cable, H.C., Rejmanova, P., Kopecek, J. & Lloyd, J.B. (1984). Biochim Biophys. Acta 799, 1-8.
Duncan, R. & Kopecek. J. (1984). Adv. in Polymer Sci. 57, 51-101.
Duncan, R., Kopecek, J. & Lloyd, J.B. (1984). Biochem. Soc. Trans. 608th Meeting 12, 913-914.
Duncan, R., Lloyd, J.B., Rejmanova, P. & Kopecek, J. (1985). Makromol. Chem. Suppl.9, 3-12.
Duncan, R. (1986). CRC Critical Reviews in Biocompatibility 2(2), 127-145.
Duncan, R., Seymour, L.C.W., Scarlett, L., Lloyd, J.B., Rejmanova, P. & Kopecek, J. (1986). Biochim. Biophys. Acta 880, 62-67.
Duncan, R. (1987). Personal communication.
Duncan, R., Kopeckova-Rejmanova, P., Strohalm, J., Hume, I., Cable, C. & Pohl, J. (1987). Br. J. Cancer 55, 165-174.

De Duve, C. (1963). Lysosomes Ciba Found. Symp. (ed. De Ruck, A.V.S. & Camerson, M.B.), Churchill, London.
Edelman, G.M. (1970). Sci. Am. 223(2), 34-42.
Ehrlich, P. (1956). Immunology & Cancer Reseach Vol. 2, London Permagon Press, pp442-447.
Embleton, M.J. (1986). Biochem. Soc. Trans. 14, 393-395.
Embleton, M.J. (1987). Personal communication.
Embleton, M.J. (1987). Brit. J. Cancer 55, 227-231.
Erwin, B.G., Stoscheck, C.M. & Florini, J.R. (1981). Anal. Biochem. 110, 291-294.
Fan, Y.J., Carpentier, J.L., Gordon, P., Obberghen, E.V., Blackett, N.M., Grunfield, C. & Orci, L. (1982). Proc. Natl. Acad. Sci. USA 79, 7788-7794.
Farqhar, M.G. & Palade, G.E. (1981). J. Cell Biol. 91, 775-797.
Feizi, T. (1984). Biochem. Soc. Trans. 12, 545-549.
Feizi, T. (1985). Nature 314, 53-57.
Feun, L.G., Lee, Y.Y., Wallace, S., Charnsangavej, C., Sawaray, N., Carrasco, L.H., Giantwco, C. & Yung, W.-K.A. (1985). Prog. Exp. Tumor Res. 29, 131-139.
Finch, C.A. & Heuber, H. (1982). New Eng. J. Med., 306(25), 1520-1527.
Flessner, M.F., Parker, R.J. & Sieber, S. (1983). Am. J. Physiol. 244 (Heart Circ. Physiol. 13) H89-H96.
Flessner, M.F., Deadrick, R.L. & Schultz (1985). Am. J. Physiol. 248, (Heart Circ. Physiol. 17), H15-H25.
Flessner, M.F., Fenstermacker, J.D., Blasberg, R.G. & Dedrick, R.L. (1985). Am. J. Physiol. 248, (Heart Circ. Physiol. 17) H26-H32.
Foley, P. (1965). Cancer 18, 522-526
Ford, C.H.J. & Casson, A.G. (1986). Cancer Chemother. Pharmacol. 17, 197-208.
Forrester, J.A., McIntosh, D.P., Cumber, A.J., Parnell, G.D. & Ross, W.C.J. (1984). Cancer Drug Delivery 1(4), 283-91
Forsbeck, K., Ericsson, J., Birgegard, G., Malmgren, M. & Nilson, K. (1986). Acta Path. Microbiol. Immunol. Scand. Sect. A. 94, 245-252.
Fraker, P.J. & Speck, J.C. (1978). Biochem. Biophys. Res. Commun. 80, 849-857.
Freitas, A.A., Rocha, B. & Coutintio, A.A. (1986). Immunol. Rev. 91, 5-37.
Froese, A. & Paraskevas, F. (1983). Structure and function of Fc receptors. Marcel Dekker, Inc. N.Y.
Gallego, J., Price, M.R. & Baldwin, R.W. (1984). Int. J. Cancer 33, 737-744.
Galloway, C.J., Dean, G.E., Marsh, M., Rudnick, G. & Mellman, I. (1983). Proc. Natl. Acad. Sci. USA. 80, 3334-3338.
Garnett, M.C., Embleton, M.J., Jacobs, E. & Baldwin, R.W. (1983). Int. J. Cancer 31, 661-70.
Garnett, M.C., Embleton, M.J., Jacobs, E. & Baldwin, R.W. (1985). Anti-cancer drug design 1, 3-12.
Gatter, K.C., Brown, G., Trowbridge, I.S., Woolston, R.E. & Mason, D.Y. (1983). J. Clin. Pathol. 36, 539-545.
Geuze, H.J., Slot, J.M., Strous, G.J.A.M., Lodish, H.F. & Schwartz, A.L. (1983). Cell 32, 277-287.
Geysen, H.M., Barteling, S.J. & Meloen, R.H. (1985). Proc. Natl. Acad. Sci. USA, 82, 178-182.
Ghose, T. & Blair, H. (1978). J. Natl. Cancer Inst. 61(3), 657-676.
Golding, H., McCluskey, J., Munitz, T.I., Germain, R.N., Margulies, D.H. & Singer, A. (1985). Nature 317, 425-427.
Gorevic, P.D., Prelli, F.C. and Frangione, B. (1985). Methods in Enzymology 116, 3-26.

Gorman, R.M. & Poretz, R.D. (1987). J. Cellular Physiol. 131, 158-164.
Greaves, M.F. (1979). Tumour Markers: Impact and Prospects (ed. E. Boelsma & P.H. Rumke) Elseveier, Amsterdam, 201-230.
Gregoriadis, G. (1984). Nature 310, 136-137.
Griffiths, P., Milson, J.P. & Lloyd, J.B. (1978). Clinical Chimica Acta 90, 129-141.
Grollman, C.W.J. (1982). Proc. Int. Conf. Biomed. Polymers (London, The Biol. Eng. Soc., 203-240.
Hamblin, T.J., Cattan, A.R., Glennie, M.J., Mackenzie, M.R., Stevenson, F.K., Watts, H.F. & Stevenson, G.T. (1987). Blood 69(3), 790-797.
Hamilton, T.A., Wada, G.H. & Sussman, H.H. (1979). Proc. Natl. Acad. Sci. USA 76(12), 6406-6410.
Hanra, D.J. & Sharma, R.C. (1982). Nucl. Med. Comm. 3, 210-223.
Harding, C., Heuser, J. & Stahl, P. (1984). Eur. J. Cell Biol. 35, 256-263.
Harding, C., Levy, A.L. & Stahl, P. (1985). Eur. J. Cell Biol. 36, 230-238.
Hazra, D.J. & Sharma, R.C. (1982). Nucl. Med. Comm. 3, 210-223.
Hazra, D.K. & Dass, S. (1984). Cur. Sci. 53(16), 842-846.
Helenius, A., Hellman, I., Wall, D. & Hubbard, A. (1983). TIBS 8(7), 245-250.
Hellstrom, K.E., Doolittle, R.F. & Dreyer, W.J. (1982). Nature 296, 171-3.
Herberman, R.B. & Holden, T.H. (1978). Adv. Cancer Res. 27, 305-311.
Herberman, R.B. (1980). Natural Cell-Mediated Immunity Against Tumours Academic Press (N.Y.).
Hill, J.M., Ruff, M.R., Weber, R.J. & Pert, C.B. (1985). Proc. Natl. Acad. Sci. USA 82, 4553-4557.
Hirakawa, K., Kubo, S., Utsuyama, M., Kurashima, C. & Sado, T. (1986). Cellular Immunol. 100, 443-451.
Hopkins, C. (1983). Cell 35, 321-330.
Hopkins, C.R. & Trowbridge, I.S. (1983). J. Cell Biol. 97(8), 508-521.
Hopkins, C.R. (1986). Site Specific Drug Delivery (ed. Tomlinson, E. & Davis, S.S.) John Wiley & Sons Ltd., 27-48.
Hozumi, N., Tonegawa, S. (1976). Proc. Natl. Acad. Sci. USA 73, 3628-3632.
Hulhoven, R. & Harvengt, C. (1982). Pharmacolog. 24(4), 253-260.
Hunt, R.C. (1986). Developmental and Comparative Immunol. 10, 273-277.
Hunt, R.C. & Mashall-Carlson, L. (1986). J. Biol. Chem. 261(8), 3681- 3686.
Ihler, G.M., Glew, R.W. & Schnure, F.W. (1973). Proc. Natl. Acad. Sci. USA 70, 2633-2666.
Illum, L., Jones, P.D.E., Kreuter, J., Baldwin, R.W. & Davis, S.S. (1983). Int. J. Pharm. 17, 65-76.
Ishihara, A., Hou, Y. & Jacobson, K. (1987). Proc. Natl. Acad. Sci. USA 84, 1290-1293.
Jeffries, W.A. (1984). Nature 312, 162-163.
Judd, W., Poodry, C.A. & Strominger, J.L. (1980). J. Exp. Med. 152, 1430-5.
Jung, G., Kohlein, W. & Luden, G. (1981). Biochem. Biophys. Res. Comm. 101(2), 599-606.
Kabat, E.A. (1976). Structural Concepts in Immunology & Immunochemistry, 2nd Ed. (N.Y.) Holt, Rinehart & Winston.
Kolb-Bachofen, V., Schlepper-Schafer, J. & Vogell, W. (1982). Cell 29, 859-866.
Kolb-Bachofen, V. (1985). TIBS 10(3), 107-108.

Konieczny, M., Charytonowicz, O. & Inglot, A.D. (1982). Arch. Immunol. Ther. Exp. 30, 1-9.
Kooistra, T. & Lloyd, J.B. (1985). Int. J. Biochem. 17(17), 805-811.
Kopecek, J. & Spincl, L. (1973). J. Biomed. Mat. Res. 7, 179-201.
Kopecek, J., Cifkova, I., Rejmanova, P., Strohalm, J., Obereigner, J. & Ulbrich, K. (1981). Makromol. Chem. 182, 2941-2949.
Kopecek, J., Rejmanova, P. & Chytry, V. (1981). Makromol. Chem. 182, 799-809.
Kopecek, J. (1984). Biomaterials 5(1), 19-25.
Kopecek, J. (1984). Recent Advances in Drug Delivery Systems (ed. Kim, S.W. & Anderson, J.M.) Penum Press (N.Y.), 41-62.
Kopecek, J., Rejmanova, P., Duncan, R. & Lloyd, J.B. (1985). Ann. N.Y. Acad. Sci. 446, 93-104.
Kornfeld, S. (1969). Biochim. Biophys. Acta 194, 25-31.
Kroczek, R.A., Gunter, K.C., Germain, R.N. & Shevach, E.M. (1986). Nature 322, 181-184.
Kulkarni, P.N., Blair, H. & Ghose, T.I. (1981). Cancer Res. 41, 2700-2706.
Laakso, T., Andersson, J., Artursson, P., Edman,P. & Sjoholm, J. (1986). Life Sciences 38, 183-190.
Langone, J.J. (1982). J. Immunol. Methods 55, 277-296.
Lazarus, A.H. & Baines, M.G. (1985). Cellular Immunol. 96, 255-266.
Lennox, E.S. (1985). Immunity to Cancer (Ed. Reif, A.E. & Mitchell, M.S.) Academic Press, 17-27.
Letvin, N.L., Chalifoux, L.V., Reimann, K.A., Ritz, J., Schlossman, S.F. & Lambert, J.M. (1986). J. Clin. Invest. 78, 666-673.
Lloyd, J.B., Duncan, R. & Pratten, M. (1983). Brit. Polymer J. 15th Dec., 158-159.
Lloyd, J.B., Duncan, R. & Kopecek, J. (1984). Pure & Appl. Chem. 56(10), 1301-1304.
Lloyd, J.B. & Forster, S. (1986). TIBS 11(9), 365-368.
Lloyd, J.B. & Williams, K.E. (1984). Biochem. Soc. Trans. 605th Meeting, 527-528.
Low, M.G. & Kincade, P.W. (1985). Nature 318, 62-66.
Lowry, O.H., Roberts, N.R. and Kapphahn, J.I. (1957). Amer. Soc. Biol. Chem. Inc. 1047-1064.
Manabe, Y., Tusbota, T., Haruta, Y., Kataoka, K., Okazaki, M., Haisa, S. Nakamura, K. & Kimura, I. (1984). J. Lab. Clin. Med. 104(3), 445-454.
Mangat, S. & Patel, H.M. (1985). Biochem. Soc. Trans. 13(4), 699-700.
Marsh, M., Bolzau, E. & Helenius, A. (1983). Cell 32, 931-940.
Marx, J.L. (1984). TIBS 9(11), 819-821.
Mather, S.J. (1986). Appl. Radiat. Isot. 37(8), 727-733.
May, Jr, W.S. & Cuatrecasas, P. (1985). J. Membrane Biol. 88, 205-215.
McCormick, L.A., Seymour, L.C.W., Duncan, R. & Kopecek, J. (1986). J. Bioact. Compatible Polymers 1(1), 1-19.
Merion, M., Schlesinger, P., Brooks, R.M., Moehring, J.M., Moehring, T.J. & Sly, W.S. (1983). Proc. Natl. Acad. Sci. USA 80, 5315-5319.
Milstein, C. (1980). Sci. Amer. 243(4), 66-74
Milstein, C. & Cuello, A. (1984). Immunol. Today 5(10), 299-305.
Milstein, C. (1986). Science 231, 1261-1268.
Morgan, E.H., Smith, G.D. & Peters, T.J. (1986). Biochem. J. 237, 163-173.
Morrison, S.L., Johnson, M.J., Herzenberg, L.A. & Oi, V.T. (1984). Proc. Natl. Acad. Sci. USA. 81, 6851-6855.
Mung, D.L., Alavi, A., Koprowski, H. & Herlyn, D. (1986). J. Nucl. Med. 27, 1739-1745.

Musgrove, E., Rugg, C., Taylor, I. & Hedley, D. (1984). J. Cell Physiol. 118, 6-12.
Neuberger, M.S., Williams, G.T. & Fox, R.O. (1984). Nature 312, 604-608.
Neufeld, E.F., Lim, T.W. & Shapiro, L.J. (1975). Ann. Rev. Biochem. 44, 357-376.
Neutra, M.A., Ciechanover, A., Owen, L.S. & Lodish, H.F. (1985). J. Histochem. & Cytochem. 33(11), 1134-1144.
Newman, C.E. & Ford, C.H.J. (1977). Lancet July 23rd 163-166.
Newman, R., Schneider, C., Sutherland, R., Vodinelich, L. & Greaves, M. (1982). TIBS 7(11), 397-400.
Nishimura, Y., Yokoyama, M., Araki, K., Ueda, R., Kudo, A. & Watanabe, T. (1987). Cancer Res. 47, 999-1005.
Nisonoff, A., Hopper, J.E. & Spring, S.B. (1975). The Antibody Molecule, N.Y. Academic Press.
Nvotny, J., Handschumacher, M., Haber, E., Bruccoleri, R.E., Carlson, W.B., Fanning, D.W., Smith, J.A. & Rose, G.D. (1986). Proc. Natl. Acad. Sci. USA 83, 226-230.
Octave, J.-N., Schneider, Y-J., Trouet, A. & Crichton, R.R. (1979). FEBS Lett. 108(1), 127-130.
Octave, J.-N., Schneider, Y.-J., Crichton, R.R. & Trouet, A. (1981). Eur. J. Biochem. 115, 611-618.
Octave, J.N., Schneider, YU-J., Trouet, A. & Crichton, R.R. (1983). TIBS 8(6), 217-220.
Omary, M.B., Trowbridge, T.S. & Minowada, J. (1980). Nature 286, 888- 891.
Oudemans, P.B., de la Riviere, G.B., Hart, G.A.M., van Heerde, P., Scholte, G. & Vroom, T.M. (1986). Cancer 58, 1252-1259.
Padlan, E.A., Davies, D.R., Rudikoff, S. & Potter, M. (1976). Immunochem. 13(11), 945-949.
Pastan, I.H. & Willingham, M.C. (1981). Ann. Rev. Physiol. 43, 239-250.
Pastan, I.H. & Willingham, M.C. (1983). TIBS 8(7), 250-253.
Patel, H.M. (1984). Biochem. Soc. Trans. 12, 141-144.
Pato, J., Azori, M. & Tudos, F. (1983). Makromol. Chem. Rapit. Commun. 4, 25-27.
Pearse, B.M.F. & Bretscher, M.S. (1981). Ann. Rev. Biochem. 50, 85-101.
Peterson, O.W. & van Deurs, B. (1983). J. Cell Biol. 96(1), 277-281.
Pitha, J. (1981). Biomedical and Dental Applications of Polymers (ed. Gebelen, C.G. & Koblitz, F.K.) Plenum Press (N.Y.), 203-232.
Porter, R.R. (1973). Science 180, 713-716.
Poste, G. & Kirsh, R. (1983). Biotechnology 1, 869-878.
Poste, G., Kirsh, R. & Bugelski, P. (1984). Novel Approaches to Cancer Chemotherapy Academic Press, (N.Y.) 165-230.
Poste, G. (1985). Receptor Mediated Targeting of Drugs (Ed. Gregoriadis, G., Poste, G., Senior, J. & Trouet, A.) Plenum Press, (N.Y.) pp427-474.
Poznansky, M.J. & Juliano, R.L. (1984). Pharmacol. Rev. 36, 277-334.
Poznanzky, M.J., Singh, R. & Singh, B. (1984). Science 223, 1304-1306.
Pressman, D. (1980). Cancer Res. 40, 2960-2967.
Prieels, J.-P., Pizzo, S.V., Glasgas, L.R., Paulson, J.C. & Hill, R.L. (1978). Proc. Natl. Acad. Sci. USA 75(3), 2215-2219.
Rejmanova, P., Kopecek, J., Duncan, R. & Lloyd, J.B. (1985). Biomaterials 6, 45-48.
Rejmanova, P. (1987). Personal communication.
Rieber, E.P., Rank, G. & Reithmuller, G. (1986). Klin. Wochenschr. 64, 1119-1123.

Rihova, B. & Riha, I. (1981). Am. J. Reprod. Immunol. 1, 164-167.
Rihova, B., Tuckova, L. & Riha. I. (1981). Folia biologica (Praha) 27, 1-14.
Rihova, B., Ulbrich, K., Kopecek, J. & Mancal, P. (1983). Folia Microbiol. 28, 217-277.
Rihova, B., Kopecek, J., Ulbrich, K., Pospisil, M. & Mancal, P. (1984). Biomaterials 5(3), 143-148.
Rihova, B. & Kopecek, J. (1985). J. Cont. Rel. 2, 289-310.
Rihova, B., Kopecek, J., Ulbrich, K. & Chytry, V. (1985). Makromol. Chem. Suppl. 9, 13-24.
Rihova, B., Kopecek, J., Kopecek, P., Strohlam, J., Plocova, D. & Jemoradova, H. (1986). J. Chrom. 376, 221-233.
Rihova, B. & Riha, I. (1986). CRC Critical Reviews in Therapeutic Drug Carrier Systems 1(4), 311-375.
Rihova, B. (1987). Personal communication.
Roche, A.C., Barzilay, M., Midoux, P., Junqua, S., Sharon, N. & Monsigny, M. (1983). J. Cell Biochem. 22(3), 131-140.
Rodwell, J.D., Grearhart, P.J. & Karush, F. (1983). J. Immunol. 130, 313-316.
Rodwell, J.D., Alvarez, V.L., Lee, C., Lopes, A.D., Goeb, J.W.F., King, H.D., Powsner, H.J. & McKearn, T.J. (1986). Proc. Natl. Acad. Sci. USA 83, 2632-2636.
Rudland, P.S., Durbin, H., Clingan, D.& de Asua, L.J. (1977). Biochem. Biophys. Res. Commun. 75(3), 556-562.
Ruud, E., Blomhoff, H.K., Funderud, S. & Gobal, T. (1986). Eur. J. Immunol. 16. 286-291.
Ryser, H.J.P. & Shen, W.C. (1978). Proc. Natl. Acad. Sci. USA, 75(8), 3867-3870.
Salacinski, P.R.P., McLean, C., Sykes, J.E.C., Clement-Jones, V.V. & Lowry, P.J. (1981). Analyt. Biochem. 117, 136-146.
Sauvage, C.A., Mendelsohn, J.C., Lesley, J.F. & Trowbridge, I.S. (1987). Cancer Res. 47, 747-753.
Savoca, K.V., Abuchowski, A., van Es, T., Davis, F.F. & Palczuk, N.C. (1979). Biochim. Biophys. Acta 578, 47-53.
Scatchard, G. (1948). Ann. N.Y. Acad. Sci. 51, 667-672.
Scheinberg, D.A. & Strand. M. (1982). Cancer Res. 42, 44-49.
Schlabach, M.R. & Bates, G.W. (1975). J. Biol. Chem. 250, 2182-2188.
Schneider, C., Sutherland, R., Newman, R.J. & Greaves, M. (1982). J. Biol. Chem. 257(14), 8516-8522.
Schneider, C., Owen, M.J., Banville, D. & Williams, J.G. (1984). Nature 311, 675-680.
Schneider, C. & Williams, J.G. (1985). J. Cell Sci. Suppl. 3, 139-149.
Schneider, Y.-J., Tulkens, P., de Duve, C. & Trouet, C. (1979). J. Cell Biol. 82, 449-465.
Schneider, Y.-J., de Duve, C. & Trouet, A. (1981). J. Cell Biol. 88, 380-387.
Schneider, Y.-J. (1983). PhD Thesis, 70-71.
Schwartz, A.L., Fridovich, S.E. & Lodish, H.F. (1982). Biol. Chem. 257(8), 4230-4237.
Senior, J., Waters, J.A. & Gregoriadis, G. (1986). FEBS Lett. 196(1), 54-58.
Seymour, L.W., Duncan, R., Strohalm, J. & Kopecek, J. (1987). J. Biomed. Mater. Res. (In press).
Shen, W.C. & Ryser, H.J.P. (1978). Proc. Natl. Acad. Sci. USA 75, 3867-3876.
Shen, W.C. & Ryser, H.J.P. (1979). Mol. Pharmacol. 16(2), 614-622.
Shen, W.C. & Ryser, H.J.P. (1981). Fed. Proc. 40, 642-670.
Sherwin, C. (1980). PhD Thesis (unfinished) University of Keele.

Silverton, E.W., Navia, M.A. & Davies, D.R. (1977). Proc. Natl. Acad. Sci. USA. 74(11), 5140-5144.
Smyth, M.J., Pietersz, A., Classon, B.J. & McKenzie, F.C. (1986). J. Mat. Com. Inst. 76(3), 503-510.
Staerz, U.D., Kanagawa, O.L. & Bevan, M.J. (1985). Nature 314 628-632.
Stahl, P. (1983). Reception and Recognition Series B 15 (ed Cuatrecasas, P. & Roth, T.) Chapman Hall, London 141-165.
Stahl, P. & Schwartz, A.L. (1986). J. Clin. Invest. 77, 657-662.
Stein, B.S., Bensch, K.G. & Sussman. H.H. (1984). J. Biol. Chem. 259(23), 14762-14777.
Stein, B.S. & Sussman, H.H. (1986). J. Biol. Chem. 261(22), 10319-10331.
Steinman, R.M., Brodie, S.E. & Cohn, Z.A. (1976). J. Cell Biol. 68, 665-687.
Steinman, R.M., Mellman, I.S., Muller, W.A. & Cohn, Z.A. (1983). J. Cell Biol. 96, 1-27.
Stepkowski, S.M. & Duncan, W.R. (1986). Transplantation 42(4), 406-412.
Stevenson, G.T., Glennie, M.J., Paul, F.E., Stevenson, F.K., Watts, H.F. & Wyeth, P. (1985). Biosci. Rep. 5, 991-998.
Stoorvogel, W., Greuze, H.J. & Strous, G.J. (1987). J. Cell Biol. 104, 1261-1268.
Straus, W. (1964). J. Cell Biol. 21, 295-308.
Suemura, M., Kikutani, H., Barsumian, E.L., Hattori, Y., Kishimoto, S., Sato, R., Maeda, A., Nakamura, H., Owaki, H., Hardy, R.R. & Kishimoto, T. (1986). J. Immunol. 137(4), 1214-1220.
Sutherland, R. (1981). Proc. Natl. Acad. Sci. USA 78, 4515-4519.
Tainer, J.A., Getzoff, E.D., Alexander, H., Houghten, R.A., Olsen, A.J. & Lerner, R.A. (1984). Nature 312, 127-134.
Tang, P.W., Gool, H.C., Hardy, M., Leu, Y.C. & Feizi, T. (1985). Biochem. Biophys. Res. Comm. 132(2), 474-480.
Takeda, S., Naito, T., Hama, K., Noma, T. & Hong, T. (1985). Nature 314, 452-454.
Teh, J.G., Stacker, S.A., Thompson, C.H. & McKenzie, I.F.C. (1985). Cancer Surveys 4(1), 149-184.
Teilland, J-L., Desaymard, C., Giush, A.M., Hazeltine, B., Pollock, R.R., Yelton, D.E., Zack, D.J. & Scharft, M.D. (1983). Science 222, 721-726.
Teradaira, R., Kolb-Bachofen, V., Schlepper-Schafer, J. & Kolb, H. (1983). Biochim. Biophys. Acta 759(3), 306-310.
Testa, E.P., Testa, U., Samoggia, P., Salvo, G., Camagna, A. & Peschle, C. (1986). Cancer Res. 46, 5330-5334.
Testa, U. (1985). Curr. Topics Haematol. 5, 127-161.
Thines-Simpoux, D. (1984). Lysosomes in Biology & Pathology Vol. 3 (eds. Dingle, J.T., Dean, R.T. & Sly, W.) Elsevier, Amsterdam.
Thompson, R.J. & Jackson, A.P. (1984). TIBS 9(1), 1-3.
Thorpe, P.E., Ross, W.C.J., Brown, A.N.F., Myers, C.D., Cumber, A.J., Foxwell, B.M.J. & Forrester, J.T. (1984). Eur. J. Biochem. 140, 63-71.
Tomlinson, E. (1986). Site Specific Drug Delivery (ed. Tomlinson, E. & Davis, S.S.) John Wiley & Sons Ltd. 1-26.
Tonegawa, S., Moucan, A.M., Tizard, R., Bernard, O. & Gilbert, W. (1978). Proc. Natl. Acad. Sci. USA 73(3), 1485-1489.
Tonegawa, S. (1983). Nature 302, 575-581.
Trouet, A. & Sokal, G. (1979). Cancer Chemotherapy 63, 895-920.
Trouet, A., Bourain, D., Deprez-De Campenere, C., Layton, D. & Masquelier, M. (1980). Recent Results Cancer Res. 75, 229-235.

Trouet, A., Bawain, R., Deprez-De Campaneere, D., Masquelier, M. & Pirson, P. (1982). Targeting of Drugs (ed. Gregoriadis, G., Senior, J. & Trouet, A.) Plenum Press (N.Y.) 19-30.
Trowbridge, I.S. & Domingo, D.L. (1981). Nature 294, 171-173
Trowbridge, I.S. & Omary, M.B. (1981). Proc. Natl. Acad. Sci. USA 78(5), 3039-3043.
Trowbridge, I.S. & Lopez, F. (1983). Proc. Natl. Acad. Sci. USA 79, 1175-1179.
Trowbridge, I.S. (1985). Gene Expression During Normal and Malignant Differentiation, Academic Press, London. 95-105.
Tsavaler, L., Stein, B.S. & Sussman, H.H. (1986). J. Cell Physiol. 128, 1-8.
Tulkens, P., Beaufay, H. & Trouet, A. (1974). J. Cell Biol. 63, 383-401.
Ulbrich, K., Zacharieva, E.I., Obereigner, B. & Kopecek, J. (1980). Biomaterials 1, 199-204.
Ulbrich, K., Stohalm, J. & Kopecek, J. (1981). Makromol. Chem. 182, 1917-1924.
Ulbrich, K., Mersmann, G., Fleischer, M. & Von Figura, K. (1978). Hoppe-Seyler's Z. Physiol. Chem. 359, 1591-1598.
Ushiko, T. (1986). Cell Tissue Res. 244, 285-298.
Varki, N.M., Reisfeld, R.A. & Walker, L.E. (1985). Monoclonal antibodies and cancer therapy. Alan R. Liss Inc., 207-214.
Van Deurs, B.O., Peterson, O.W. & Bundgaard, M. (1983). TIBS 8(11) 400-401.
Van Renswoude, J., Bridges, K.R., Harford, J.B. & Klausner, R.D. (1982). Proc. Natl. Acad. Sci. USA 79, 6186-6190.
Vitols, S.G., Masquelier, M. & Peterson, C.O. (1985). J. Med. Chem. 28, 451-454.
Wall, D.A., Wilson, P. & Hubbard, A.L. (1980). Cell 21, 79-93.
Wall, D.A. & Hubbard, A.L. (1985). J. Cell Biol. 101, 2104-2112.
Ward, J.H., Kushner, J.P. & Kaplan, J. (1982). J. Biol. Chem. 257(17), 10317-10323.
Watts, C. (1985). J. Cell Biol. 100, 633-637.
Weibel, E.R. (1986). Handbook Physiol, Section 3 iii(1) The respiratory system (eds. Fishman, A.P., Macklem, P.T., Mead, J. & Geiger, S.R.) Am. Physiol. Soc. 89-113.
Weigele, M., De Bernardo, S.L. Tenzi, J.P. & Leingruber, W. (1972). J. Amer. Chem. Soc. 94(16), 5927-5928.
Weinstein, J.N., Black, C.D.V., Barbet, J., Eger, R., Parker, R.J., Holton, O.D., Mulshine, J.L., Keenan, A.M., Larson, S.M., Carrasquillo, J.A., Sieber, S.M. & Covell, D.G. (1986). Site Specific Drug Delivery (eds. Tomlinson, E. & Davis, S.S.) John Wiley & Sons Lted., 27-48.
Weisse, E. & de Leeuw, A.M. (1984). Microsphores and Drug Therpay. Pharmaceutical, Immunological and Medical Aspects (Ed. Davis, S.S., Illum, L., McVie, J.G. & Tomlinson, E.) Elsevier, Biomed. Press, Amsterdam, ppl- 23.
Weissman, A.M., Klausner, R.D., Rao, K. & Harford, J.B. (1986). J. Cell Biol. 102, 951-958.
Weller, N.K. (1974). J. Cell Biol. 63, 699-707.
Westhof, E., Alfschuh, D., Moras, D., Bloomer, A.C., Mondragon, A., Flug, A. & Van Regenmortel, M.H.V. (1984). Nature 313, 123-126.
Wileman, T., Harding, C. & Stahl, P. (1985). Biochem. J. 232, 1-14.
Williams, A.F. & Gagnon, J. (1982). Science 216, 696-702.
Williams, A.F. & Woollett, G.R. (1984). Biochem. Soc. Trans. 13(1), 1-3.
Williams, A.F. (1985). Nature 314, 579-580.
Williams, K.E., Kidston, E.M., Beck, F. & Lloyd, J.B. (1975). J. Cell Biol. 64, 113-122.

Williams, R.J.P. & Moore, G.R. (1985). TIBS 10(3), 96-97.
Willingham, M.C., Hanover, J.A., Dickson, R.B. & Pastan, I. (1984). Proc. Natl. Acad. Sci. USA 81, 175-179.
Willingham, M.C. & Pastan, I. (1984). TIBS 8(3), 93-94.
Willingham, M.C. & Pastan, I. (1984). Int. Rev. Cytol. 92. 51-92.
Willingham, M.C. & Pastan, I. (1985). TIBS 10(5). 190-191.
Wisse, E. & de Leeuv, A.M. (1984). Microspheres and Drug Delivery. Pharmaceutical, Immunological and Medical Aspects (Eds. Davis. S.S., Illum, L., McView, J.G. & Tomlinson, E.) Elsevier Biomed. Press, Amsterdam, 1-23.
Witz, I.P. (1977). Adv. Cancer Res. 25. 95-148.
Wolf, B. & Gregoriadis, G. (1984). Biochim. Biophys. Acta 302. 259-273.
Worobec, E.A., Paranchych, W., Parker, J.M.R., Tanya, A.K. & Hodges, R.S. (1985). J. Biol. Chem. 260(2). 938-948.
Worrell, N.R., Cumber, A.J., Parnell, G.D., Ross, W.C.J. & Forrester, J.A. (1986). Biochem. Pharm. 35(3), 417-423.
Worrell, N.R., Cumber, A.J., Parnell, G.D., Mirza, A., Forrester, J.A. & Ross, W.C.J. (1986). Anti-cancer drug design 1. 179-188.
Wu, G.Y. & Wu, C.H. (1986). J. Biol. Chem. 261(36). 16834-16837.
Wu, T.T. & Kabat, E.A. (1970). J. Exp. Med. 132, 211-250.
Young, S.P. & Aisen, P. (1981). Hepatology 1, 114-120.
Zerial, M., Melancan, P., Schneider, C. & Garroff, H. (1986). EMBO J. 3(7), 1543-1550.

Appendices

Appendix 1

Characteristics of the HPMA copolymers and protein-HPMA copolymer conjugates used in this study.

Code Number	Structure	Comment
1	P*-gly-gly-aminopropanol \TyrNH$_2$	Used as a control polymer
2	P-gly-gly-Transferrin(Tf)	human transferrin; non-degradable linkage
Immunoconjugates		
3	P-gly-gly-IgG	human IgG, non-specific; non-degradable linkage
4	P-gly-gly-anti-Thy-1.2	Rabbit, anti-mouse, polyclonal antibody; specific for Thy-1 antigen; non-degradable linkage
4a	P-gly-gly-anti-Thy-1.2	Fc region of antibody masked
4b	P-gly-gly-anti-Thy 1.2	Fc presenting
5	P-gly-gly-B3/25	murine anti-human transferrin receptor monoclonal antibdoy
Transferrin-polymer-drug conjugates		
6	P-gly-gly-transferrin \gly-gly-Daunomycin (DNM)	DNM attached to P via non-degradable linkage
7	P-gly-gly-transferrin \gly-phe-leu-gly-DNM	DNM attached to P via a degradable linkage

* P; HPMA copolymer backbone

Appendix 2

Details of HPMA copolymers and protein-HPMA copolymer conjugates (supplied by Kopecek, ref. 9).

code	Mol. wt HPMA copolymer precursor	Mol. % reactive ONp groups	Mol. % gly-gly-DNM	Mol. % gly-phe-leu-gly-DNM
1	15K	11	-	-
2	15K	11	-	-
3	15K	11	-	-
4	15K	11	-	-
5	13K	10.2	-	-
6	15K	5.2	2.3	-
7	17K	5.2	-	4.2

Appendix 3

Statistical approach to the determination of $\bar{M}w$.

1. Construct a calibration graph of log Mol.wt. against elution volume (tube number).

In the examples which follow the 4B/6B protein calibration line (see Fig. 3.5b) was used. The $\bar{M}w$ of conjugates 2 and 5 was determined.

Calibration protein	log Mw	Tube number
transferrin	4.903	67
IgG	5.1761	62
ferritin	5.6628	54
thyroglobulin	5.826	51

slope of calibration line = 8.8026227

= constant a

intercept = -0.0583012

= constant b

Appendix 3.1

Data relating to the elution of HPMA copolymer conjugate 2 through a Sephadex 48/6B column (Fig. 3.10).

Tube number	radioactivity (cpm) detected
45	617
46	809
47	1011
48	1454
49	1873
50	2481
51	3329
52	4179
53	5204
54	6700
55	7956
56	9796
57	11206
58	12661
59	13693
60	13809
61	13661
62	12430
63	11008
64	9901
65	8391
66	7115
67	6285
68	5462
69	4797
70	4337
71	3920
72	3577
73	3197
74	3116
75	2826

Appendix 3.1 cont...

number of tubes = 31

constants a = -0.0583012

b = 8.8026227

Using computer programme in Appendix 4

$\bar{P}_w$ = 240K

Appendix 3.2

Data relating to the elution of HPMA copolymer conjugate 3 through a sephadex 4B/6B GPC column (Fig. 3.11).

Tube number	Radioactivity (cpm) corrected	uncorrected
28	1326	1016
29	1460	2952
30	1595	4120
31	1730	3159
32	1865	2816
33	1999	2638
34	2134	2637
35	2269	2697
36	2403	2669
37	2538	2616
38	2673	2752
39	2807	
40	2780	
41	2960	
42	3051	
43	197	
44	3337	
45	3467	
46	3639	
47	3827	
48	3823	
49	4064	
50	4140	
51	4265	
52	4434	
53	4576	
54	4580	
55	4495	
56	4160	
57	3824	
58	3379	
59	2973	2642
60	2611	2325
61	2216	2370
62	1821	2350

cont...

Appendix 3.2 contd...

Tube number	Radioactivity (cpm) corrected	uncorrected
63	1426	2795
64	1030	3251
65	636	3742
66	241	4598
67	0	5238

number of tubes = 4

constants a = -0.0583012

b = 8.8026227

$\bar{P}w = \rangle 2M$

Appendix 4

Computer programme used for the statistical determination of $\bar{M}_w$ (and $\bar{M}_n$).

```
0010PRINT"PRAGUE PROGRAMME"
0020DIMA(90,2)
0030PRINT"ENTER CONSTANTS"
0040PRINT"'a'="
0050INPUTA
0060PRINT"'b'="
0070INPUTB
0080PRINT"ENTER FIRST PEAK COUNT-'C1'"
0090INPUTC1
0100PRINT"ENTER NO. OF COUNTS"
0110INPUTC
0120MATA=ZER(C,2)
0130PRINT"ENTER PEAK HEIGHTS"
0140X=C1-1
0150FORI=1TOC
0160X=X+1
0170A(I,1)=X
0180PRINT"COUNT";X
0190INPUTA(I,2)
0200NEXTI
0210H1=0
0220D1=0
0230P=0
0240FORI=1TOC
0250H1=H1+A(I,2)
0260S1=A+(B*A(I,1))
0270S2=10 S1^
0230D1=D1+(A(I,2)/S2)
0290P1=P1+(S2*A(I,2))
0300NEXTI
0310W=P1/H1
0320N=H1/D1
0330U=W/N
0340PRINT"PEAK PARAMETERS:"
0350PRINT"COUNT VALUES","HEIGHTS"
0360MATPRINTA
0370PRINT
0380PRINT"'a'=";A
0390PRINT"'b'=";B
0400PRINT"MW=";W
0410PRINT"MN=";N
0420PRINT"U=";U
0430END
```

Appendix 5

Calculations used to estimate Total Uptake and Internalisation of HPMA copolymer conjugate 5.

As detailed in Chapter 3 (Fig. 3.2.2) conjugate 5 contains 60% unconjugated HPMA copolymer precursor.

∴ To estimate Tu and In of conjugate 5 it was necessary to correct cell-associated radioactivity in each experimental flask for the contribution attributable to ^{125}I-labelled HPMA copolymer.

At each time point 24 fibroblast cultures (3x8 experiments) were used to determine Tu and In of HPMA copolymer. The formula used to subtract the contribution of ^{125}I-labelled HPMA copolymer to cell associated radioactivity is given below, but first an example will be shown in detail.

EXAMPLE

1. If there are 200 cpm μl^{-1} medium/HBSS

   then 80 cpm μl^{-1} medium/HBSS is associated with conjugate 5

   and 120 cpm μl^{-1} medium/HBSS is associated with unconjugated HPMA copolymer

2. After 3h total cell-associated radioactivity was 153cpm

3. It was known from control experiments that

   Tu_{HPMA} = 2.68 $\mu l\ mg^{-1}$ cell protein

   and since

$$\underset{(\mu l\ mg^{-1}\ \text{cell protein})}{Tu} = \frac{\text{cell-associated radioactivity (cpm)}}{\text{medium radioactivity (cpm)}\mu l^{-1} \times \text{total cell protein (mg)}} + \Delta\text{degradation products}$$

mg^{-1} cell protein

then

$$\text{cell-associated radioactivity (cpm)} = \text{Tu} \times \text{medium radioactivity (cpm) } l \times \text{total cell protein (mg)} - \Delta\text{degradation products } mg^{-1} \text{ cell protein}$$

In this example

$$= (2.68 \times 120 \times 0.156) - 0$$

$$= 50.2 \text{ cpm}$$

$\therefore$ Of the 153 cpm cell-associated radioactivity it was assumed that 100 cpm were associated with conjugate 5

$$\therefore \text{Tu} = \frac{100}{80 \times 0.156} + 0$$

$$= 6.41 \mu l \text{ mg}^{-1} \text{ cell protein.}$$

The same form of calculation was used to determine In, but using trypsin insensitive radioactivity.

Correction for In and Tu of conjugate 5

Tu and In were routinely expressed as follows (also given in Chapter 2, 2.2.5.4).

$$\text{Tu } (\mu l \text{ mg}^{-1} \text{ cell protein}) = \frac{\text{Cell-associated radioactivity (cpm)}}{\text{Medium radioactivity (cpm } \mu l^{-1}) \times \text{Total cell protein (mg)}} + \Delta\text{Degradation products } (mg^{-1} \text{ cell protein})$$

$$\text{In } (\mu l \text{ mg}^{-1} \text{ cell protein}) \quad \frac{\text{Trypsin insensitive cell-associated radioactivity (cpm)}}{\text{Medium radioactivity (cpm } \mu l^{-1}) \times \text{Total cell protein (mg)}} + \Delta\text{Degradation products } (mg^{-1} \text{ cell protein})$$

cell-associated radioactivity (CAR) attributable to HPMA copolymer

$= TU_{HPMA} \times \text{Medium radioactivity}_{HPMA} \times \text{Total cell protein (mg)}$

$= D$ cpm

$\therefore CAR_{\text{conjugate 5}} = (\text{Total CAR} - D)$ cpm

$= E_{cpm}$

$$TU_{\text{conjugate 5}} = \frac{E \text{ cpm}}{\text{Medium radioactivity}_{\text{conjugate 5}} \times \text{Total cell protein (mg)}}$$

$+ \Delta$Degradation products

Similarly In can be determined by correction of trypsin insensitive radioactivity.

APPENDIX 6

Calculations used in Chapter 7 to quantify the body distribution of conjugate 5 (contains 60% unconjugated HPMA copolymer).

As detailed in Chapter 3 (see Fig. 3.8) this preparation contains 60% non-conjugated HPMA copolymer.

The radioactivity administered that corresponds to conjugate 5 is always 40% of the total counts administered.

To estimate the body distribution of conjugate 5 it was necessary to correct each organ/tissue examined for the previously determined distribution of HPMA copolymer (Table 7.1).

The formula used for this calculation is given below, but first an example will be shown in detail.

Detailed Example

If 4,550,077 cpm of a preparation of conjugate 5 were administered

1. That is, 2,730,046 cpm correspond to the administered dose (A.D.) of HPMA copolymer

   1,820,031 cpm correspond to the administered dose of conjugate 5.

2. Recovered radioactivity in the liver after 5h was 97,238 cpm.

3. It was known from previous experiments that 0.5% (expressed as % administered dose) of HPMA copolymer would be found in the liver after 5h (Table 7.1).
   In this case this would correspond to 2730046 x 0.005 cpm
   = 13,650 cpm.

Of the 97,238 cpm recoverd in the liver it was assumed that

13,650 cpm corresponded to HPMA copolymer,

and the remainder, that is

83,588 cpm corresponded to conjugate 5.

The percentage (administered dose) of conjugate 5 in the liver was:

$$\frac{83,588}{1,820,036} \times 100$$

$$= 4.59\%$$

General Calculation

Radioactivity detected in each organ was routinely expressed as a percentage of administered dose (%A.D.).

$$\%(A.D.) = \frac{\text{Radioactivity (cpm) present in the organ}}{\text{Radioactivity (cpm) administered}} \times 100$$

Calculation specific for conjugate 5

1. Total A.D. = HPMA copolymer conjugate 5 (40%) + unconjugated HPMA copolymer precursor (60%)

2. The body distribution of HPMA copolymer was known (Table 7.1).

3. The radioactivity in an organ/tissue due to the presence of HPMA = [60% Total A.D.] x % A.D. localised in the organ

= Xcpm

4. Radioactivity in the same organ due to the presence of conjugate 5

= Total radioactivity detected in the organ (cpm) - Xcpm

= Zcpm

5. Radioactivity in this organ expressed in terms of % administered dose

$$= \frac{Zcmp \times 100}{40\% \text{ Total A.D.}}$$

Chromatography (Pd-10) of urine, collected 5h after i.v. administration of HPMA-copolymer to DBA_2 male mice (Table A.6), showed that 95% of urine-associated radioactivity eluted at the Vo. This indicated that undegraded HPMA copolymer had passed readily through the kidney (consistent with the work of Seymour et al. 1986). Therefore, any radioactivity detected in the urine after administration of conjugate 5 could be analysed as described above.

Table A:6

Percentage urine-associated radioactivity detected in Peak I (high molecular weight ligand) and Peak II (low molecular weight degradation products) after elution through a Sephadex G-15 gel permiation column.

Ligand	Urine-associated radioactivity	
	Peak I	Peak II
HPMA	95%	5%
HPMA copolymer conjugate 5	57% *	43%

*Corresponds to the calculated percentage of counts attributable to unconjugated HPMA copolymer.

Appendix 7

Organ weight as a percentage of mouse body weight.

Organ	mean percentage weight ± S.E. n = 24
Heart	0.55 ± 0.1
Liver	5.08 ± 0.09
Lung	0.54 ± 0.01
Kidney	1.87 ± 0.2
Spleen	0.38 ± 0.09
Thymus	0.13 ± 0.01
Submaxillary gland	0.86 ± 0.05
Skin	13.88 ± 0.2
Bone	6% taken from Kooistra (1979)
Stomach	2.77 ± 0.19
Intestine	11.1 ± 0.2